NATIONAL TECHNICAL UNIVERSITY OF ATHENS

SCHOOL OF CIVIL ENGINEERING
DEPARTMENT OF WATER RESOURCES
AND ENVIRONMENTAL ENGINEERING

Diploma thesis

Optimizing the management of small hydroelectric plants: from the synergetic operation of the turbine system to day-ahead energy forecasting

KORINA KONSTANTINA DRAKAKI

Supervisor : Andreas Efstratiadis, Assistant Professor, NTUA

Athens, November 2021

Στον παππού μου, Κώστα Α. Μαρμαρέλη (+24.10.2020)

CONTENTS

Πρόλογος

Σα βγεις στον πηγαιμό για την Ιθάκη,
να εύχεσαι να 'ναι μακρύς ο δρόμος,
γεμάτος περιπέτειες, γεμάτος γνώσεις….

Κ.Π. Καβάφης, «Ιθάκη»

Ένα ταξίδι γεμάτο γνώσεις, πρωτόγνωρες εμπειρίες και ποικίλα δυνατά συναισθήματα ήταν και το δικό μου ταξίδι στη σπουδή της επιστήμης του Πολιτικού Μηχανικού, στο Εθνικό Μετσόβιο Πολυτεχνείο.

Ένα ταξίδι σε *λιμένας πρωτοϊδωμένους,* όπως λέει και ο ποιητής.

Και τώρα που έφθασα στον *προορισμό* μου, νιώθω να πλημμυρίζω από ικανοποίηση και θαυμασμό, *πλούσια για όσα κέρδισα στον δρόμο,* ευγνώμων *για το ωραίο ταξίδι.*

******

Κάνοντας μια ανασκόπηση σε αυτά τα πέντε χρόνια των σπουδών μου, αισθάνομαι πως πέτυχα να κατακτήσω τους αρχικούς μου στόχους. Συχνά αναλογίζομαι πως ίσως και να τους ξεπέρασα…

Δεν ξεχνώ πως κατά την πρώτη μου επίσκεψη στην ιστοσελίδα της Σχολής, λίγο μετά την ανακοίνωση των αποτελεσμάτων των εισαγωγικών εξετάσεων, ένιωσα μια ξεχωριστή έλξη για την κατεύθυνση του Υδραυλικού Μηχανικού, λες και ήταν φτιαγμένη για μένα. Κι όταν άρχισα να εντρυφώ σε αυτήν, ως φοιτήτρια πλέον φωτισμένων δασκάλων, τότε με άγγιξε στην ψυχή όσο καμία άλλη. Ταίριαξε λες περισσότερο από τις άλλες με εκείνη την, από παιδί, αθεράπευτή μου αγάπη για τη φύση.

Θεωρώ πως υπήρξα τυχερή, γιατί στα πέντε χρόνια των σπουδών μου γνώρισα ανθρώπους που πίστεψαν σε μένα και στάθηκαν αρωγοί δίπλα μου σε στιγμές χαράς μα και αγωνίας, πέρα και πάνω από τη συμβολή τους στην «κοινωνία» μου με το γνωστικό αντικείμενο και τον εφοδιασμό μου με στέρεες επιστημονικές βάσεις.

Ο κ. Ανδρέας Ευστρατιάδης, ο πρώτος καθηγητής της σχολής που διέκρινε την αγάπη μου για το επάγγελμα και πίστεψε στις ικανότητές μου, με ενέταξε στην επιστημονική μου οικογένεια, της οποίας τα μέλη συνδέονται με δεσμούς αλληλοστήριξης και πνεύμα συνεργασίας. Μαζί του πέρασα το μεγαλύτερο μέρος του *ταξιδιού* μου, το οποίο γέμισε όχι μόνο με τις πάμπολλες επιστημονικές του γνώσεις αλλά και με τις αξίες που αρμόζει να χαρακτηρίζουν έναν επιστήμονα. Ο ίδιος στάθηκε δίπλα μου σε κάθε απορία, δυσκολία και προβληματισμό, τόσο ως καθηγητής μου, καθ' όλη τη διάρκεια των σπουδών μου, όσο και ως επιβλέπων καθηγητής της διπλωματικής μου εργασίας. Για την καθοριστική συμβολή του σε όλη την πορεία του *ταξιδιού* τον ευχαριστώ μέσα από την ψυχή μου.

Για τη σπουδαία υποστήριξη στην ερευνά μου, κατά την εκπόνηση της διπλωματικής μου, αισθάνομαι βαθιά την ανάγκη να εκφράσω τις ειλικρινείς μου

ευχαριστίες και στους καθηγητές κ. Δημήτρη Κουτσογιάννη και κ. Νίκο Μαμάση, μέλη της τριμελούς επιτροπής.

Χάρη στη βοήθεια, επιστημονική και ηθική, της υποψήφιας δρ. Τζωρτζίνας Σακκή, του δρ. Γιάννη Τσουκαλά και του δρ. Παναγιώτη Κοσσιέρη, η έρευνά μου για τη διπλωματική μου εργασία πραγματοποιήθηκε με μεγαλύτερη ευκολία και ενδιαφέρον. Καθένας τους αποτελεί πρότυπο για μένα και χαίρομαι πολύ τόσο που συνεργάστηκα επιστημονικά μαζί τους όσο και που τους γνώρισα ως ανθρώπους. Από καρδιάς τους ευχαριστώ.

Τον υποψήφιο δρ. Διονύση Νικολόπουλο και τον ερευνητή Σπύρο Τσατταλιό, επίσης ευχαριστώ, για την προθυμία τους να με διευκολύνουν, όποτε τους το ζήτησα, μα και που έκαναν πιο όμορφα τα διαλείμματά μου από το διάβασμα….

Την οικογένειά μου, τους γονείς μου και τα αδέρφια μου, για την, με κάθε τρόπο, στήριξη στο *ταξίδι* και την ευόδωση του στόχου, ολόψυχα ευχαριστώ. Όσες δυσκολίες και αν προέκυψαν ήταν πάντα παρόντες.

******

Τέλος, θέλω να αναφερθώ σε έναν από τους πιο σημαντικούς ανθρώπους της ζωής μου, που με περιέβαλλε με πολλή τρυφερότητα και πίστευε σε μένα και στις επιλογές μου, στον εκ μητρός παππού μου.

Ο παππούς ένιωθε πολύ περήφανος που θα γινόμουν μηχανικός. Έτσι, εκτός από το να μου γράφει και να μου αφιερώνει ποιήματα, συγκέντρωνε μανιωδώς όποιο άρθρο εφημερίδας έπεφτε στα χέρια του και αναφερόταν στους Υδραυλικούς Μηχανικούς!

Παππού μου, ξέρω ότι με βλέπεις από εκεί ψηλά και με καμαρώνεις. Πόσο περήφανος και γελαστός θα είσαι απόψε…

Στην Κορίνα μου

Μες στην καρδιά μου βρίσκεσαι
θέλω να το κατέχεις
να με θυμάσαι τακτικά
και φυλαχτό να μ' έχεις

και όταν κάπου ζορίζεσαι
ζήτα μου την ευχή μου
και θα στην στέλνω πάντοτε
μέσα απ' την ψυχή μου.

Κ.Μ. , παππούς

Abstract

Motivated by the challenges induced by the so-called Target Model and the associated changes to the current structure of the energy market, we revisit two different aspects regarding the everyday management of Small Hydropower Plants (SHPPs) without storage capacity. The first focuses on determining an optimal operational rule for a given turbine system, while the second confronts the problem of day-ahead prediction of energy by looking for a credible forecasting model with minimal data requirements and little complexity. The task of establishing an efficient operational policy is addressed through extended theoretical analysis, in which we investigate alternative configurations of potential turbine combinations. In order to obtain generic conclusions, we provide a dimensionless formulation of the turbine mixing and the power production procedure. The proposed operation policy, next referred to as synergetic, is compared by using as reference a simpler operation rule, the so-called hierarchical. On the other hand, for the day-ahead energy forecasting problem we use as example a typical run-of-river SHPP, in the upper course of river Achelous ,Western Greece. Based on daily hydrological data for a 39-year period, we test alternative forecasting schemes of varying complexity (from regression-based to machine learning) that take advantage of different levels of information. In this respect, we investigate whether it is preferable to use as predictor the known energy production of previous days, or to predict the day-ahead inflows and next estimate the resulting energy production via simulation. Our analyses indicate that the second approach becomes clearly more advantageous when the expert's knowledge about both the hydrological regime and the technical characteristics of the SHPP is incorporated within the model training procedure. Beyond these, we also focus on the predictive uncertainty that characterize such forecasts, with overarching objective to move beyond the standard, yet risky, point forecasting methods, providing a single expected value of power production. Finally, we discuss the use of the proposed forecasting procedure under uncertainty in the real-world electricity market.

Συνοπτική περίληψη

Έχοντας ως γνώμονα τις ραγδαίες εξελίξεις που έφερε η είσοδος του νέου θεσμικού πλαισίου λειτουργίας (Target Model) στο Ευρωπαϊκό Χρηματιστήριο Ενέργειας, σε συνδυασμό με την ένταξη των Μικρών Υδροηλεκτρικών Έργων (ΜΥΗΕ) σε αυτό, επιλέξαμε, μέσω της παρακάτω εργασίας, να αναζητήσουμε τρόπους βελτιστοποίησης της παραγόμενης ενέργειας που υπόσχεται ένα ΜΥΗΕ αμελητέας αποθηκευτικής ικανότητας. Η έρευνά μας αποτελείται από δύο διαφορετικών ειδών προσεγγίσεις για την εν λόγω βελτιστοποίηση, όπου η μία διαδέχεται την άλλη, για την τελική παρουσίαση του βέλτιστου μοντέλου παραγωγής ενέργειας. Η πρώτη προσέγγιση αφορά την εύρεση ενός αποδοτικότερου κανόνα λειτουργίας των στροβίλων, σε σχέση με τον απλοϊκό που ορίζει το ιεραρχικό μοντέλο. Δοκιμάζεται ένα μείγμα στροβίλων διαφορετικών χαρακτηριστικών και διαμορφώνεται ένας νέος, βελτιωμένος κανόνας, ο συνεργατικός, εκφρασμένος μέσω γενικευμένων μαθηματικών εξισώσεων, ώστε να μπορεί να προσαρμοστεί σε κάθε περίπτωση. Η δεύτερη προσέγγιση δημιουργεί ικανά μοντέλα πρόγνωσης της ενέργειας,. Τα δεδομένα που αξιοποιήθηκαν στην έρευνα των παραπάνω προσεγγίσεων αναφέρονται σε δεδομένα παροχής και βροχόπτωσης του ποταμού Αχελώου, στη Δυτική Ελλάδα για 39 έτη. Κάθε μοντέλο πρόγνωσης χρησιμοποιεί διαφορετική πληροφορία ως μεταβλητή εισόδου. Επιλέξαμε να προσεγγίσουμε το πρόβλημα της πρόγνωσης μέσω δύο οδών. Η πρώτη χρησιμοποιεί ως πληροφορία εισόδου την ενέργεια των προηγούμενων ημερών, σε συνδυασμό με τη βροχόπτωση, επιστρέφοντας ως αποτέλεσμα την ενέργεια της επόμενης ημέρας. Αντιθέτως, η δεύτερη οδός έχει ως δεδομένα εισόδου την παροχή των προηγούμενων ημερών με την αντίστοιχη βροχόπτωση, από τα οποία προκύπτει η παροχή της επόμενης ημέρας. Συνέχεια, λαμβάνουμε την ενέργεια της επόμενης ημέρας, εισάγοντας την παροχή στον βέλτιστο κανόνα λειτουργίας των στροβίλων. Στόχος μας είναι να διαπιστώσουμε ποιο μοντέλο πρόγνωσης είναι πιο αποδοτικό, το άμεσο ή το έμμεσο. Οι υπολογισμοί μας έδειξαν ότι το έμμεσο μοντέλο γίνεται πιο αξιόπιστο, όταν συμπεριλάβει την τεχνολογική γνώση περί της λειτουργίας του συστήματος. Το πλέον βελτιωμένο μοντέλο διαμορφώθηκε κατάλληλα, έτσι ώστε να περιλαμβάνει και την αβεβαιότητα στη δομή του, ως αναπόφευκτο παράγοντα ενός μοντέλου πρόγνωσης που στηρίζεται στη συλλογή ιστορικών καιρικών δεδομένων. Τέλος, προκειμένου να έχουμε μια πρακτική εφαρμογή της έρευνας και των αποτελεσμάτων της, εφαρμόσαμε το πιο αποδοτικό μοντέλο πρόγνωσης στη δημιουργία τριών πολιτικών αγορών, ανάλογα με τον χαρακτήρα (συντηρητικό, ασφαλές, ριψοκίνδυνο) που θέλει ο χρήστης του έργου να υιοθετήσει, κατά τη συμμετοχή του στο χρηματιστήριο ενέργειας.

Συμπερασματικά, θα λέγαμε ότι η παρούσα εργασία επιτυγχάνει να προτείνει στον λειτουργό του ΜΥΗΕ μια εύχρηστη και αξιόπιστη μεθοδολογία πρόγνωσης της ενέργειας επόμενης ημέρας, βάσει κατάλληλου μαθηματικού μοντέλου, καθώς και έναν βελτιωμένο προγραμματισμό της λειτουργίας μείγματος στροβίλων, υποσχόμενο μέγιστη δυνατή παραγωγή ενέργειας.

Εκτενής περίληψη

Σκοπός εργασίας

Η συγκεκριμένη Διπλωματική εργασία έχει διττό χαρακτήρα, καθώς προσεγγίζει και στοχεύει στη βέλτιστη μοντελοποίηση δύο διαφορετικών όψεων του ίδιου, όμως, "νομίσματος". Ως νόμισμα νοείται η βελτιστοποίηση της διαχείρισης των Μικρών Υδροηλεκτρικών Έργων (ΜΥΗΕ), από τη σκοπιά του λειτουργού του έργου. Η έρευνά μας επικεντρώνεται σε δύο ζητήματα:

I. την εύρεση της βέλτιστης ρύθμισης λειτουργίας του μείγματος των στροβίλων, διαμορφώνοντας έναν πρότυπο κανόνα προγραμματισμού λειτουργίας ("Συνεργατικό κανόνα");

II. τη δημιουργία μοντέλων πρόγνωσης της παραγόμενης ενέργειας της επόμενης ημέρας, λαμβάνοντας υπόψιν τον παράγοντα της αβεβαιότητας, λόγω σφαλμάτων του μοντέλου και αδυναμίας ακρίβειας της γνώσης των καιρικών φαινομένων.

Άξονας προσέγγισης των δύο παραπάνω στόχων αποτελεί η δημιουργία κανόνα λειτουργίας και μοντέλων πρόβλεψης, εύκολων στην εφαρμογή και εποπτεία από τον χρήστη του έργου, χωρίς να θεωρείται αναγκαία προϋπόθεση οποιαδήποτε εξειδικευμένη γνώση ή χρήση περίπλοκων τεχνολογιών υπολογισμού.

Περιοχή μελέτης

Στο πλαίσιο της παραπάνω ανάλυσης, θεωρήσαμε ένα υποθετικό ΜΥΗΕ εκτροπής (run-of-river) στον άνω ρου του Αχελώου ποταμού, Δυτικής Ελλάδας. Η παροχή που φθάνει στην υδροληψία εκτρέπεται, μέσω ενός ανοικτού καναλιού, σε μια δεξαμενή φόρτισης, και έπειτα, μέσω ενός αγωγού πτώσης και συστήματος στροβίλων, παράγει ηλεκτρική ισχύ, εξαιτίας υψομετρικής διαφοράς, ίσης με 150 m.

Η διαθέσιμη υδρολογική πληροφορία που αξιοποιήσαμε ήταν τα υδρολογικά δεδομένα βροχόπτωσης από 10 διαφορετικούς σταθμούς στην ευρύτερη περιοχή του έργου υδροληψίας, καθώς και τα δεδομένα παροχών στο σημείο αυτό. Η τελευταία πληροφορία ανακτήθηκε με τη μέθοδος προσαρμογής των παρατηρημένων παροχών στα κατάντη, από τον ταμιευτήρα των Κρεμαστών (Efstratiadis et al., 2014), λαμβάνοντας υπόψιν τον λόγο των αντίστοιχων λεκανών απορροής (προσεγγιστικά 1:40). Η περίοδος καταγραφής δεδομένων εκτείνεται στα 39 χρόνια (Μάιος 1969 έως Δεκέμβριο του 2008), με μέση παρατηρούμενη τιμή παροχής 2.15 m^3/s. Στο **Σχήμα 1** παρουσιάζεται η χρονοσειρά μέσης ημερήσιας παροχής ενός υδρολογικού έτους (1971-72).

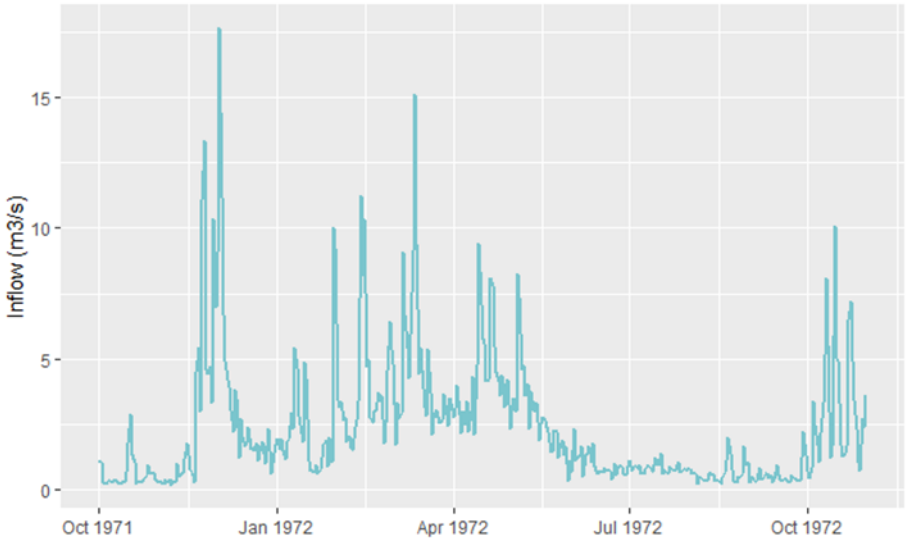

Σχήμα 1 : Χρονοσειρά παροχής υδρολογικού έτους 1971-1972.

Βελτιστοποίηση λειτουργία μείγματος στροβίλων: από τον Ιεραρχικό στον Συνεργατικού Κανόνα

Η ανάγκη αναζήτησης ενός πρότυπου κανόνα προγραμματισμού λειτουργίας στροβίλων αποτελεί απόρροια του γνωρίσματος των ΜΥΗΕ, ως έργων που στην πλειονότητά τους έχουν αμελητέα αποθηκευτική ικανότητα. Ως αποτέλεσμα τούτου, η παροχή που καλούνται να εκμεταλλευτούν για παραγωγή ενέργειας παρουσιάζει διαρκείς διακυμάνσεις. Μέσω της χρήσης μείγματος τουρμπινών, όπου κάθε μια λειτουργεί σε ένα διαφορετικό εύρος παροχών ($q_{i,min}$, $q_{i,max}$), πετυχαίνουμε επαρκή αξιοποίηση του υδατικού δυναμικού, με όρια λειτουργίας ($q_{min} = min(q_{i,min})$, $q_{max} = \sum_{i=1}^{N} q_{i,max}$), και, συνακόλουθα, μειωμένη την επίδραση της διακυμάνσης της παροχής. Ο αντίκτυπος της μεταβαλλόμενης παροχής ως προς την εξασφάλιση παραγωγής ενέργειας μπορεί να ελαχιστοποιηθεί ακόμα περισσότερο μέσω της βελτιστοποίησης του προγραμματισμού των στροβίλων.

Ένας απλός και αποδοτικός κανόνας λειτουργίας του συστήματος στροβίλων είναι ο λεγόμενος "Ιεραρχικός κανόνας" ,(**Σχήμα 3**). Αυτός ο κανόνας προϋποθέτει την ύπαρξη δύο στροβίλων, ενός κυρίαρχου και του αντίστοιχου δευτερεύοντα. Ο πρώτος, έχοντας μεγαλύτερη ονομαστική παροχή, εκμεταλλεύεται παροχές μεγαλύτερης κλίμακας, σε αντίθεση με τον τελευταίο, όπου είναι υπεύθυνος για την παραγωγή ενέργειας μέσω της αξιοποίησης χαμηλών παροχών. Πιο συγκεκριμένα, όταν η εκτρεπόμενη ροή έχει τιμή μικρότερη από την ελάχιστη δυνατή παροχή του συστήματος προς εκμετάλλευση, q_{min}, και οι δύο στρόβιλοι είναι εκτός λειτουργίας. Όταν η παροχή που διέρχεται το σύστημα ξεπερνάει την μέγιστη δυνατή παροχή του συστήματος, q_{max} , και οι δύο στρόβιλοι λειτουργούν στη μέγιστη απόδοσή τους, επιστρέφοντας τυχόν υπερχειλίσεις στη ροή του ποταμού. Για ενδιάμεσες τιμές παροχών το Ιεραρχικό μοντέλο θέτει σε λειτουργία μόνο τον δευτερεύοντα στρόβιλο, όταν $q_a \in (q_{2,min}, q_{1,min})$. Από την άλλη πλευρά, ο κυρίαρχος στρόβιλος τίθεται σε προτεραιότητα, όταν $q_b \in (q_{1,max}, q_{1,max} + q_{2,max})$, αφήνοντας το ενδεχόμενο να λειτουργεί ο δευτερεύων μόνο για παροχή $\Delta q = q_b - (q_{1,max} + q_{2,max}) \geq q_{2,min}$.

Η παραπάνω απλουστευμένη ρύθμιση του κανόνα λειτουργίας μείγματος στροβίλων παρουσιάζεται συνοπτικά μέσω των ακόλουθων εξισώσεων :

$$q_1 = \min(q, q_{1,max})$$

Αν $q > q_{1,max}$ τότε η επιπλέον παροχή που διέρχεται από τον δευτερεύοντα στρόβιλο ισούται με :

$$q_2 = \min(q - q_1, q_{2,max})$$

Για $q_i < q_{i,min}$ το σύστημα παράγει μηδενική ισχύ, ενώ για $q_i > q_{i,min}$ η παραγόμενη ισχύς από τον έκαστο στρόβιλο ισούται με :

$$p_i = \begin{cases} 0 & q_i < q_{i,min} \\ \rho\, g\, \eta_i(q_i)\, q_i h_n(q_i) & q_{i,min} \le q_i < q_{i,max} \\ p_{i,max} & q_{i,max} \le q_i \end{cases}$$

όπου q συμβολίζεται η παροχή που φτάνει στο σημείο πρόσληψης ροής από τον ποταμό, έχοντας αφαιρέσει την περιβαλλοντική παροχή q_e, σύμφωνα με την αντίστοιχη νομοθεσία, $\eta_i(q_i)$ είναι ο συνολικός βαθμός απόδοσης του συστήματος, και $h_n(q_i)$ το καθαρό ύψος πτώσης, το οποίο αντιθέτως είναι φθίνουσα συνάρτηση της παροχής q_i. Σημειώνεται ότι ο βαθμός απόδοσης των στροβίλων είναι μια έντονα μη γραμμική σχέση που δίνεται με μορφή νομογραφήματος (**Σχήμα 2**), ως συνάρτηση του λόγου της διερχόμενης παροχής προς την ονομαστική, q/q_{nom}(μονότονα αύξουσα έως το ονομαστικό σημείο). Για ευκολία στους υπολογισμούς, η σχέση αυτή μπορεί να προσεγγιστεί από την ακόλουθη αναλυτική έκφραση:

$$\eta_T = \eta_{min} + \left(1 - \left(1 - \left(\frac{\frac{q}{q_{nom}} - \theta}{1 - \theta}\right)^a\right)^b\right)(\eta_{max} - \eta_{min})$$

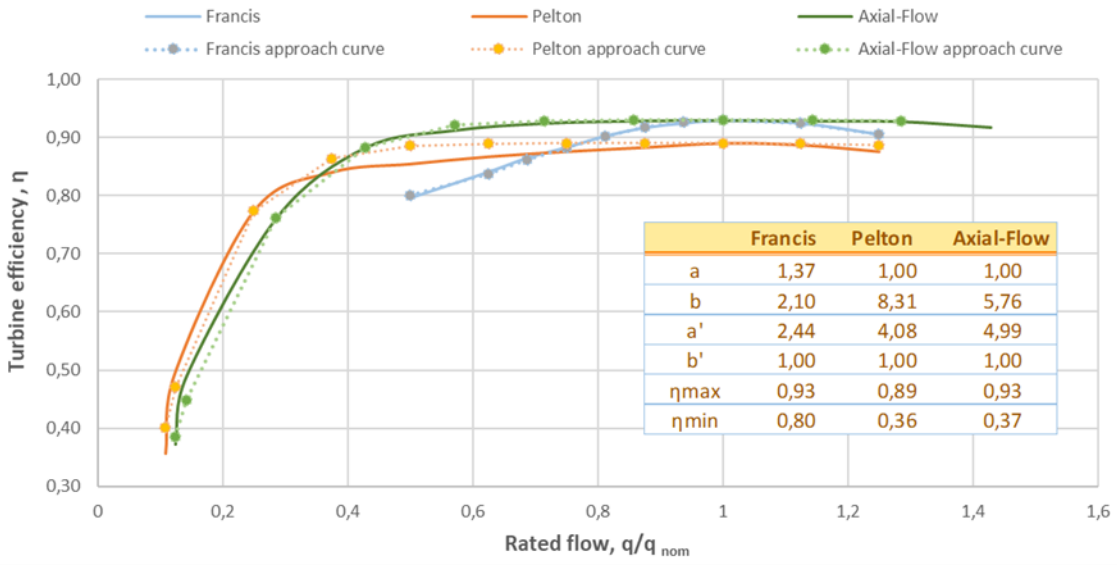

	Francis	Pelton	Axial-Flow
a	1,37	1,00	1,00
b	2,10	8,31	5,76
a'	2,44	4,08	4,99
b'	1,00	1,00	1,00
ηmax	0,93	0,89	0,93
ηmin	0,80	0,36	0,37

Σχήμα 2 : Καμπύλες βαθμού απόδοσης διαφόρων τύπων στροβίλων.

Η παραπάνω πολιτική λειτουργίας μπορεί να είναι απλή στην εφαρμογή αλλά δεν συνεπάγεται ότι είναι και πιο αποδοτική. Η μη γραμμική συμπεριφορά του γινομένου $\eta_i(q_i)\, q_i$, όπου ο δείκτης i χαρακτηρίζει τον κάθε στρόβιλο, η οποία εκφράζεται από καμπύλες του παρακάτω διαγράμματος, οδήγησε σε ένα νέο βέλτιστο κανόνα λειτουργίας, τον αποκαλούμενο ως "Συνεργατικό κανόνα" (**Σχήμα 4**). Ο κανόνας αυτός ρυθμίζει τους στροβίλους σύμφωνα με τα παρακάτω βήματα :

- Όταν $q < q_{2,min}$, κανένας στρόβιλος δεν λειτουργεί, άρα δεν υπάρχει παραγωγή ενέργειας·
- Όταν $q_{2,min} < q < q_{1,min}$, μόνο ο μικρότερος σε δυναμικό στρόβιλος λειτουργεί·
- Όταν $q_{1,min} < q < q_{2,max}$, μόνο ένας στρόβιλος σε χρήση, εκείνος που υπόσχεται μεγαλύτερο γινόμενο $\eta_i q_i$·
- Όταν $q_{2,max} < q < q_{1,max}$, μόνο ένας στρόβιλος σε χρήση, εκείνος με το μεγαλύτερο δυναμικό·
- Όταν $q_{1,max} < q < q_{1,max} + q_{2,min}$, σημείο δανεισμού, και οι δυο στρόβιλοι σε χρήση, σύμφωνα με τον πιο αποδοτικό συνδυασμό λειτουργίας, δηλαδή ο μικρότερος στρόβιλος λειτουργεί με τη μέγιστη απόδοση και ο μεγάλος με απόδοση λίγο χαμηλότερη από τη μέγιστη, για μικρό εύρος παροχών·
- Όταν $q_{1,max} + q_{2,min} < q < q_{1,max} + q_{2,max}$, και οι δυο στρόβιλοι σε χρήση, σύμφωνα με τον πιο αποδοτικό συνδυασμό λειτουργίας
- Όταν $q > q_{1,max} + q_{2,max}$, και οι δυο στρόβιλοι λειτουργούν με την μέγιστη απόδοσή τους.

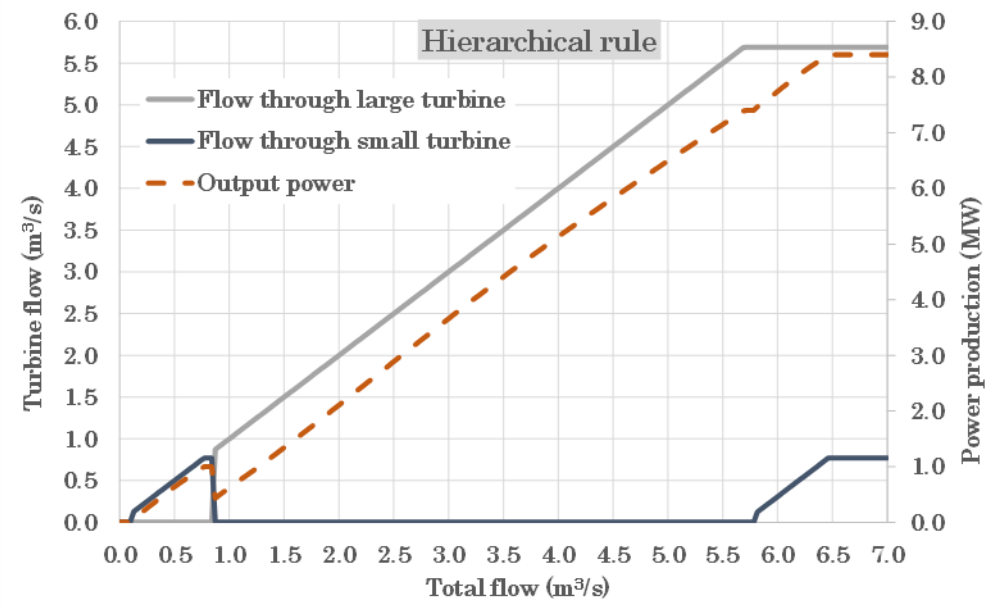

Σχήμα 3 : Διερχόμενη παροχή από το μείγμα στροβίλων, συναρτήσει της εισερχόμενης στο σύστημα και η αντίστοιχη παραγωγή ισχύος, βάσει του Ιεραρχικού κανόνα λειτουργίας.

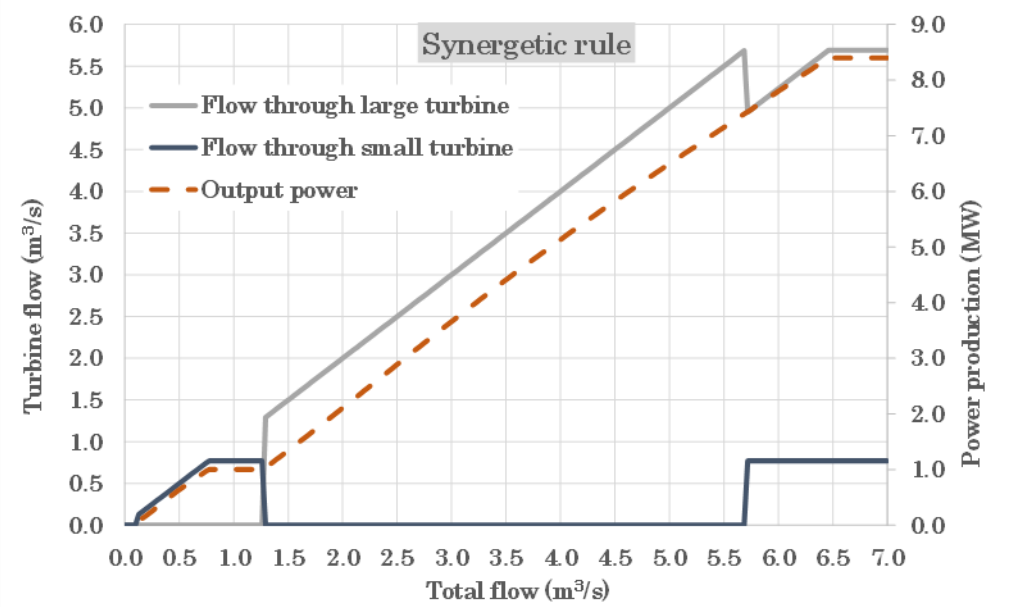

Σχήμα 4 : Διερχόμενη παροχή από το μείγμα στροβίλων, συναρτήσει της εισερχόμενης στο σύστημα και η αντίστοιχη παραγωγή ισχύος, βάσει του Συνεργατικού κανόνα λειτουργίας .

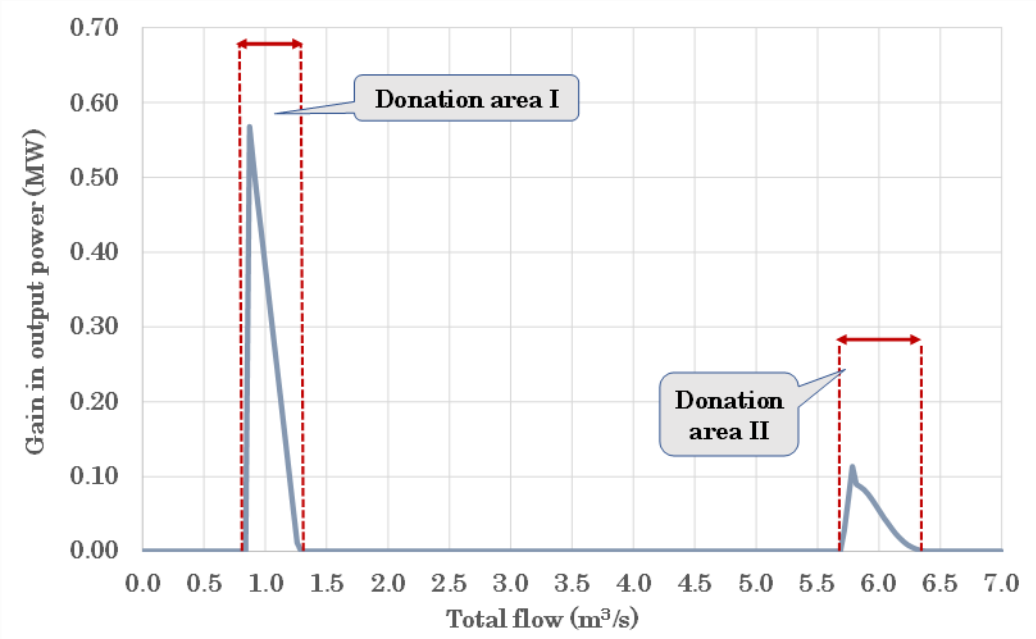

Σχήμα 5 : Το πλεονέκτημα σε όρους παραγωγής ισχύος του Συνεργατικού κανόνα έναντι του Ιεραρχικού διαμορφώνοντας χαρακτηριστικές "Περιοχές Δωρεάς".

Στο **Σχήμα 5** παρουσιάζεται το πλεονέκτημα που κερδίζουμε σε παραγωγή ισχύος με την εφαρμογή του Συνεργατικού κανόνα έναντι του Ιεραρχικού. Δύο χαρακτηριστικές περιοχές, "Περιοχή Δωρεάς Ι" και "Περιοχή Δωρεάς ΙΙ", καθορίζουν τα εύρη των παροχών, όπου ο μεγαλύτερης δυναμικότητας στρόβιλος 'δωρίζει' μία

ποσότητα της δυνατής διερχόμενης παροχής του στον μικρότερο στρόβιλο, καθώς, μέσω αυτής της προσφοράς, το συνολικό γινόμενο $\eta_i(q_i)\, q_i$ του συστήματος αυξάνεται. Η σχέση που περιγράφει τη συνολική παραγωγή ισχύος από τη συμμετοχή κάθε στροβίλου, φαίνεται παρακάτω, (για λόγους απλότητας το καθαρό ύψος πτώσης h_n θεωρείται σταθερό, καθώς η διάμετρος του αγωγού πτώσης έχει επιλεχθεί ικανή σε διαστάσεις, ώστε να είναι αμελητέου βαθμού οι απώλειες κατά μήκους αυτού):

$$p_{tot} = \rho\, g\, h_n \left(\eta_1 \left(\frac{q_1}{q_{1,max}} \right) q_1 + \eta_2 \left(\frac{q_2}{q_{2,max}} \right) q_2 \right)$$

- Η πρώτη περιοχή δωρεάς ξεκινάει όταν η διερχόμενη παροχή από τους στροβίλους ισούται με το ελάχιστο όριο του μεγαλύτερου στροβίλου, $q_{1,min}$ (0.85 m^3/s), όπου όλη η παροχή διέρχεται από τον μικρό στρόβιλο με τη μέγιστη απόδοσή του, καθώς $q_{1,min} > q_{2,max}$ και άρα $\frac{q_2}{q_{2,max}} = 1$ Αντιθέτως, αν, σύμφωνα με τον ιεραρχικό κανόνα, λειτουργούσε ο μεγάλος στρόβιλος, το συνολικό παραγόμενο γινόμενο $\eta_i(q_i)\, q_i$, θα ήταν μικρότερο, καθώς ο βαθμός απόδοσής του για χαμηλές παροχές είναι αρκετά χαμηλός. Το σημείο περάτωσης της πρώτης περιοχής δωρεάς, όπου ο μεγάλος στρόβιλος αποκτά προτεραιότητα, ορίζεται όταν:

$$\eta_1 \left(\frac{q_1}{q_{1,max}} \right) q_1 = \eta_{2,max} q_{2,max}$$

- Η δεύτερη περιοχή δωρεάς ξεκινάει όταν η διερχόμενη παροχή ισούται με $q_{1,max}$(5.69 m^3/s), όπου η διερχόμενη παροχή από τον μεγάλο στρόβιλο μειώνεται κατά $q_{2,max}$ (0.77 m^3/s), με σκοπό να λειτουργεί ο μικρός στρόβιλος με μέγιστο βαθμό απόδοσης, και ο μεγάλος με ελάχιστα χαμηλότερο από τον μέγιστο, δίνοντας πάλι υψηλότερο γινόμενο $\eta_i(q_i)\, q_i$. Η δεύτερη περιοχή εμφανίζεται μέχρι και το σημείο όπου $q = q_{1,max} + q_{2,max}$.

Προκειμένου να εξαγάγουμε συμπεράσματα, ως προς την πραγματική (σύμφωνα με τα υδρολογικά δεδομένα στη θέση του έργου) επιπλέον ισχύ που μπορεί να προσφέρει ο Συνεργατικός κανόνας έναντι του Ιεραρχικού, κατατάσσουμε τις τιμές της παροχής σε φθίνουσα σειρά και αντιστοιχούμε σε κάθε τιμή την πιθανότητα υπέρβασης που της αναλογεί $p_i = (1/n+1)$, όπου n είναι η n-οστή φθίνουσα τιμή. Στη συνέχεια, για κάθε τιμή παροχής υπολογίζεται η αντίστοιχη παραγόμενη ισχύς από κάθε κανόνα και εκφράζεται συναρτήσει της πιθανότητας υπέρβασης, σύμφωνα με τα παρακάτω διαγράμματα:

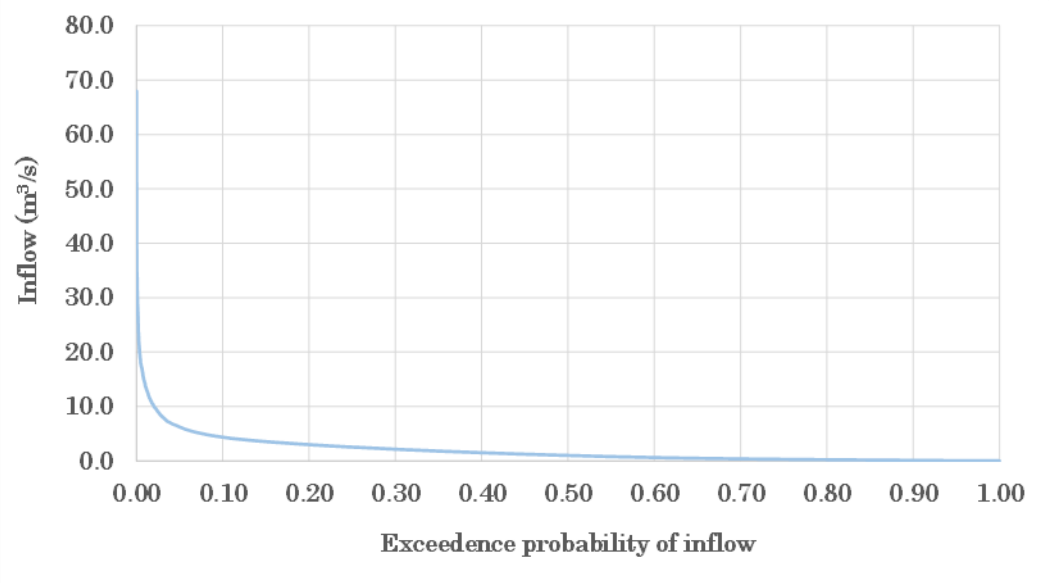

Σχήμα 6 : Καμπύλη διάρκειας παροχής.

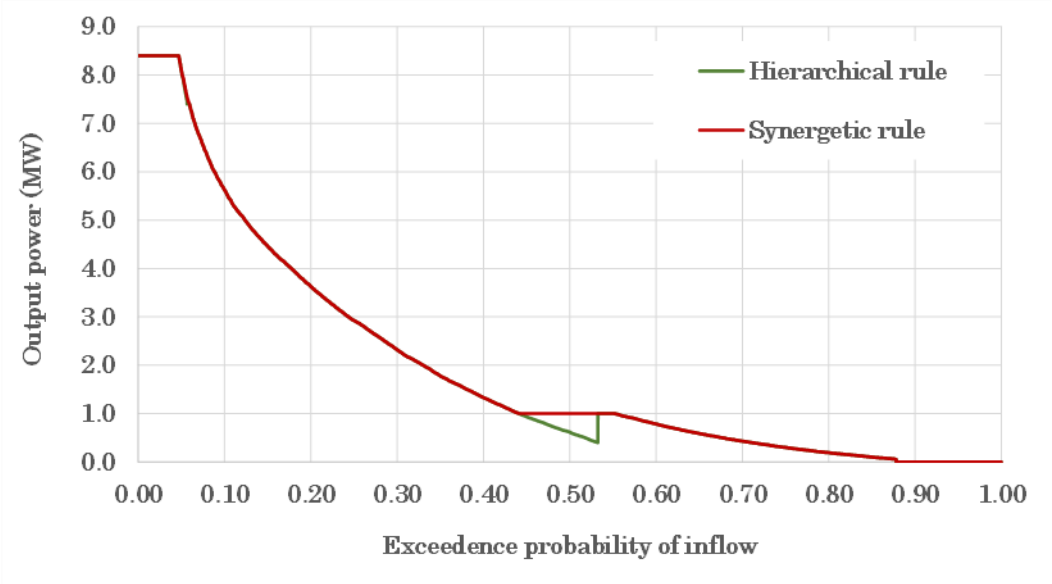

Σχήμα 7 : Προσομοιωμένη παραγωγή ισχύος ως συνάρτηση της εμπειρικής πιθανότητας υπέρβασης παροχής, για τους δύο κανόνες λειτουργίας.

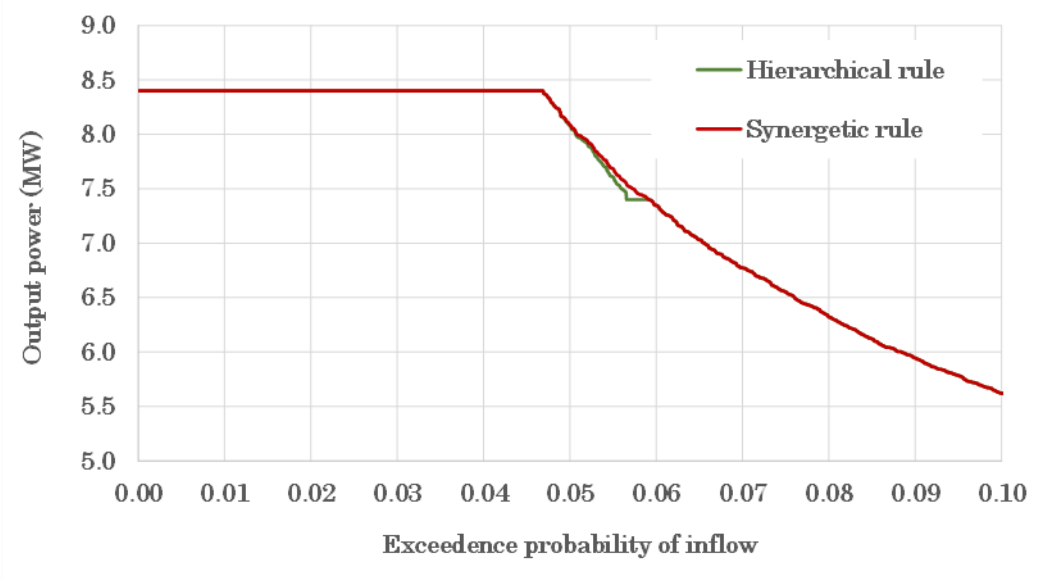

Σχήμα 8 : Λεπτομέρεια του άνω σχήματος, εμβαθύνοντας στην περιοχή δωρεάς ΙΙ.

Όπως φαίνεται στο **Σχήμα 7**, ο Συνεργατικός κανόνας λειτουργίας υπερέχει του Ιεραρχικού, ειδικά στην περιοχή δωρεάς Ι, όπου η διερχόμενη στο σύστημα παροχή είναι μέσης τάξης και η αντίστοιχη πιθανότητα υπέρβασής της είναι 45 με 55%. Αυτό σημαίνει ότι για ένα 10% ποσοστό χρόνου το Συνεργατικό μοντέλο προσφέρει παραπάνω ισχύ σε σχέση με το Ιεραρχικό. Από την άλλη, το όφελος σε ισχύ που παράγεται στην περιοχή δωρεάς ΙΙ είναι αμελητέο (**Σχήμα 8**). Καθένα από τα παραπάνω διαγράμματα αποτελεί αποκλειστική αντιπροσώπευση του επιλεγμένου προβλήματος, με τα δικά του υδρολογικά χαρακτηριστικά, συνεπώς τα παραπάνω συμπεράσματα διαφέρουν ανά περιοχή μελέτης και ανά έργο.

Στη συνέχεια, προκειμένου να διατυπώσουμε σε γενικευμένη μορφή την παραγόμενη ισχύ από την εφαρμογή μείγματος στροβίλων, θεωρούμε ένα υδροηλεκτρικό έργο με χρήση δυο στροβίλων συνολικής ονομαστικής ισχύος $p^*_{max} = 1$, με αξιοποιήσιμο καθαρό ύψος πτώσης $h^*_n = 1$.

Γενικά, το είδος των στροβίλων θεωρείται διαφορετικό, και η καμπύλη απόδοσης $\eta_i = f(q/q_{nom})$ περιγράφεται από διαφορετικές παραμέτρους, $\eta_{i,max}$, θ_i, a_i και b_i για τον κάθε στρόβιλο. Θεωρούμε ότι κάθε στρόβιλος λειτουργεί με μέγιστη διερχόμενη παροχή ίση με την ονομαστική του, άρα εύλογα θέτουμε $q_{nom} = q_{max}$ και $p_{nom} = p_{max}$. Επίσης, ο βαθμός απόδοσης η_i αναφέρεται στην ολικό βαθμό απόδοσης του συστήματος, δεδομένου ότι οι απώλειες στα υπόλοιπα στάδια της εγκατάστασης, μέσω του γινομένου $\eta_{TR}\eta_G\eta_E$ (μετασχηματιστής, γεννήτρια, ηλεκτρικό δίκτυο), είναι σταθερές, και κατά προσέγγιση ίσες με 95%.

Τελευταίο βήμα για την γενίκευση του κανόνα λειτουργίας είναι η εισαγωγή ενός δείκτη διαμερισμού $\varphi \geq 0.50$, ορίζοντας έτσι την ονομαστική ισχύ κάθε στροβίλου ίση με $p^*_{1,max} = \varphi$ και $p^*_{2,max} = 1 - \varphi$. Επιπλέον ορίζονται παρακάτω η διερχόμενη παροχή για κάθε στρόβιλο και του συστήματος συνολικά, ήτοι μέγιστη $(q^*_{i,max}, q^*_{max})$ και ελάχιστη $(q^*_{i,min}, q^*_{min})$, αντίστοιχα.

$$q^*_{i,max} = \frac{p^*_{i,max}}{\rho\ g\ \eta_{i,max} h^*_n}$$

$$q^*_{i,min} = \theta_i \frac{p^*_{i,max}}{\rho\ g\ \eta_{i,max} h^*_n}$$

$$q^*_{max} = \frac{1}{\rho\ g h^*_n}\left(\frac{\varphi}{\eta_{1,max}} + \frac{1-\varphi}{\eta_{2,max}}\right)$$

$$q^*_{min} = \frac{1}{\rho\ g h^*_n} min\left(\frac{\theta_1\ \varphi}{\eta_{1,max}}, \frac{\theta_2(1-\varphi)}{\eta_{2,max}}\right)$$

Θέτοντας $u = q/q_{max}$, εκφράζουμε την αδιαστατοποιημένη παροχή και την αντίστοιχη παραγωγή ισχύος ως:

$$q^* = u\ q^*_{max}$$

$$p^*_i = \rho\ g\ \eta_i(u) q^* h^*_n$$

Έπειτα δοκιμάσαμε τις παραπάνω γενικευμένες φόρμουλες για διάφορους συνδυασμούς του συντελεστή διαμερισμού φ και της παραμέτρου $\theta_i = {}^{q_{i,min}}/_{q_{i,nom}}$ για τους δυο πιο συνήθεις τύπους στροβίλων (Pelton, Francis). Παρακάτω παρουσιάζεται ένας από τους συνδυασμούς που εφαρμόστηκαν, με χαρακτηριστικά στροβίλων όπως φαίνονται στον **Πίνακα 1**.

Τέλος, κάθε συνδυασμός στροβίλων εφαρμόστηκε με σκοπό την αξιολόγηση της απόκλισης του Συνεργατικού από το Ιεραρχικό μοντέλο σε παραγωγή αδιαστατοποιημένης ισχύος $\Delta p_{i,operational} = (p^*_{opt,i} - p^*_{hier,i})$, όπου, $\Delta p_i = (p_{0,i} - p^*_i)$ και $p_{0,i} = \rho\ g\ q^*(\varphi, \theta_i, \eta_{i,max}, a_i, b_i)\ h^*_n$, η παραγόμενη ισχύς από έναν ιδανικό στρόβιλο με βαθμό απόδοσης 100% για όλα τα εύρη παροχών. Ο αντίστοιχος συνδυασμός παρουσιάζεται στο **Σχήμα 10**.

Πίνακας 1: Χαρακτηριστικά του συστήματος στροβίλων συνδυασμού ΙΙ.

Συνδυασμός ΙΙ	Στρόβιλος 1	Στρόβιλος 2
Τύπος στροβίλου	Francis	Francis
Παράμετρος θ_i	0.15	0.15
$\eta_{i,max}$	0.93	0.93
a_i	0.78	0.78
b_i	3.11	3.11

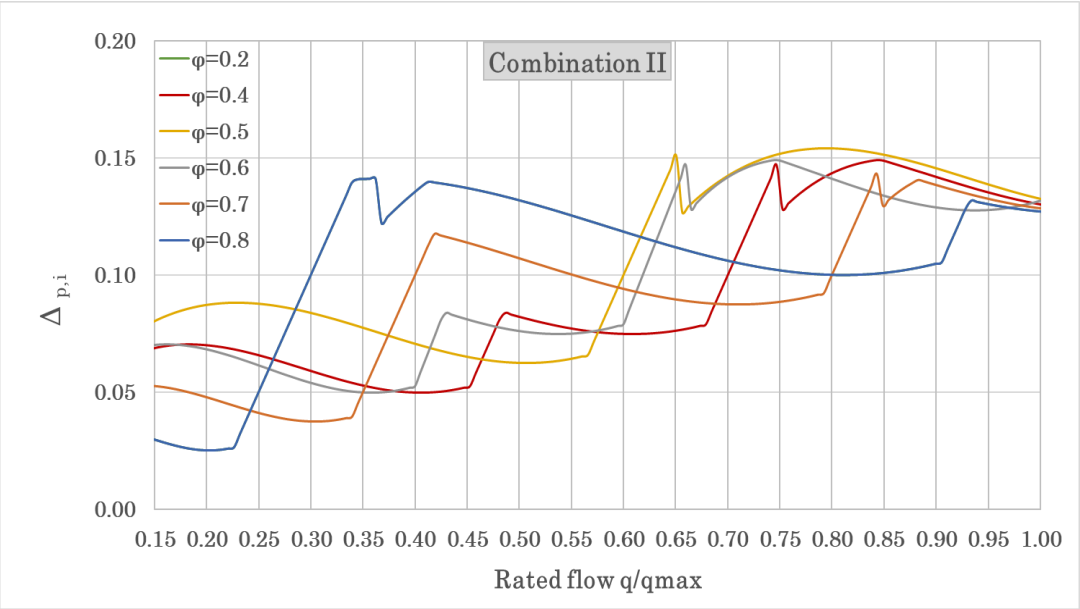

Σχήμα 9 : Διάφορα σενάρια συντελεστή διαμερισμού για δεδομένα συνδυασμού ΙΙ, συγκρίνοντας την απόδοσή τους σε παραγωγή ισχύος συγκριτικά με ένα ιδανικό σύστημα στροβίλων.

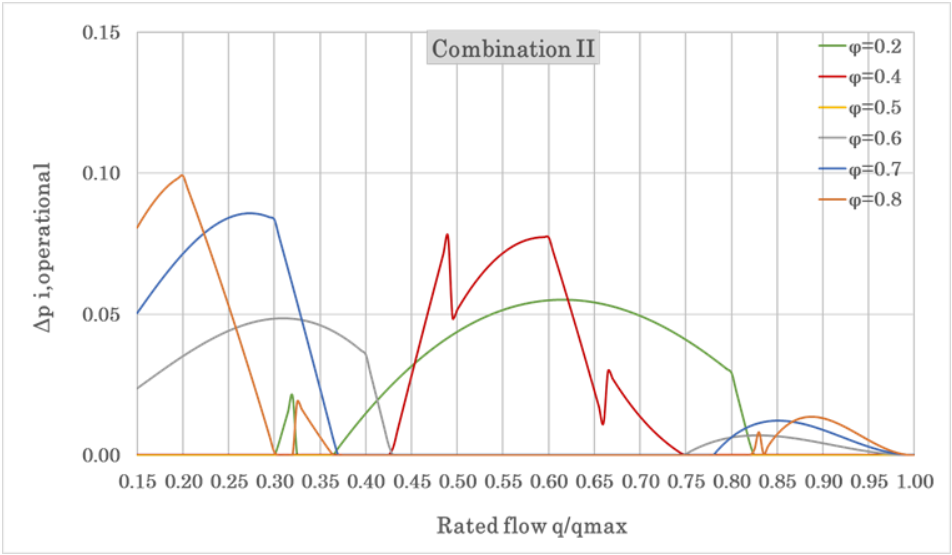

Σχήμα 10 : Διάφορα σενάρια συντελεστή διαμερισμού για δεδομένα συνδυασμού ΙΙ, συγκρίνοντας την απόδοσή τους σε παραγωγή ισχύος βάσει του Συνεργατικού κανόνα συγκριτικά με τον Ιεραρχικό.

Το πρόβλημα πρόγνωσης της ημερήσιας παραγωγής ενέργειας

Επόμενος στόχος της παρούσας διπλωματικής εργασίας είναι η δημιουργία ενός βέλτιστου μεν, εύχρηστου δε, μοντέλου πρόγνωσης της παραγόμενης ενέργειας επόμενης ημέρας από ένα Μικρό Υδροηλεκτρικό Έργο (ΜΥΗΕ). Αιτία της παραπάνω προσέγγισης είναι η μελλοντική ένταξη των ΜΥΗΕ στο χρηματιστήριο ενέργειας, στο πλαίσιο της δημιουργίας ενιαίας αγοράς ηλεκτρικής ενέργειας, όπως ορίζει το νέο θεσμικό πλαίσιο "Target Model". Το προαναφερθέν, σε συνδυασμό με το γεγονός

ότι ελάχιστη είναι η έως τώρα έρευνα γύρω από την πρόβλεψη ενέργειας σε ΜΥΕ, μας προέτρεψαν στην παρακάτω έρευνα.

Στην προσπάθειά μας για εύρεση ενός ικανού μοντέλου πρόβλεψης της ενέργειας, βάσει ιστορικών δεδομένων, καθώς και τεχνολογικής γνώσης, παρήγαμε ποικίλα μοντέλα, με διαφορετικά δεδομένα εισόδου - εξόδου, καθώς και μέτρων απόδοσης, Προκειμένου να βαθμονομήσουμε κάθε μοντέλο πρόγνωσης, καθώς και να συγκρίνουμε την αξιοπιστία τους, εισήχθη το παρακάτω μέτρο απόδοσης,:

$$F = 1 - \frac{\sum_{t=1}^{n}\left(E_{t,\,obs} - E_{t,\,forecast}\right)^2}{\sum_{t=1}^{n}\left(E_{t,obs} - E_{t,\,bencmark}\right)^2}$$

όπου $E_{t,\,obs}$ είναι η παρατηρούμενη ενέργεια την ημέρα t, γνωστή σε μας από την εφαρμογή του κανόνα λειτουργίας στα ιστορικά μας δεδομένα παροχής, $E_{t,\,forecast}$ η προβλεπόμενη τιμή της ενέργειας, εκτιμώμενη βάσει της διαθέσιμης πληροφορίας του παρελθόντος $(x_{t-1}, x_{t-2}, \dots)$, εκφρασμένη από διαφορετικές μεταβλητές ανά μοντέλο πρόβλεψης, και $E_{t,\,bencmark}$ αποτελεί την τιμή πρόβλεψης αναφοράς, βάσει ενός μοντέλου benchmark. Το μέτρο αυτό είναι πολύ πιο αυστηρό, συγκριτικά με τον κλασικό δείκτη αποτελεσματικότητας.

Ακολουθήσαμε δύο οδούς με σκοπό την πρόγνωση της ενέργειας. Η πρώτη δέχεται ως μεταβλητές εισόδου την ενέργεια των δύο προηγούμενων ημερών (E_t, E_{t-1}), την παροχή της προηγούμενης ημέρας (q_t), καθώς και τις βροχοπτώσεις της προηγούμενης ημέρας (p_t) (ως προσεγγιστικό μέτρο της υγρασίας του εδάφους, που συνιστά επιπλέον πληροφορία στο μοντέλο), δίνοντας ως μεταβλητή εξόδου την προβλεπόμενη ενέργεια της επόμενης ημέρας. Για αυτόν τον λόγο το συγκεκριμένο μοντέλο ονομάζεται direct model, και ανάλογα με τον συνδυασμό που επιλέξαμε να ακολουθούν οι μεταβλητές εισόδου, προέκυψαν δύο εκδοχές του, η General (**Σχήμα 11**) και η Crossroad (**Σχήμα 12**), με την τελευταία να είναι πιο αποδοτική.

General direct εκδοχή :

$$E_{t+1} = \begin{cases} 4.79\,(E_t)^{0.48}\,(q_t)^{0.06}(E_{t-1})^{0.12}(p_t)^{0.15}, & p_t > 0.1\ mm \\ E_t, & p_t \le 0.1\ mm \end{cases}$$

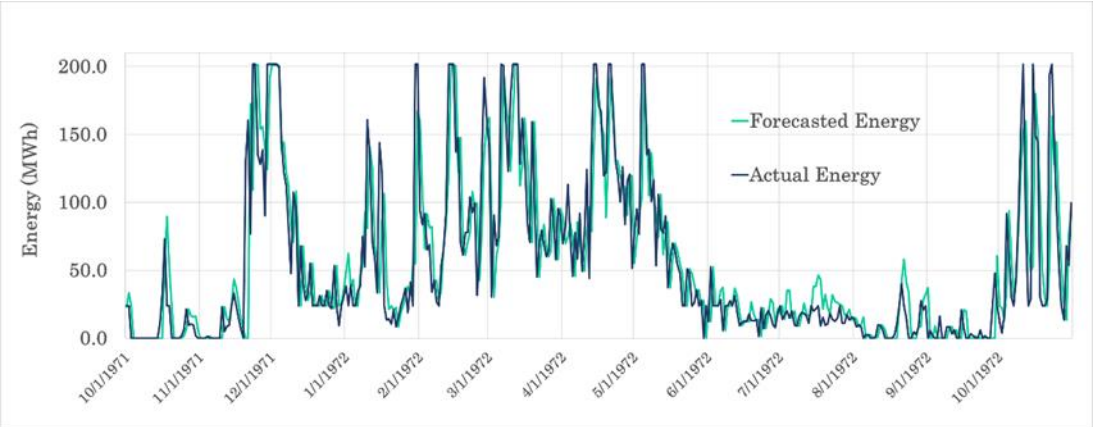

Σχήμα 11 : Χρονοσειρά ενέργειας πρόγνωσης και πραγματικής, σύμφωνα με το μοντέλο General direct, για το υδρολογικό έτος 1971-72.

Crossroad direct εκδοχή :

$$E_{t+1} = \begin{cases} 3.88\ (E_t)^{0.54}(E_{t-1})^{0.12}(p_t)^{0.16}, p_t > 0.1\ mm \\ 1.51\ (E_t)^{0.63}(E_{t-1})^{0.25}, \quad p_t \leq 0.1\ mm \end{cases}$$

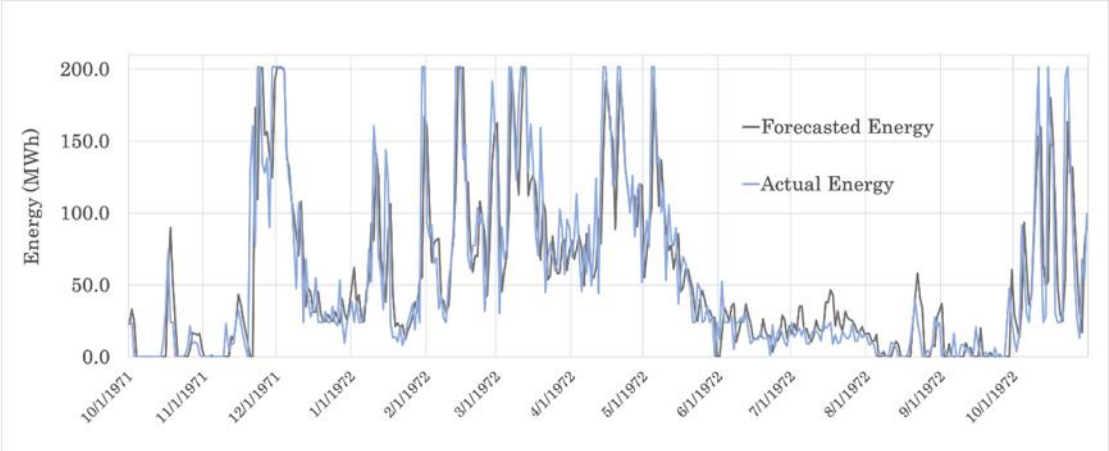

Σχήμα 12 : Χρονοσειρά ενέργειας πρόγνωσης και πραγματικής, σύμφωνα με το μοντέλο Crossroad direct, για το υδρολογικό έτος 1971-72.

Η δεύτερη οδός που ακολουθήσαμε είναι η indirect, καθώς η πρόβλεψη σε αυτήν την περίπτωση αναφέρεται στο μέγεθος της παροχής της επόμενης ημέρας, η οποία στη συνέχεια αξιοποιείται μέσω του κανόνα λειτουργίας για την εξαγωγή της αντίστοιχης ενέργειας επόμενης ημέρας. Πάλι και σε αυτήν την προσέγγιση παρήγαμε δυο διαφορετικές εκδοχές της, την Simple (**Σχήμα 13**) και την Smart (**Σχήμα 14**). Η διαφορά τους έγκειται στο γεγονός ότι η δεύτερη λαμβάνει υπόψιν τα λειτουργικά χαρακτηριστικά των στροβίλων και τη γνώση γύρω από την λειτουργία τους, καθώς στον υπολογισμό του σφάλματος αδιαφορεί όταν η προβλεπόμενη τιμή είναι μεγαλύτερη από $q_{max,tot}$ και μικρότερη από $q_{min,tot}$, εφόσον ταυτόχρονα και η πραγματική τιμή παροχής ικανοποιεί τις αντίστοιχες συνθήκες. Δεν έχει αξία λοιπόν να λαμβάνουμε σφάλμα, όταν $q_{forecast} < q_{min,tot}$ και $q_{forecast} > q_{max,tot}$, αντίστοιχα. Και στις δύο εκδοχές, ως δεδομένα εισόδου χρησιμοποιήσαμε την τιμή

της παροχής προηγούμενης ημέρας (q_t), τη μέση παροχή του μήνα, που υπολογίζουμε την προβλεπόμενη, την ελάχιστη παροχή των πέντε τελευταίων ημερών, καθώς και τη βροχή της προηγούμενης ημέρας. Όλες οι παραπάνω μεταβλητές έχουν ως στόχο να ποσοτικοποιήσουν, μέσω της βαθμονόμησης, τη συσχέτιση της παροχής της επόμενης ημέρας με το υδρολογικό καθεστώς του μήνα αλλά και την αποθηκευμένη κατάσταση εδαφικής υγρασίας.

Simple, Smart Indirect εκδοχή :

$$q_{t+1} = \begin{cases} a_1\,(q_{min5}) + \beta_1(q_t) + \gamma_1(q_{meant}), & p_t < 0.1\ mm \\ a_2\,(q_{min5}) + \beta_2(q_t) + \gamma_2(q_{meant}) + \delta(p_t),\ p_t \geq 0.1\ mm \end{cases}$$

Smart εκδοχή, ορισμός σφάλματος :

$$e = \begin{cases} q_{max,tot} - q_{forecast}, & q_{obs} > q_{max,tot}\ and\ q_{forecast} < q_{max,tot} \\ q_{forecast} - q_{min,tot}, & q_{obs} < q_{min,tot}\ and\ q_{forecast} > q_{min,tot} \\ q_{obs} - q_{forecast}, & q_{obs} > q_{min,tot}\ and\ q_{obs} < q_{max,tot} \end{cases}$$

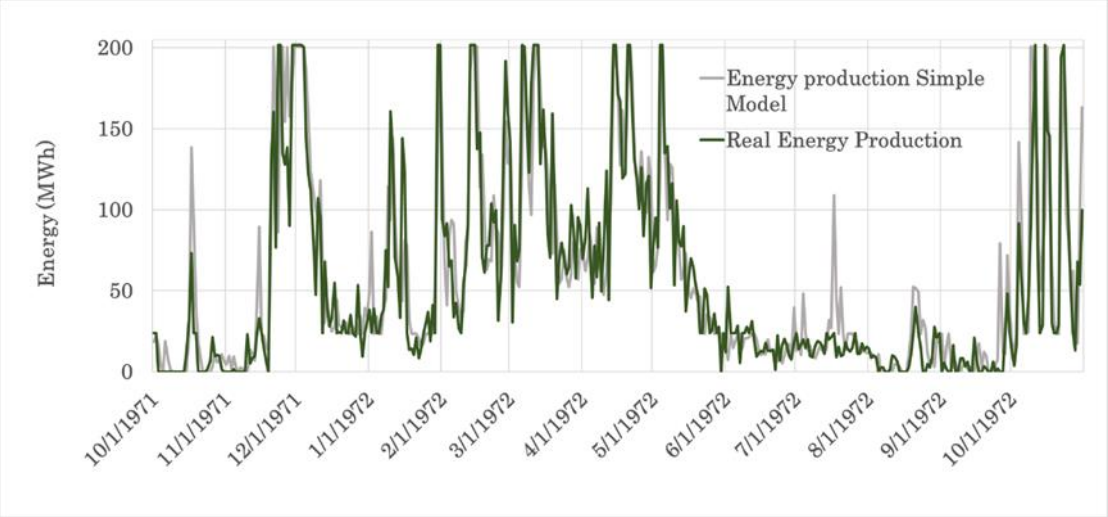

Σχήμα 13 : Χρονοσειρά ενέργειας από μοντέλο πρόγνωσης παροχής Simple indirect και της πραγματικής, για το υδρολογικό έτος 1971-72.

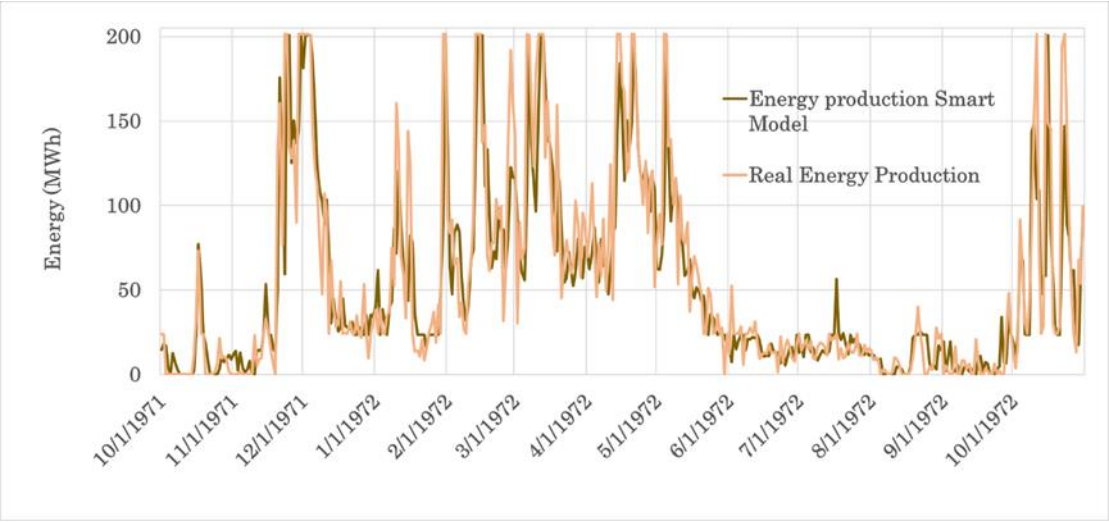

Σχήμα 14 : Χρονοσειρά ενέργειας από μοντέλο πρόγνωσης παροχής Smart indirect και της πραγματικής, για το υδρολογικό έτος 1971-72.

Θέλοντας να δοκιμάσουμε την απόκριση ενός αρκετά πιο προηγμένου τύπου πρόγνωσης αλλά και να συγκρίνουμε την απόδοσή του, σε σχέση με το καλύτερο έως τώρα μοντέλο μας (Smart model), εφαρμόσαμε ένα μοντέλο μηχανικής μάθησης (Machine Learning), με ονομασία Deep Feedforward Neural Network (DNN), το οποίο όμως δεν λαμβάνει υπόψιν του την τεχνική πληροφορία. Το DNN μοντέλο αποτελείται από τρία κρυφά επίπεδα 128, 64 και 32 νευρώνες, αντίστοιχα, με την Rectified Linear Unit (ReLu) να αποτελεί την συνάρτηση ενεργοποίησης για κάθε έναν από αυτούς.

Ως δεδομένα εισόδου χρησιμοποιήσαμε την παροχή των τελευταίων 5 ημερών και την βροχή των προηγούμενων 2 ημερών (πληροφορία υγρασίας εδάφους). Από τα επόμενα σχήματα γίνεται εμφανές ότι ενώ το DNN καταφέρνει να προσεγγίσει πιο αποδοτικά από το Smart Model την παροχή (R^2 = 0.82 και 0.63, αντίστοιχα) (**Σχήμα 15**), ενώ στην πρόγνωση της ενέργειας παρουσιάζει σαφώς χειρότερη απόδοση (R^2 = 0.55 και 0.83, αντίστοιχα) (**Σχήμα 16**).

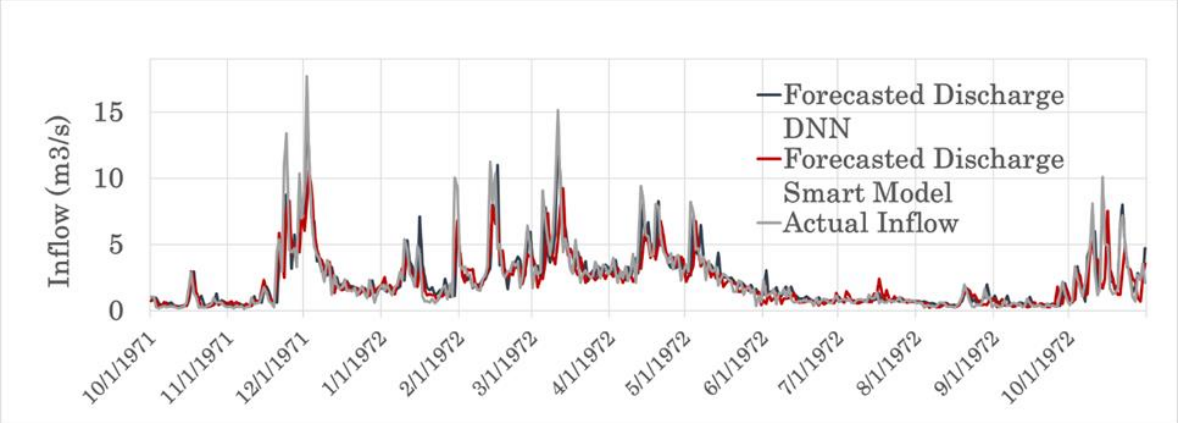

Σχήμα 15 : Χρονοσειρά παροχής πρόγνωσης και πραγματικής, σύμφωνα με το μοντέλο DNN, για το υδρολογικό έτος 1971-72.

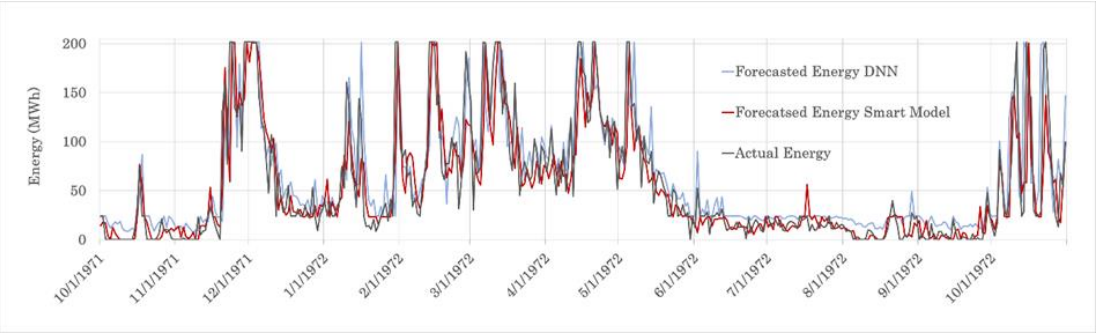

Σχήμα 16 : Χρονοσειρά ενέργειας από μοντέλο πρόγνωσης παροχής DNN και της πραγματικής, για το υδρολογικό έτος 1971-72.

Η έννοια της αβεβαιότητας στην πρόγνωση της ημερήσιας παραγωγής ενέργειας

Το πιο αποδοτικό μοντέλο πρόγνωσης της ενέργειας (Smart Model) θεωρήθηκε και το πιο αντιπροσωπευτικό. Επιθυμώντας να εισαγάγουμε τον παράγοντα της αβεβαιότητας στην πρόγνωσή μας, δημιουργήσαμε ένα πλήθος συνθετικών τιμών του σφάλματος $w_t = E_{t,obs} - E_{t,for}$ που ακολουθεί Γάμα Κατανομή, εφόσον τα στατιστικά χαρακτηριστικά του σφάλματος έδωσαν σημαντική ασυμμετρία και αμελητέο συντελεστή αυτοσυσχέτισης (συντελεστής ασυμμετρίας = 1.23, αυτοσυσχέτισης = 0.066). Στη συνέχεια χρησιμοποιήσαμε τη συνθετική χρονοσειρά του σφάλματος στη δημιουργία συνθετικών χρονοσειρών παραγόμενης ενέργειας, εξάγοντας εν τέλει τις τρεις πιο σημαντικές σε ενεργειακή πληροφορία, όσον αφορά την αξιοποίησή τους στην αγορά ενέργειας, από τον χρήστη το έργου.

Αυτές οι τρείς είναι τα 0.10, 0.50 και 0.90 ποσοστημόρια (quantiles), που αντιπροσωπεύουν αντίστοιχα σενάριο ριψοκίνδυνο, ασφαλές και συντηρητικό (**Σχήμα 19**). Η προσέγγιση της ποσοτικοποίησης της αβεβαιότητας, καθώς και η ενσωμάτωσή της στο μοντέλο πρόβλεψης της ενέργειας, πραγματοποιήθηκε για δύο διαφορετικές προσεγγίσεις στην αναπαράσταση της δομής του σφάλματος. Στην πρώτη, το σφάλμα μοντελοποιείται ως στάσιμη διεργασία, θεωρώντας ότι το δείγμα έχει κοινά στατιστικά χαρακτηριστικά, ανεξαρτήτως εποχών. Ωστόσο, μια σημαντική παρατήρηση μας οδήγησε στην εξαγωγή αντίστοιχων συνθετικών χρονοσειρών για μία πιο σύνθετη διαδικασία, την κυκλοστάσιμη, η οποία προβλέπει διαφορετικά στατιστικά χαρακτηριστικά ανά μήνα. Η παρατήρηση που οδήγησε στην δημιουργία της τελευταίας και ορθότερης προσέγγισης είναι ότι κατά την πρώτη παρατηρήθηκε μεγάλο εύρος αβεβαιότητας κατά τους ξηρούς μήνες, το οποίο δεν συμβαδίζει με του χαμηλού ύψους απορροών που τους αντιστοιχούν (**Σχήμα 17,18**).

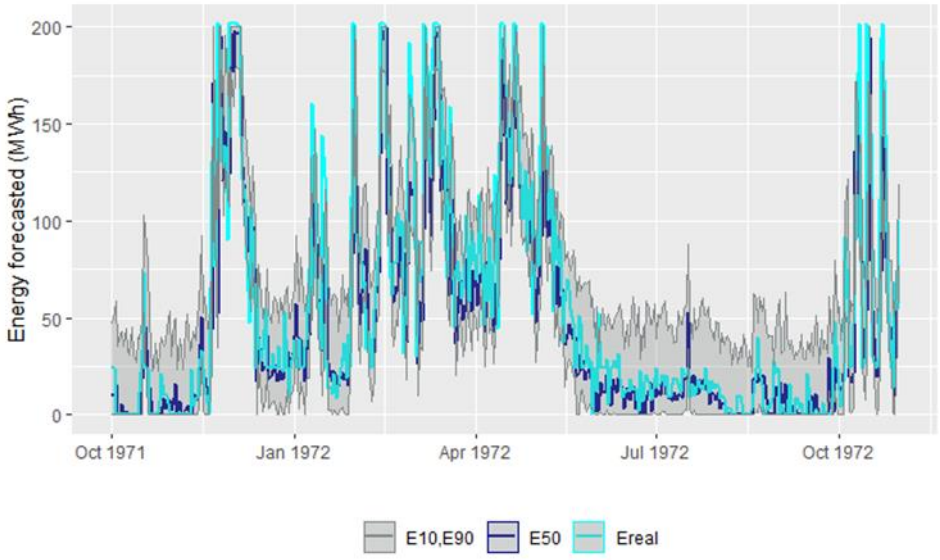

Σχήμα 17 : Χρονοσειρά ενέργειας πρόγνωσης με αβεβαιότητα των 0.1, 0.5 και 0.9 quantiles, συγκριτικά με την πραγματική, για το υδρολογικό έτος 1971-72, (στάσιμο σφάλμα).

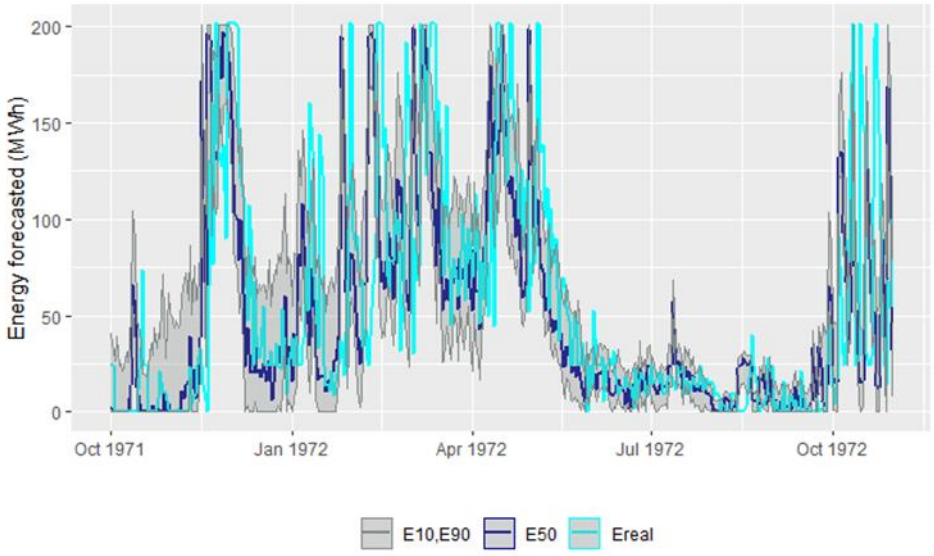

Σχήμα 18 : Χρονοσειρά ενέργειας πρόγνωσης με αβεβαιότητα των 0.1, 0.5 και 0.9 quantiles, συγκριτικά με την πραγματική, για το υδρολογικό έτος 1971-72, (κυκλοστάσιμο σφάλμα).

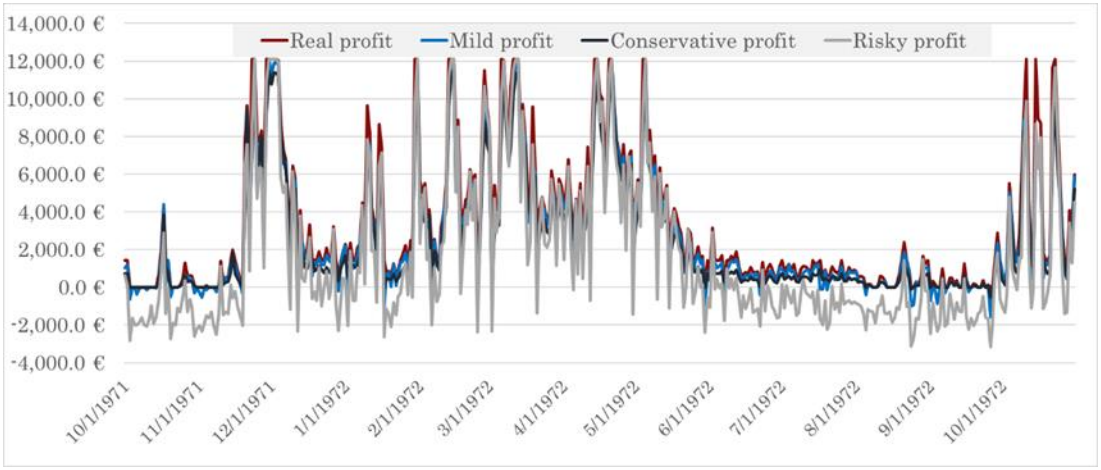

Σχήμα 19 : Χρονοσειρά οφέλους ανάλογα με την πολιτική πώλησης ενέργειας, για το υδρολογικό έτος 1971-72.

Αποτελέσματα έρευνας και μελλοντικοί στόχοι

Μέσω της παρούσας διπλωματικής εργασίας επιτυγχάνουμε να προτείνουμε στον λειτουργό του ΜΥΗΕ δύο χρήσιμα εργαλεία για τη βέλτιστη εκμετάλλευση της εγκατάστασής του. Το πρώτο εργαλείο είναι ο βελτιωμένος αλγόριθμος προγραμματισμού της λειτουργίας μείγματος στροβίλων, ικανός να υποσχεθεί μέγιστη δυνατή παραγωγή ενέργειας. Δεύτερο εργαλείο αποτελεί το μαθηματικό μοντέλο πρόγνωσης της ενέργειας επόμενης ημέρας, βασιζόμενο σε μια εύχρηστη και αξιόπιστη μεθοδολογία.

Μελλοντικοί στόχοι επέκτασης της παρούσας έρευνας συμπεριλαμβάνουν την εφαρμογή του βέλτιστου συνεργατικού κανόνα λειτουργίας στροβίλων σε διαφορετικά υδρολογικά καθεστώτα, με σκοπό την αξιολόγηση της απόδοσής του, σε σχέση με τον ιεραρχικό. Όσον αφορά το πρόβλημα πρόγνωσης ενέργειας επόμενης ημέρας, υπάρχει πληθώρα προς αξιοποίηση μοντέλων, βασιζόμενων σε εργαλεία καιρικών προγνώσεων, καθώς και εξελιγμένων μεθόδων τεχνητής νοημοσύνης. Εκμεταλλευόμενοι τα παραπάνω, σκοπεύουμε να βελτιώσουμε τη στοχική έκφραση του μοντέλου DNN ορίζοντας το RMSE, όμοια με του βέλτιστου μοντέλου (Smart model). Συνεπώς, στοχεύουμε στη δημιουργία ενός ακόμα καλύτερου μοντέλου πρόγνωσης, έχοντας πάντα ως γνώμονα να μην απαιτεί από τον λειτουργό εφαρμογή εξειδικευμένων γνώσεων ή και χρήση τεχνικών εργαλείων, δύσκολων στην επίβλεψη και επεξεργασία.

1 Introduction

1.1 Motivation

The humanity has been consuming, as main sources for power, oil and coal, and since there is a limit in their use, a need for alternative energy sources has been created. Those are known to us as renewable sources and no matter their peculiarities and additional challenges that these forms of energy production pose, nowadays, humanity relies on them.

When we deal with energy production by renewable sources such as Hydropower, Wind, Solar, Geothermal, on the one hand we develop and take advantage of far cleaner forms of energy, thus preserving our ecosystem's balance, but on the other hand it does not nullify the fact that the associated investments are generally more expensive, comparing to oil, coal, natural gas and nuclear energy. Nevertheless, the key challenge that defines renewable energy is the issue of unpredictability, which is even more amplified due to the lack of means for energy storage.

Short-term scheduling of energy production is a of high importance for power systems of all forms and scales. This task becomes even more crucial for the renewable sources, which are governed by stochastic drivers, namely weather-related processes (e.g., wind velocity, solar radiation, streamflow). The dependence between renewable energy production and weather prediction make it particularly difficult to ensure a credible power supply scheduling.

The topic of our thesis is a specific type of hydroelectricity, which are referred to as Small Hydropower Plants (SHPPs). Among several configurations of such systems, we investigate the most typical case, which are either in-stream or run-of-river plants of negligible storage capacity. In particular, we revisit two different aspects regarding the everyday management of SHPPs, namely the optimal co-operation of their turbines, and the problem of next day energy forecasting. In this respect, our research objective is twofold. The first is the determination of generic operational rules across different turbine mixing schemes, while the second focuses on minimizing the uncertainty which accompanies SHPPs, by seeking for credible forecasting approaches for day-ahead energy scheduling, in terms of a credible forecasting model with minimal data requirements and little complexity.

1.2 Research objectives

The main objectives, and at the same time novelties, of our research our summarized as follows:

- improving a recently introduced analytical formula to approximate the full range of commercial efficiency curves;

- recognizing the shortcomings of the classical "hierarchical" operational rule, which is typically applied in SHPP simulations;
- providing generic formulas for establishing a more effective operational rule, in order to be applied in a wide range of turbine characteristics;
- approaching the problem of energy production forecasting from two different point-of-views, direct prediction of energy through past values of energy and indirect prediction of energy through discharge forecasting models;
- quantifying uncertainties on forecasting error;
- proposing an uncertainty-aware framework to take advantage of uncertain forecasts in the context of energy market policies;

1.3 Thesis outline

This thesis has been composed through ten chapters.

The **first chapter** is an introduction to our motivation for the following research and the objectives which we will be focusing on and dealing with through it.

The **second chapter** summarizes the importance of Hydropower through the years till our days and presents as well the various facilities we can construct in order to benefit from this form of renewable energy. Also, it includes the essential mathematical formulas to be used in next calculations.

The **third chapter** presents the various types of turbines, their technical and operational characteristics along with some of their most important charts. Also, we present an analytical configuration of turbine efficiency curves, as an extension of the work by Sakki (2020) and Sakki et al. (2021).

The **fourth chapter** presents the calculations and methodologies which take place in order to create a new operational rule which can ensure higher energy production comparing to the hierarchical one.

The **fifth chapter** revises to the new legal framework, named as "Target Model", and the various regulations behind it. In addition, it summarized the research progress so far on the topic of day-ahead energy forecasting in SHPPs.

The **sixth chapter** describes the study area and the hydrological information which we collect and process, along with the technical characteristics of our run-of-river system.

The **seventh chapter** presents the different approaches of forecasting models and their results through various diagrams and tables.

The **eighth chapter** draws the attention on the modelling procedure in order to include the issue of uncertainty in our forecasting model.

The **ninth chapter** illustrates the computational implementation of the algorithms that were built in the R environment,.

The **tenth chapter** summarizes the conclusions from our research and the future perspectives to accompany its progress.

2 Hydropower as an essential renewable source

2.1 Historical background

Since the dawn of civilization, humans have come to the realization of hydropower's importance. The wide use of watermills in ancient times for grinding wheat into flour for more than 2000 years ago by the Greeks, of Archimedes' screw pump as irrigation machine by the Egyptians and hushing, also known as hydraulic mining, by the Romans are some examples of what impact water had in our lives and society's evolution since the beginning of times.

The very first progress in the field of modern hydropower turbine was marked in the mid-1700s by the French hydraulic and military engineer, Bernard Forest de Belidor and his innovative book 'Architecture Hydraulique'.

In the 19th century, the improvement of technological knowledge accompanied by the work of French engineer Benoit Fourneyron, led to the replacement of the open water mill to an enclosed turbine, as known to us today. It was James B. Francis, a British-American engineer, the one who managed to improve the turbine's operational efficiency up to 90%, in 1848 , through his research in the optimization of turbine design, by means of applied scientific principles and testing methods. Another breakthrough in the field of hydraulic turbines, was established by Lester Allan Pelton, an American inventor, in 1870, after developing the high efficiency Pelton wheel impulse turbine, which used hydropower from the high streams characteristic of the Sierra Nevada, a mountain range in California.

More details about the operation of the above mention turbines and others which have been later invented, are presented in **Chapter** 3.

2.2 Hydropower nowadays

2.2.1 Overview

One of the most efficient sources of renewable energy is Hydropower. To be more specific, the ability of storing huge quantities of water downstream of a advantageous mountain basin by the creation of dams or by extracting a part of the natural river flow, through a diversion structure (**Figure 2.1**), proves how flexible and wide applied this element of nature can be in order to produce energy. Not only the various establishments of hydropower but also the water's natural properties, like density, affect its performance.

Each hydropower facility is driven by the kinetic energy and pressure of flowing water as it streams through the penstock. This energy is a transformation of the water's gravity energy, which is ensured either with dams (creating a high water level through storage) or by taking advantage the favorable relief in mountainous regions (Small Hydropower Plants). Hydropower plants include turbines and generators, that are activated by the hydrodynamic energy and convert it into electricity, which is then delivered to electrical grid in order to provide households, industries and urban facilities with power.

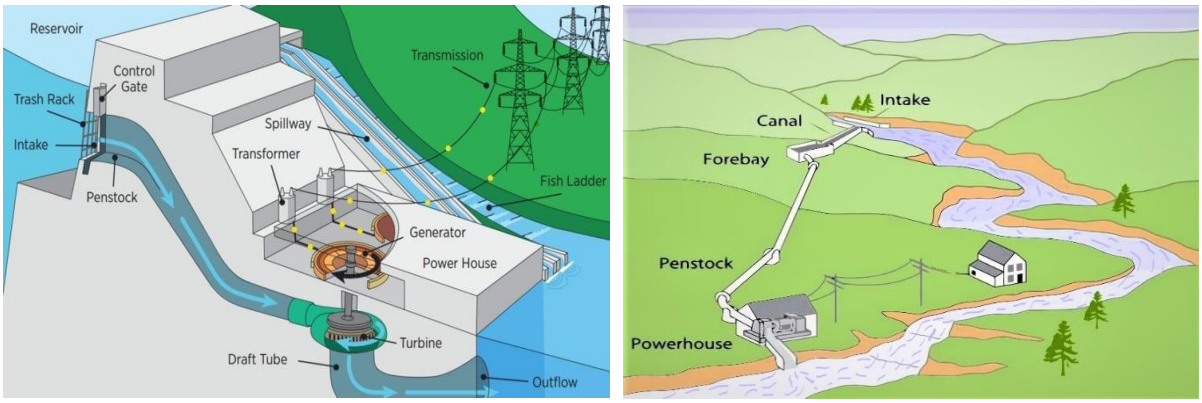

Figure 2.1: Sketch of a hydropower plant which storages water due to a dam and also provides safety measures in case of flood incidents (left), and a Small Hydropower Plant (run-off-river type), which is benefits from the facility's geographical relief (right).

2.2.2 Classification of hydropower plants

As it is implied from the previous paragraph, there are different type of hydropower facilities by which we can take advantage of water's power to produce electricity.

a. Impoundment facilities are the most common type of hydropower plant. As main characteristics we should point out the use of dams in order to store the water, that flows from upstream of the basin from different torrents, in a reservoir. Also as an important difference comparing with the Small Hydropower Plants is that impoundment plants are bigger facilities thus more expensive. Moreover, since the outflow is manageable and can be controlled depending the demand and the scheduling of the producer, impoundment plants can produce predictable amount of energy. Last but not least, those type of facilities, can also play the role of flood control safety plant, water supply and/or for irrigation needs.

b. Small Hydropower Plants (SHPPs) which are plants of up to a certain power capacity limit, which is specified from national standards, e.g., 15 MW, 30 MW and 50 MW, according to Greek, South America /USA, Canada/China and New Zealand legislation law, respectively. Diversion facilities, also known as run-off-river plants, are the most common type of SHPPs. These have negligible water storage and utilize the streamflow as it arrives by extracting a part of the river's inflow by leading it through a channel and then taking advantage of the height difference, due to rough terrain, passing the flow through a penstock and the to the turbines system for energy production. As a result, they have limited requirements from the investment's perspective, but their most important shortcoming is the lack of storage capacity, thus the unpredictable quantity of water passing through the turbine systems and produced energy. In order to face the above obstacle, day-ahead energy forecasting methods should be established to minimize the uncertain power production from SHPPs'. Except from run-off-river type, SHPPs can also be settled downstream of large dams in order to take advantage of the environmental flow, which is released from an independent intake, such as bottom outlet. Another type of SHPP's is the in-stream, which utilize the streamflow to produce energy, by installing a low-head dam across large rivers (and, occasionally, channels).

2.3 Governing equations

The governing equation for electric power production via transformation of the dynamic and kinetic energy of water is

$$P = \eta(q)\, \rho\, g\, q\, h_n(q) \tag{2.1}$$

where ρ is the water density with a typical value for clean water of 1000 kg/m^3; g is the gravity acceleration with a typical value of 9.81 m/s^2; q is the discharge; h_n is the net or effective head, i.e. the dynamic energy, expressed as elevation difference, after subtracting the hydraulic losses across the water transfer to the turbine, which depend on q; and η is the total efficiency of the electromechanical system, that changes with q. The issue of efficiency is been emphasized more in **Chapter** 3. The Both h_n and q may vary in time, and therefore so does P. By applying the SI units for q (m^3/s) and h_n (m), the power P is expressed in Joules per second (J/s) or Watts (W).

The energy produced or consumed during a time interval $[t_1,\ t_2]$ is the integral of P, i.e.

$$E = \int_{t_1}^{t_2} P(t)dt \tag{2.2}$$

After simplifications, we get the following formula, expressing the average energy produced over a specific time interval

$$E = \rho\, g\, V\overline{H}_n\bar{\eta} \tag{2.3}$$

where V is the water volume of that passes through the turbines during the time interval $[t_1,\ t_2]$ and $\overline{H}_\mathrm{n}$ and $\bar{\eta}$ are the net head and efficiency during this period, respectively, averaged over time.

3 Hydro-turbines: technology and operation

3.1 Key principles of hydro-turbine operation

By turbine system is implied a rotary mechanical structure that transforms hydraulic energy (kinetic energy and pressure of water) to rotational kinetic energy by which an electro-magnetic field is been activated (of low-voltage) through an inductor inside the generator unit.

The turbines and associated electromechanical equipment are hosted in the power station.

In the case of impoundment systems (i.e., hydroelectric reservoirs and dams), there are several options for location of the power station. Specifically:

- power stations installed close to the dam;
- power stations installed at a significant distance downstream of the dam;
- power stations installed at an adjacent river basin (inter-basin water transfer).

The typical case is the first, thus involving a penstock of relatively small length, in order to minimize the friction losses and the environmental impacts. Yet, there are cases where it is more advantageous to construct the power plant at a downstream location in order to increase the available head. Apparently, such a layout is economically efficient only when the river slope is large, so that the gains from elevation difference exceed the hydraulic losses due to the water being transferred at a long distance. An important issue to account for is the environmental impacts, since the water does not return to the river just downstream of the dam, as happens in typical configurations where the power station is located close to the foot of the dam.

Another case is the installation of the power station in a neighboring basin, where the water is transferred through a pipeline connecting the two basins. This layout is preferred when there is a significant elevation difference between the upstream catchment, in which the water is gathered, to the one downstream, where the power station is installed. Typically, in large-scale inter basin systems Pelton type turbines are used, as this option becomes economically efficient when the head is large enough. However, if the transfer is implemented for other reasons (e.g. if the principal objective is the transfer of water per se), then the head may be small.

3.1.1 Turbine types

The turbines used in hydroelectric plants are classified into two categories, according to their reaction degree(re), which is defined as the ratio of the static pressure drop in the rotor to the static pressure drop in the stage :

i. **impulse turbines**, re=0, (e.g. Pelton, Cross-flow, Turgo), with partial flow impact and activation of only a specific area of the runner each time, take

advantage of the kinetic energy of water falling from a large elevation (outflow to the atmosphere); the flow velocity is substantially amplified by passing water through a nozzle;

ii. **reaction turbines**, re=1, (e.g. Francis, Kaplan, Deriaz, Bulb), with total flow impact, operate under pressure, as the chamber of the runner remains completely filled by water;

In the following paragraphs are presented the main mechanical characteristics of each turbine type:

The design of Pelton's turbine, which was first introduced by the American engineer Lester Allan Pelton in 1889, lays on the philosophy of the traditional overshot water wheel. Since 1767, it was well known that in order to have the maximum efficiency in power production, the water should enter the wheel with high momentum and exit with negligible velocity.

Taking this principal as a guideline, a Pelton wheel extracts high-speed jets of water, that emerge through the injectors (their number can vary from one to six) at atmospheric pressure, that hit the center of the bucket where the water jet is divided into two streams. The two separate streams then flow along the inner curve of the bucket and leave in the opposite direction that it came in. Water leaving those wheels typically still had high speed, carrying away much of the dynamic energy brought to the wheels. Pelton's paddle geometry was designed so that when the rim ran at half the speed of the water jet, the water left the wheel with very little speed; thus, his design extracted almost all of the water's impulse energy—which made for a very efficient turbine.

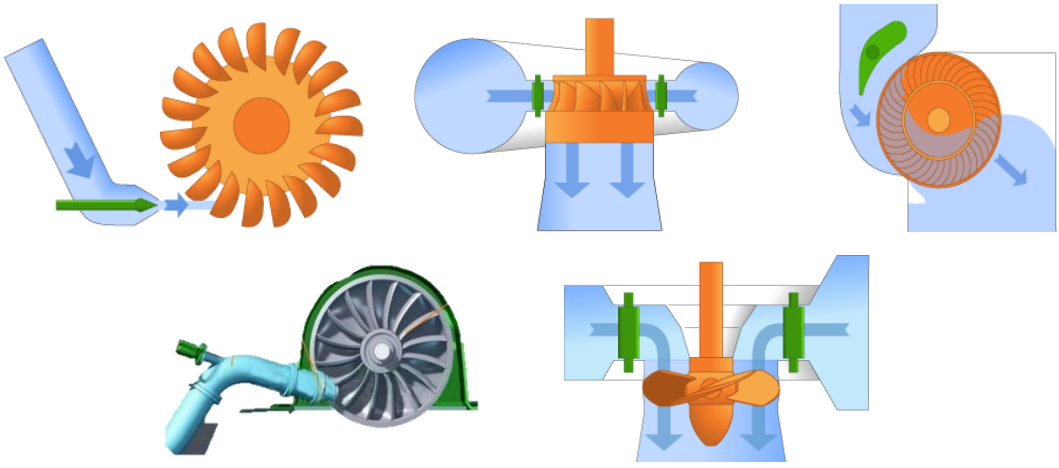

Figure 3.1: Various types of hydraulic turbines; from left to right: Pelton, Francis, Cross-Flow, Turgo, Kaplan.

Up until 1960, Pelton wheels were designed only with horizontal axis of operation with one or two maximum injectors, but after realizing how more efficient the turbine system can be if the jets of water extract from more injectors (without affecting each other in a negative way), Pelton wheels with vertical operation and the ability to combine up to six injectors, have been manufactured.

Francis turbines were the first hydraulic turbines that had a radial inflow, designed by American scientist James Francis around 1920. High pressure water enters these turbines radially meaning that it enters the turbine perpendicular to the rotational axis. This lowers the pressure as the water curls through the tube, but the speed of the water is maintained. Once the water has flown through the turbine, it exits axially - parallel to the rotational axis out of a draft tube to the tail race. This tube reduces the exit velocity of the water to obtain the maximum amount of energy from the input water. The water deflected through the runner blades results in a force that pushes the blades in the opposite direction as the water is deflected. This reaction force (like Newton's third law) is what causes power to be transferred from the water to the turbine's shaft, maintaining rotation. Because the turbine moves as a result of this reaction force, Francis turbines are known as reaction turbines. The change of direction of the water flow also results in a decrease in pressure within the turbine itself. They work equally well when positioned horizontally as they do when they are oriented vertically.

In cross-flow turbines the water passes through the turbine twice: on the upper part of the runner when inserting the turbine and on the lower part after, before leaving the system. Passing through the runner twice provides additional efficiency, and also allows self-cleaning from small debris, leaves etc. Another advantage of cross-flow turbines is the practically flat efficiency curve under varying loads, which makes them ideal for run-of-river plants.

Turgo has similar of operation as Pelton with main difference the angle in which the water enters the runner's level. This type of turbine can function in a more endurable way when it comes to intense sediment erosion.

Kaplan type, is the most used hydro turbine for high-flow and low-head power production. The runner is a form of a propeller, the water inserts vertical the axis of the turbine, spins and then meets with the runner. Another propeller type turbine is the Bulb, the Straflo, the S-type Kaplan and the Deriaz. Each one of them has a different operation and design mode making them suitable for a large scale of occasions.

3.1.2 Turbine selection

In order to choose the most suitable turbine type for a given net head H, (geometrical quantity, that also depends on the discharge due to friction and minor hydraulic losses), and to a nominal flow rate Q (hydraulic quantity), we will have to consult the chart shown in **Figure 3.2**. This nomograph summarizes various combinations of net head and nominal discharge, from 0.09 MW up to 1000 MW power capacity. Each colored area represents a specific type of turbine and the values of the above combinations, in which each is suitable for.

According to **Figure 3.2**, for relatively small nominal discharge and large head ($H > 250$ m), the impulse turbines are applicable, in contrary with the Francis turbines, which are more suitable for a wider range of discharge with lower head conditions.

Moreover, for even smaller hydraulic loads but with high discharges, propeller type turbines, like Kaplan, fit as best.

The selection of the turbine's type, when it comes to overlapping areas, depends also in the predicted variations in discharge during the year but mostly to financial and technical issues, as the available technical knowledge.

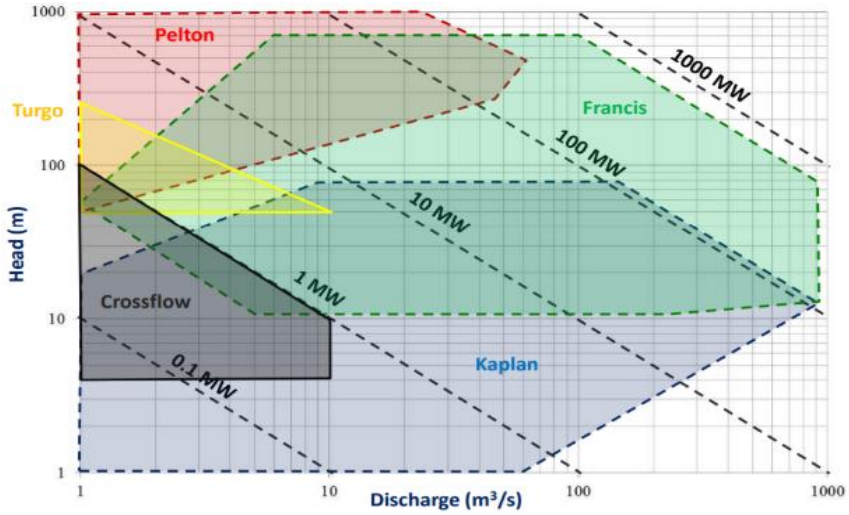

Figure 3.2: Turbine application range chart, depending on net head H(m) and nominal discharge Q (m^3/s).

3.2 Turbine efficiency

3.2.1 Definition

The total efficiency of a turbine η_T, is defined as the ratio of the output power produced by the turbine system to the input power which is provided to the turbine system. The efficiency of a turbine is always lower that one, due to energy losses. It's range also varies, depending the type of the turbine and the passing inflow. Typical ranges of efficiency are 80%-95%.

But in order to know its real value we need to take into consideration the different types of energy losses that occur inside a turbine system. Specifically:

- Hydraulic losses, due to friction losses of the fluid layers in motion and also due to water crashing on blades, local losses due to changes of the tube section;
- Volumetric losses, only for impulse turbines, due to small amounts of water that are extracted to the atmosphere, without crashing on the blade;
- Mechanical losses, that are developed in the rotating parts of the turbine.

Moreover, except from the turbine's losses, the total efficiency of our Hydropower plant is defined by the generator's efficiency η_G (~ 96%), the transformer's efficiency η_{TR} (~ 98%)and lastly by the transmission lines' efficiency η_E (~ 98%).

In conclusion, the total efficiency of our system equals to the product:

$$\eta = \eta_T \eta_{TR} \eta_G \eta_E \tag{3.1}$$

and implies the ration of the actual power provided to the electrical grid to the hydraulic energy provided to the turbine system.

3.2.2 Efficiency curves

The efficiency of the turbine system, is a nonlinear function of the net head and the inflow. Their relation can be expressed by a two-dimensional diagram, **Figure 3.3** provided by the turbine manufacturers or measured by the hydropower producers on-site. The bellowed diagram represents the percentage of typical efficiency of a turbine, η (%), as a function of the load in dimensionless terms, $^{q}/_{q_{nom}}$, where the subscript refers to the nominal operating point of the turbine.

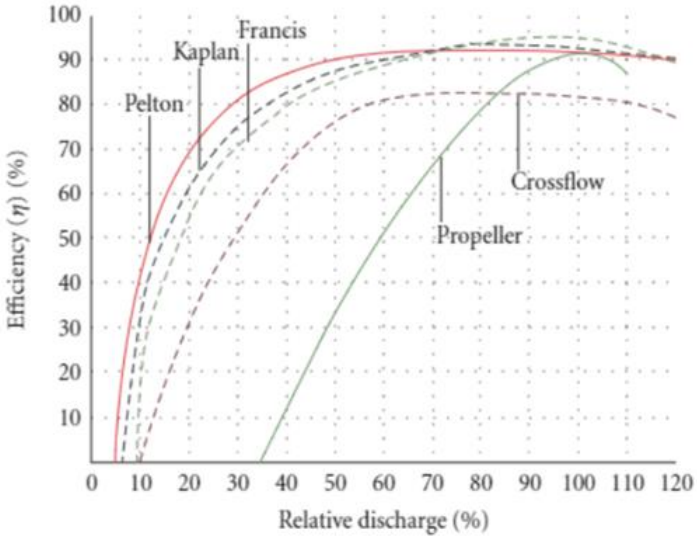

Figure 3.3: Typical efficiency curves for different types of hydropower turbines.

Some typical ranges of the maximum efficiency, in relation with the turbine type, are also given in the following **Table 3.1**.

As we can see from the above diagram in **Figure 3.3**, Pelton, Kaplan and Cross-flow machines are capable of operating close to their maximum efficiency for a large range of hydraulic load, comparing to Francis and Propeller ones.

Pelton turbines, manage to have that kind of operation due to their ability of changing the opening of the injectors, through a flow regulator (needle), resulting to keeping the fluid's velocity stable.

In addition, Kaplan exceeds the Propeller type, due to its faculty of adjusting the angle of the rotor and guide blades in the most efficient way.

Cross-flow, it may operate in a large range of $^{q}/_{q_{nom}}$ with its best efficiency but it cannot compete with Pelton, due to its higher efficiency level.

Table 3.1: Typical efficiency ranges for various turbine types.

Type	Efficiency range
Pelton	0.880-0.920
Cross-flow	0.800-0.840
Turgo	0.800-0.870
Francis	0.910-0.945
Deriaz	0.910-0.940
Kaplan	0.910-0.945
Bulb	0.900-0.940

The maximum and minimum efficiency of a turbine depends on the type of the turbine, its size and manufacturer's design criteria. To be more specific, when it comes to impulse turbines (e.g. Pelton, Cross Flow), their size does not affect in a great scale their maximum efficiency level, thus we can assume it as a constant value. On the other hand, the maximum efficiency of reaction turbines (e.g. Francis, Kaplan) varies depending on their nominal power capacity and cannot be taken as constant.

The following chart in **Figure 3.4** is the so-called hill chart, that expresses the relationship between the net head (blue dotted curve), the nominal discharge, the turbine's efficiency ranges (red dotted curves) and the opening of the turbine's guide vanes (olive green curves). The optimal efficiency point is determined as the cross point of the net head curve (depending on the gross head and the inflow) with the higher possible efficiency curve.

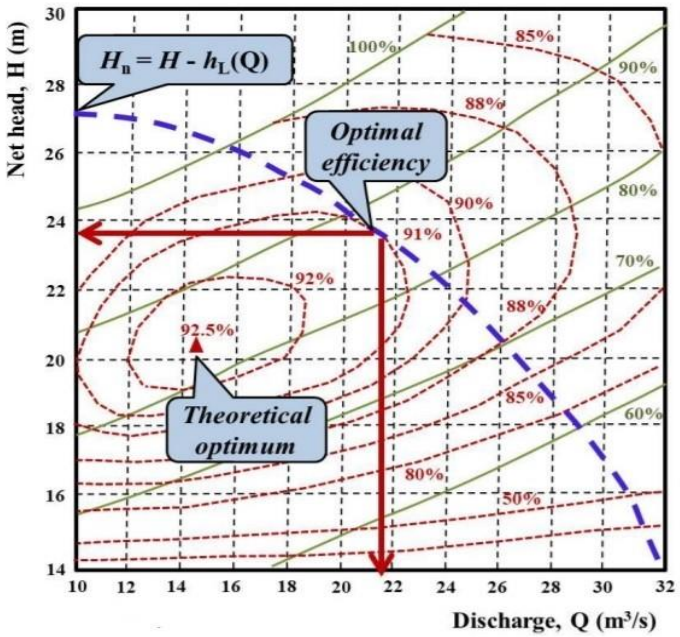

Figure 3.4: Example of determining the operation range of hydropower turbines, by drawing the flow-head relationship of the penstock.

3.2.3 Specific speed; a key variable for optimal operation of turbine systems

A lot of research has been taken place on the operation of the turbines with variable speed. This approach is of particular importance in the field of Small Hydropower Plants, when there is no storage capacity, thus meaning unsteady net head and variable efficiency rate. In order to ensure an operational range with higher efficiency levels not only in nominal values but in operating points as well, we choose a flexible scheduling of the runner by changing the speed of rotation depending on the inflow of each time, setting as goal the best operational efficiency for the incoming flow and as a result the maximization of the produced energy.

In few words, for each incoming discharge we choose the right angle of the guide vane system and the corresponding turbine speed in order to have the best efficiency point. Taken from a research on an experimental Small Hydropower Plant, with nominal head H equals to 3,5 m and nominal discharge Q equals to $3\ m^3/s$, with a propeller turbine and a permanent magnet synchronous generator, in **Figure 3.5** is shown the co-dependency of the above turbine operational values.

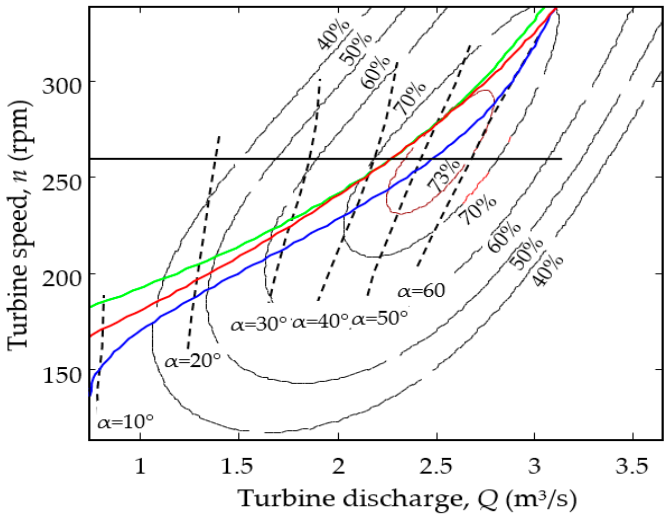

Figure 3.5: Typical hill chart of hydropower turbines.

The above technique, requires the use of power electronic converters (PECs), since we need to supply the electrical network with stable electrical frequency. The only drawback of this approach is the reduction of the total efficiency caused by the additional electromechanical equipment, which can be balanced by accompanying the PECs with permanent magnet synchronous generators. The usage of these type of generators increase the efficiency of the system since their design include a polar pair number, which allows the elimination of mechanical transmission gears.

3.3 Fundamental mathematical formulas

3.3.1 Operational range of turbines

As it is apparent from the previously presented typical efficiency curve (Figure 2.3), each turbine can operate in a specific range of inflow, in other words electricity

can be produced by the selected turbine system only if the passing discharge belongs between a minimum and a maximum value, symbolized as q_{min} and q_{max}, respectively, which differ according to the turbine model.

The nominal discharge is given by the following formula

$$q_{nom} = {}^{P}/_{\gamma\, \eta_{max}\, h_n} \tag{3.2}$$

where $\eta_{max}$is the maximum total efficiency represented by the nominal discharge, γ is the specific weight of water (9.81 KN/m^3) and h_n is the net head, i.e. the gross head, H, after subtracting hydraulic losses, h_l. Hydraulic losses include friction and minor ones, which are function of discharge and the penstock properties (roughness, length, diameter, geometrical transitions).

The minimum discharge also depends on the manufacturer, since is a ratio of the nominal, and also differs according to the type of the turbine.

The expression that gives the above value, is the following formula

$$q_{min} = \theta q_{nom} \tag{3.3}$$

where θ expresses the percentage of the q_{nom} that q_{min} equals to.

It is worth mentioned, that the discharge rate which refers to the best efficiency factor (**nominal operating point**) is not necessarily the maximum flow limit of the turbine. On the contrary, the unit is designed to produce energy for discharges up to 1.2-1.25 times the nominal rate or even greater for some turbines. Some typical ranges for common turbine types in SHPPs are shown in **Table 3.2**.In this range $\left(1 < {}^{q_i}/_{q_{nominal}} < 1.20 - 1.25\right)$ the efficiency curve becomes monotonically decreasing, in a rate that depends on the type of the turbine and the manufacturer. More details follow in the next paragraph.

Table 3.2: Typical values of range of operation for different turbine types.

Type of turbine	q_{min}/q_{nom}	q_{max}/q_{nom}
Pelton	0.1087	1.25
Francis	0.5	1.25
Cross Flow	0.285	1.428
Kaplan	0.1242	1.4286

3.3.2 Analytical formula

A more flexible and efficient method to determine the efficiency value of each incoming inflow in every time step and then extract its efficiency curve, is through an analytical formula, introduced by Sakki (2020) and Sakki et al. (2021). In the following formula, a and b are non-negative shape parameters that in combination with the appropriate values of η_{max} ,η_{min} it is possible to change the efficiency curve and extract its loyal form to the in-situ results.

$$\eta_T = \eta_{min} + \left(1 - \left(1 - \left(\frac{\frac{q}{q_{nom}} - \theta}{1 - \theta}\right)^{a}\right)^{b}\right)(\eta_{max} - \eta_{min}) \tag{3.4}$$

The above formula helps us to define the relationship between efficiency η_T and discharge , by taking into consideration the turbine's characteristics in size and type (η_{max} ,η_{min},θ, a, b). The lower limit of the expression (3.4) is (q_{min},η_{min}) and the upper (q_{nom},η_{max}).

In case that we decide the nominal discharge to also be the maximum discharge that our turbine should operate, as it happens with the present case study then there above formula is the best fit to our problem. In a more generic way, in order to include a broader approach, we also provide a second formula, as shown in expression (3.5), similar to the above. The second formula acts as a supplement to expression (3.4), since is applicable for$\eta \leq \eta_{max}$ while $q_{nom} \leq q \leq q_{max}$.

$$\eta_T = \eta_{max} - \left(1 - \left(1 - \left(\frac{\frac{q}{q_{nom}} - 1}{1 - \theta}\right)^{a\prime}\right)^{b\prime}\right)(\eta_{max} - \eta_{min}) \tag{3.5}$$

Figure 3.6 demonstrate three different types of turbines with their efficiency curve given by their manufacture. In the same diagram, the analytical formulas have been applied for each type with the appropriate turbine characteristic for each case and shape parameters.

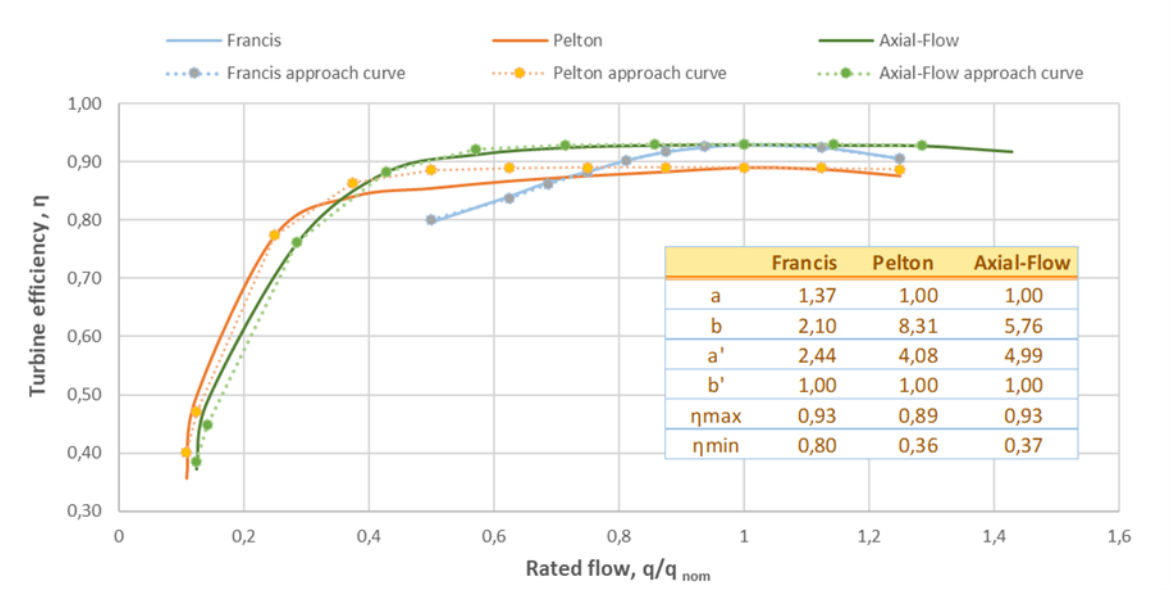

	Francis	Pelton	Axial-Flow
a	1,37	1,00	1,00
b	2,10	8,31	5,76
a'	2,44	4,08	4,99
b'	1,00	1,00	1,00
ηmax	0,93	0,89	0,93
ηmin	0,80	0,36	0,37

Figure 3.6: Turbine efficiency compared to rated flow and its analytical expression for different type of turbines.

4 Generic framework for optimizing the operational policy within turbine mixing

4.1 The concept of turbine mixing in small hydroelectric plants

For a given layout of a small hydropower plant (siting of intake, forebay, water conveyance system, and power plant), the most important design decision involves the configuration of the turbine system. This imposes the specification of the type and number of turbines, and the assignment of their power capacity. As explained in section **3.3.1**, the power capacity also determines the maximum discharge, q_{max}, that can pass through the turbine (see eq.3.2), while the type of the turbine leads to a certain value of ratio θ, thus resulting to a minimum discharge $q_{min} = \theta\, q_{max}$.

Since the majority of SHPPs have negligible storage capacity, they cannot offer regulation of the arriving streamflow (as made in the case of hydroelectric reservoirs), which exhibits significant variability across all scales. A single turbine captures a relatively limited portion of this variability, thus implying the setting of more than one turbines. The typical case is the mixing of two turbines in parallel (one large and one small), which allows for exploiting a wide range of diverted discharge values. In the generic case of N turbines, if the individual flow ranges are $(q_{i,min}, q_{i,max})$, the operational flow of the combined system ranges from $q_{min} = min(q_{i,min})$ to $q_{max} = \sum_{i=1}^{N} q_{i,max}$.

4.2 Hierarchical operational rule

By applying two (or more) turbines instead of a single one, we confront a challenging management problem, i.e. the sharing of the diverted streamflow through each turbine. A simple and effective operational rule, herein called *hierarchical*, indicates that the system of the two turbines comprises a master and a secondary one. As it is implied, the master turbine refers to the one with the larger power capacity, and thus the most extended operational flow range, while the secondary one has the lower capacity.

The hierarchical rule is structured as follows: When the diverted discharge is lower than the minimum flow limit of the turbine system, q_{min}, there both turbines are shut down and there is no power production. On the other hand, when the diverted discharge exceeds the maximum flow limit, q_{max}, then both turbines operate at their maximum power capacity, while the excess stream flow overflows to the natural bed of the river. For flow values within the range $(q_{2,min}, q_{1,min})$, the flow is conveyed to the secondary turbine, while the master one remains out of operation. Instead, between $q_{1,min}$ and $q_{1,max}$, only the master turbine is set in operation. Finally, in the range $(q_{1,max}, q_{1,max} + q_{2,max})$ the hierarchical operational rule states that the flow is by priority conveyed to the master turbine, which operates at its capacity. On the other hand, the secondary turbine receives the

remaining flow and produces energy only is this quantity exceeds the associated limit $q_{2,min}$.

The aforementioned operation policy is formalized as follows: Let q be the streamflow arriving at the intake (typically, this is the natural flow of the river, after subtracting a quantity q_e, which is imposed by the environmental legislation). The flow passing from the master turbine is given by:

$$q_1 = \min(q, q_{1,max}) \tag{4.1}$$

If $q > q_{1,max}$ then the surplus flow passing from the secondary turbine is:

$$q_2 = \min(q - q_1, q_{2,max}) \tag{4.2}$$

For $q_i < q_{i,min}$ the turbine is set out of operation, while for $q_i > q_{i,min}$ the power produced by each turbine is:

$$p_i = \begin{cases} 0 & q_i < q_{i,min} \\ \rho\, g\, \eta_i(q_i)\, q_i h_n(q_i) & q_{i,min} \le q_i < q_{i,max} \\ p_{i,max} & q_{i,max} \le q_i \end{cases} \tag{4.3}$$

where $\eta_i(q_i)$ is the total efficiency, which is typically expressed as afunction of the rated flow, q/q_{nom}(monotonically increasing, up to the nominal point), and $h_n(q_i)$ is the net head, which is, on the other hand, a decreasing function of flow q_i.

4.3 Looking for an optimal operation rule

The above policy is the simplest one, but not essentially the most effective. This is due to the nonlinearity of the product $\eta_i(q_i)\, q_i$, where i refers to a specific turbine. This nonlinearity is mainly induced by the peculiarity of the efficiency function, which retains an almost constant ceiling, for relatively high rated flow values, and then exhibits a steep drop. As described in previous section, the hierarchical rule implies the occasional use of the small (secondary) turbine, since the flow is by priority conveyed to the large (master) one. However, under some circumstances, a combined operation of the two turbines would be more beneficial, to ensure the maximization of the total energy production. This could be achieved by "donating" part of the arriving flow to the small turbine, to operate close to its nominal efficiency, with minimal efficiency loss for the large turbine.

In order to clarify this argument, we contrast the application of the hierarchical rule with a more effective policy, hereafter called *synergetic*. We use the data from the pilot small hydroelectric plant in upper Achelous, which takes advantage of a practically constant net head equal to 150 m (Chapter 6). This comprises two Francis-type turbines, which characteristics are shown in Table 4.1. The efficiency curve of the two turbines is illustrated in **Figure 4.1**.

Table 4.1: Design characteristics of the two Francis-type turbines.

	Turbine 1	Turbine 2	Total
Power capacity, P (MW)	7.40	1.00	8.40
Maximum discharge, q_{max} (m³/s)	5.69	0.77	6.46
Minimum discharge, q_{min} (m³/s)	0.85	0.12	0.12

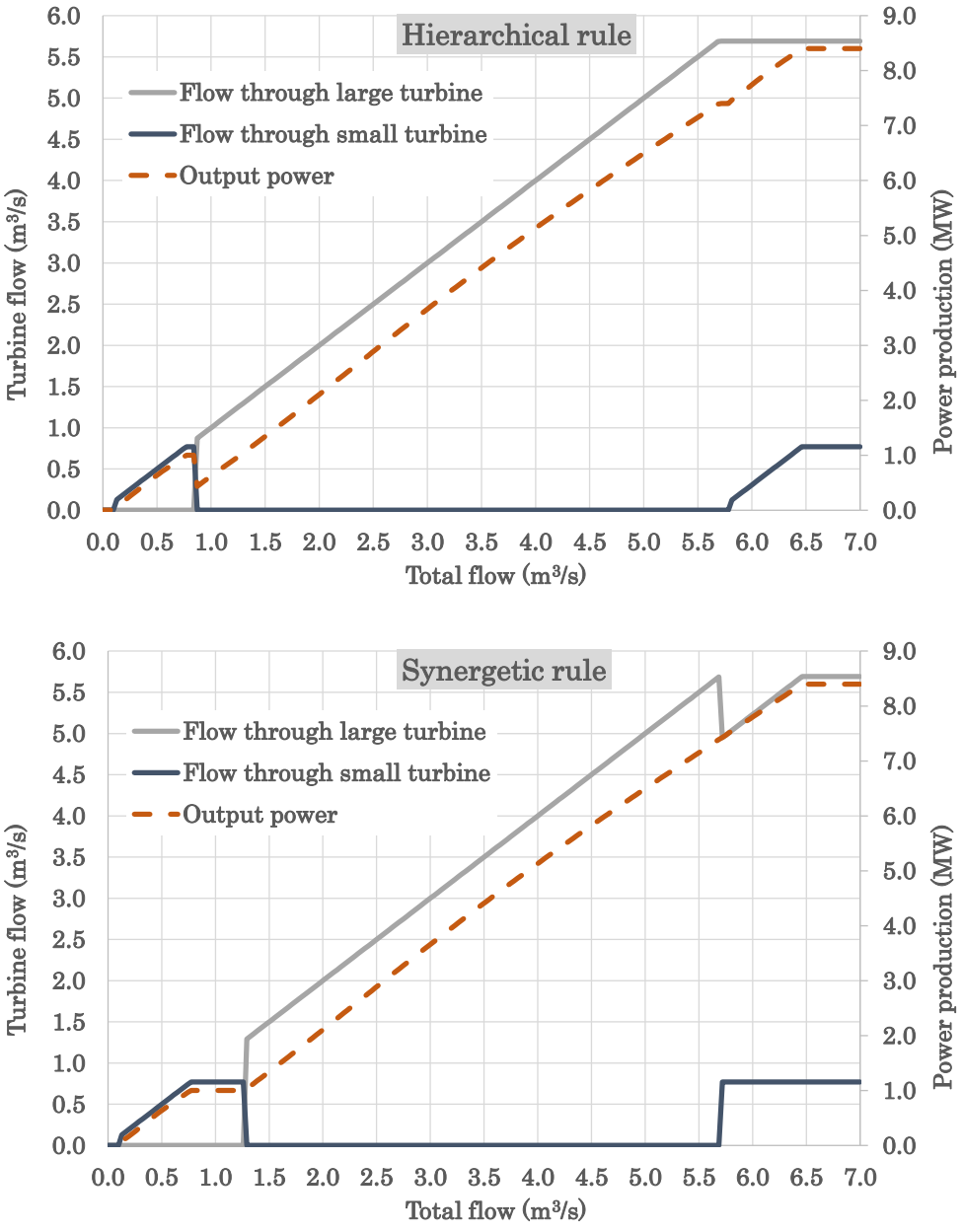

Figure 4.1: Sharing of diverted discharge across the two turbines of the pilot SHPP and associated power production for two operational rules (hierarchical, synergetic).

The contrast of the two operational rules, in terms of flow sharing and power production, is demonstrated in **Figure 4.1**. The derivation of the associated graphs is made by dividing the operational flow range of **Table 4.1** into small intervals (i.e., $q/q_{max} = 0.05$) and next applying the following methodology:

1. We calculate the flow sharing and power production for the operational scenario that implements the conventional hierarchical policy, in which the large turbine is set as the master and the small one as the secondary one;
2. We repeat the calculations for the opposite hierarchical policy, where the small turbine operates as master and the large one as secondary;
3. We compare the two scenarios, on the basis of totally produced power, and keep for each flow value the flow sharing that maximizes the output power through a synergetic operation of the two turbines. In fact, the optimal synergy is ensured when the two turbines exchange roles (master/secondary) in the most productive way.

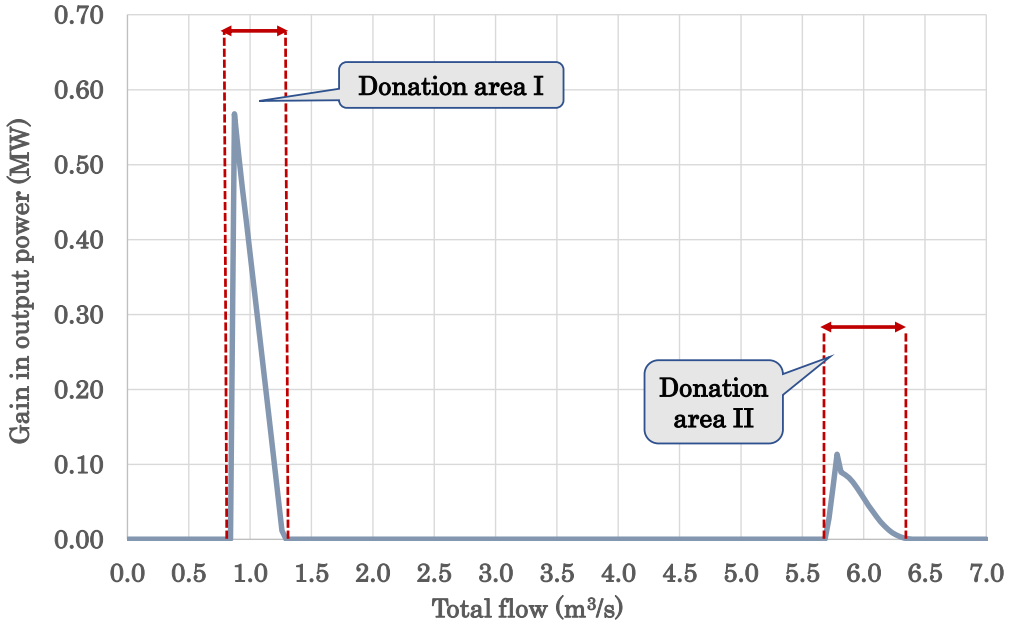

Figure 4.2: Gain in produced power by applying the synergetic instead of the hierarchical operational policy.

As shown in **Figure 4.2**, the gain in produced power by applying the synergetic instead of the hierarchical operational policy appears in two discrete flow intervals, defining the so-called *donation areas*. Term donation originates from the fact that the large turbine offers an amount of its discharge to the small one, in order to optimize the product (we remind that inthis specific case, the net head, h_n, is assumed constant, for simplicity):

$$p_{tot} = \rho\, g\, h_n \left(\eta_1 \left(\frac{q_1}{q_{1,max}} \right) q_1 + \eta_2 \left(\frac{q_2}{q_{2,max}} \right) q_2 \right) \tag{4.4}$$

The first donation area starts at $q_{1,min}$(in this case, 0.85 m³/s), where all discharge is conveyed to the small instead of the large turbine. Under this policy,

the small turbine operates with its maximum efficiency, since the rated flow$q_2/q_{2,max}$is unit (since in our case, $q_{1min} > q_{2max}$). In opposite, the hierarchical rule would require the operation of the large turbine with $q/q_{max} \ll 1$, and thus a much lower efficiency. The end point of the first donation area, where the hierarchical rule is applied again when:

$$\eta_1\left(\frac{q_1}{q_{1,max}}\right)q_1 = \eta_{2,max}q_{2,max} \tag{4.5}$$

The second donation area starts at $q_{1,max}$(in this case, 5.69 m^3/s), where the discharge which is conveyed to the large turbine is reduced by $q_{2,max}$ (in this case, 0.77 m^3/s), in order to feed the small turbine with its maximum discharge and thus operating with its maximum efficiency. This policy is applied until the system reaches its total power capacity, thus $q = q_{1,max} + q_{2,max}$.

4.4 Summary of synergetic management rule

The generic management rule for any mixing of two turbines, by applying an optimized synergetic operation, can be defined as follows:

- If $q < q_{2,min}$, both turbines are shut down, thus there is no energy production;
- If $q_{2,min} < q < q_{1,min}$, only the small turbine is in operation;
- If $q_{1,min} < q < q_{2,max}$, only one turbine is in operation, namely the one ensuring the higher product$\eta_i q_i$;
- If$q_{2,max} < q < q_{1,max}$,only one turbine in operation, the larger one (T1)
- If $q_{1,max} < q < q_{1,max} + q_{2,min}$, donation point, both of the turbines are in operation, in the most optimal combination meaning the small turbine operates with its maximum efficiency and the larger one with a slighter lower that its maximum for a small range of inflows
- If $q_{1,max} + q_{2,min} < q < q_{1,max} + q_{2,max}$, same as above step, both turbines in operation, distributing q in the most efficient way
- If $q > q_{1,max} + q_{2,max}$,both turbines operate in their maximum efficiency.

4.5 Generic formulation of operation rules

We consider a hydroelectric plant comprising two turbines, of unit total capacity, $p^*_{max} = 1$,by taking advantage of a unit net head, $h^*_n = 1$.In the generic case, the type of the two turbines differs, thus their efficiency function$\eta_i = f(q/q_{nom})$ is expressed by different parameter values,$\eta_{i,max}$,θ_i,a_i andb_i.For convenience, we assume that the system operates up to its nominal point where the efficiency is maximized, and also the power capacity of each turbine is determined. In this respect, we can set $q_{nom} = q_{max}$ and $p_{nom} = p_{max}$., We also consider that η_i refers to the total efficiency, thus it embeds the product $\eta_{TR}\eta_G\eta_E$, which refers to minor energy losses across the rest of electromechanical components (transformer, generator, electrical grid).

We next introduce a sharing factor $\varphi \geq 0.50$(dimensionless), thus the large turbine has a power capacity $p^*_{1,max} = \varphi$and the small one $p^*_{2,max} = 1 - \varphi$. Under this premise, the maximum discharge passing from each turbine is expressed in dimensionless terms as:

$$q^*_{i,max} = \frac{p^*_{i,max}}{\rho\ g\ \eta_{i,max} h^*_n} \tag{4.6}$$

Similarly, the minimum dimensionless discharge of each turbine is:

$$q^*_{i,min} = \theta_i \frac{p^*_{i,max}}{\rho\ g\ \eta_{i,max} h^*_n} \tag{4.7}$$

In this respect, the maximum dimensionless discharge of the turbine system equals to:

$$q^*_{max} = \frac{1}{\rho\ g h^*_n}\left(\frac{\varphi}{\eta_{1,max}} + \frac{1-\varphi}{\eta_{2,max}}\right) \tag{4.8}$$

On the other hand, the minimum dimensionless discharge of the system is:

$$q^*_{min} = \frac{1}{\rho\ g h^*_n} min\left(\frac{\theta_1\ \varphi}{\eta_{1,max}}, \frac{\theta_2(1-\varphi)}{\eta_{2,max}}\right) \tag{4.9}$$

By setting $u = q/q_{max}$, we can express the dimensionless discharge as:

$$q^* = u\ q^*_{max} \tag{4.10}$$

Under this premise, the dimensionless power production is:

$$p^*_i = \rho\ g\ \eta_i(u) q^* h^*_n \tag{4.11}$$

In order to determine the optimal operation of alternative configurations of the turbine system, we examine different scenarios depending on the value of the sharing factor φ,the parameter θ_i and the turbine type, which affects the efficiency function parameters$\eta_{i,max}, a_i$ andb_i.

4.6 Experimental scenarios on power production

After testing different combinations of the sharing factor φ and the parameter θ_i for the two most used turbine types (Pelton, Francis)we compared their results in terms of total dimensionless power production, $p_i{}^* = p^*_{1,i} + p^*_{2,i}$.

Depending on the mixing characteristics' for various values of the sharing factor φ_i(0.2, 0.4, 0.5, 0.6, 0.7, 0.8), we settle on the most efficient combination. In **Table 4.2**, we present all the combinations (I,II,III,IV) along with their characteristics. In order to set a measure for defying the most efficient combination, we compare with the theoretical power which can be produced by an ideal turbine system with unit efficiency, i.e.:

$$p_{0,i} = \rho\ g\ q^*\left(\varphi, \theta_i, \eta_{i,max}, a_i, b_i\right) h^*_n \tag{4.12}$$

Afterwards, for each value of the sharing factor φ_i, for the four combinations, we calculated the deviation of each's scenarios power production from the ideal system, $\Delta p_i = (p_{0,i} - p^*_i)$, as shown in **Figure 4.6 :.**

We also desire to evaluate the deviation of optimal from the hierarchical dimensionless power production,(p^*_{opt} , p^*_{hier} respectively) in each different combination of turbines mixing in type (I,II,III,IV) and sharing φ_i, meaning $\Delta p_{i,operational} = (p^*_{opt,i} - p^*_{hier,i})$.The results of the above calculations are presented in **Figure 4.10** : .

Table 4.2: Different combinations of turbine mixing

Combination I	Turbine 1	Turbine 2
Turbine Type	Francis	Francis
parameter θ_i	0.50	0.50
$\eta_{i,max}$	0.93	0.93
a_i	0.78	0.78
b_i	3.11	3.11

Combination II	Turbine 1	Turbine 2
Turbine Type	Francis	Francis
parameter θ_i	0.15	0.15
$\eta_{i,max}$	0.93	0.93
a_i	1.00	1.00
b_i	2.11	2.11

Combination III	Turbine 1	Turbine 2
Turbine Type	Pelton	Francis
parameter θ_i	0.10	0.50
$\eta_{i,max}$	0.89	0.93
a_i	1.13	0.78
b_i	12.8	3.11

Combination IV	Turbine 1	Turbine 2
Turbine Type	Pelton	Francis
parameter θ_i	0.10	0.15
$\eta_{i,max}$	0.89	0.93
a_i	1.13	1.00
b_i	12.8	2.11

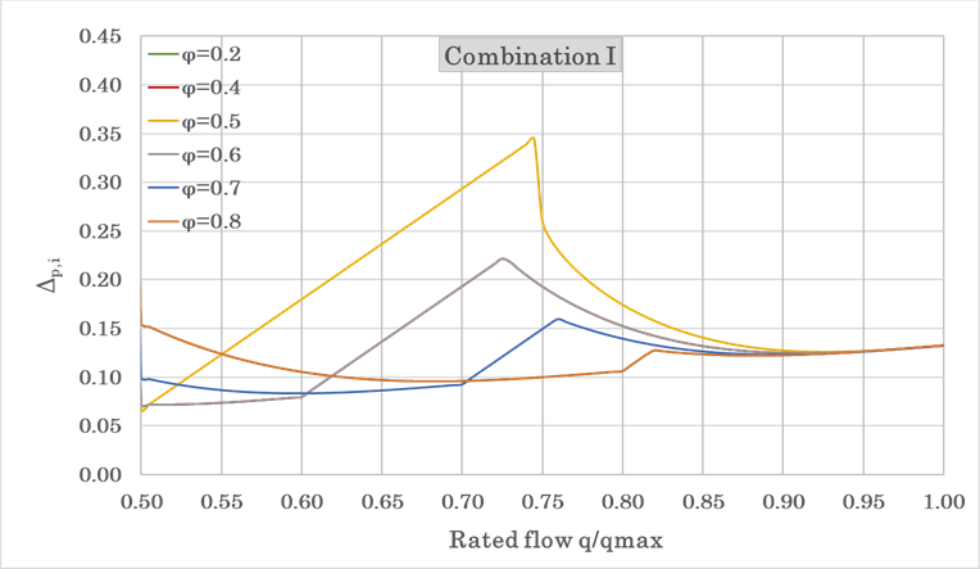

Figure 4.3 : Combination I of the deviation of dimensionless power production between real and ideal operation.

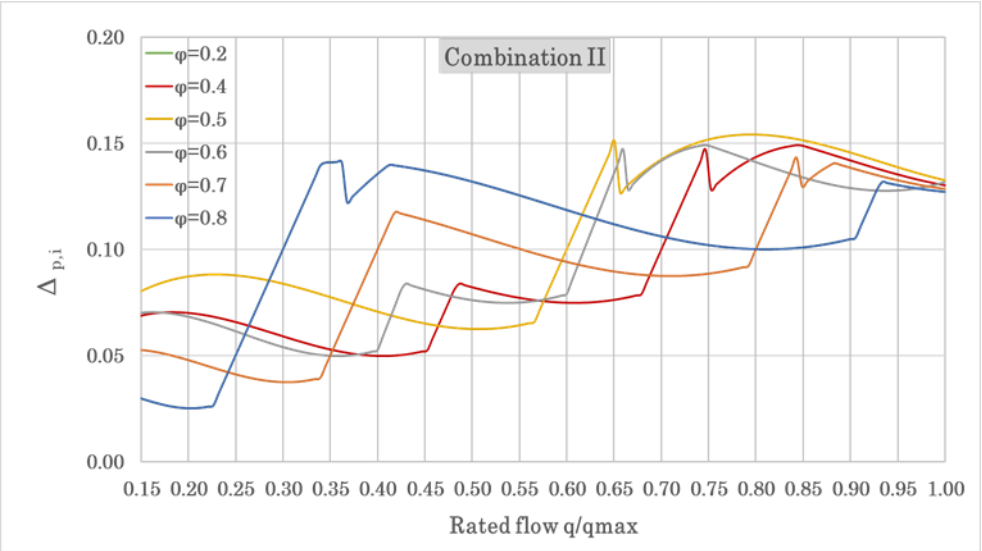

Figure 4.4 : Combination II of the deviation of dimensionless power production between real and ideal operation.

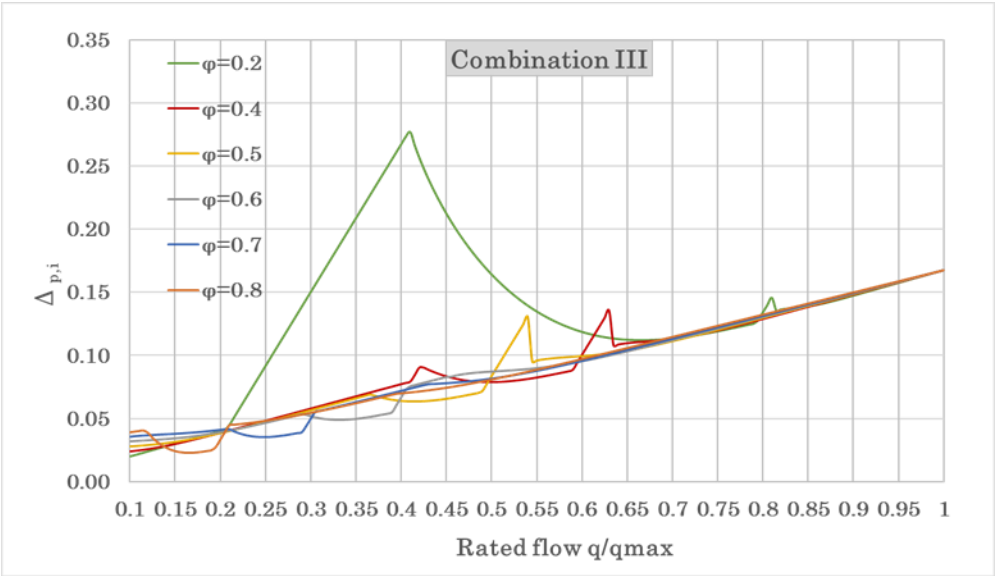

Figure 4.5 : Combination III of the deviation of dimensionless power production between real and ideal operation.

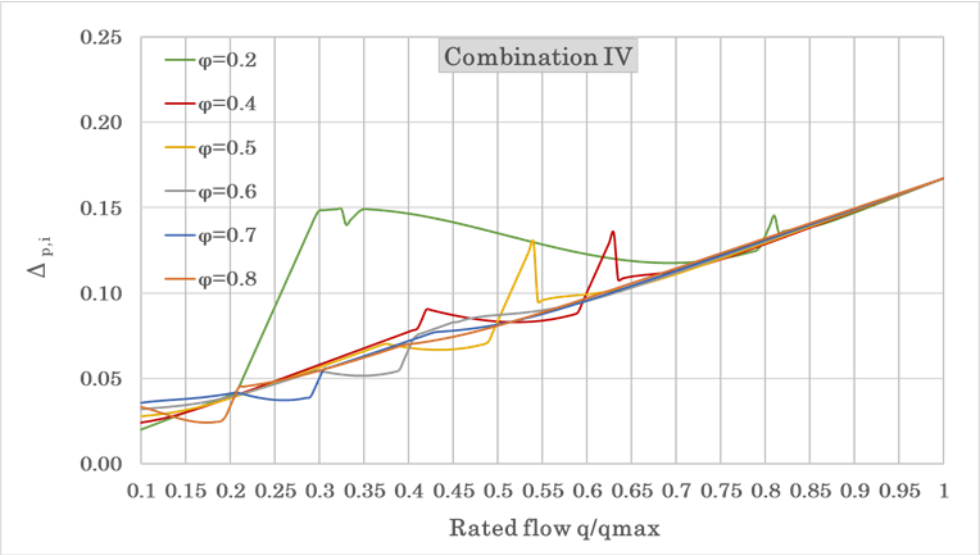

Figure 4.6 : Combination IV of the deviation of dimensionless power production between real and ideal operation.

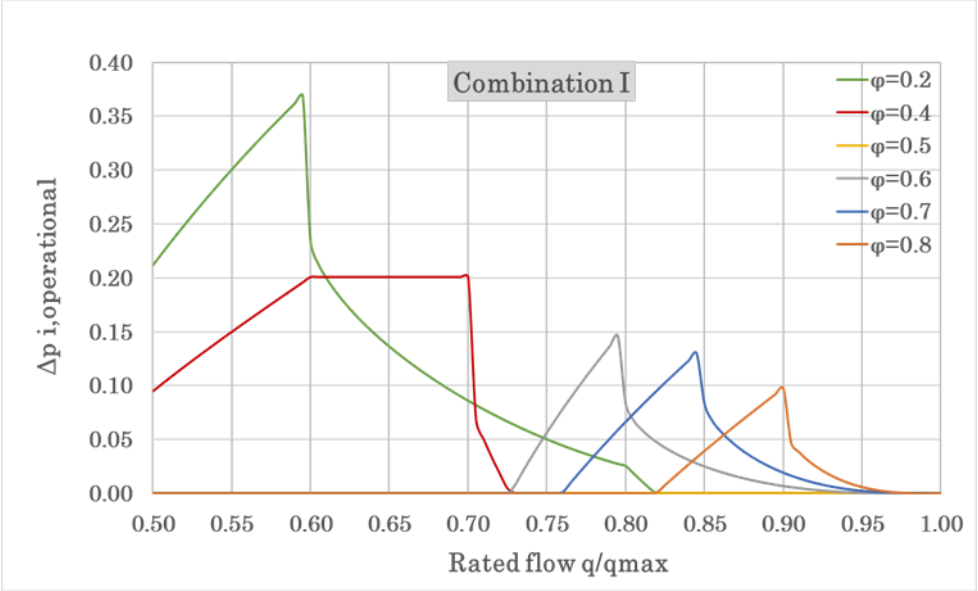

Figure 4.7 : Combination I of the deviation of dimensionless power production between optimal and hierarchical scheduling

.

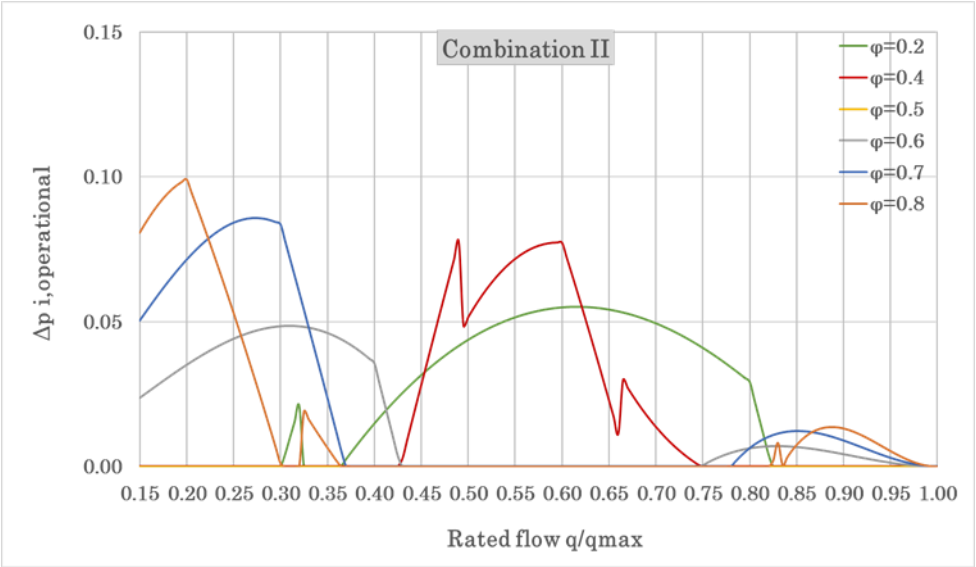

Figure 4.8 : Combination II of the deviation of dimensionless power production between optimal and hierarchical scheduling.

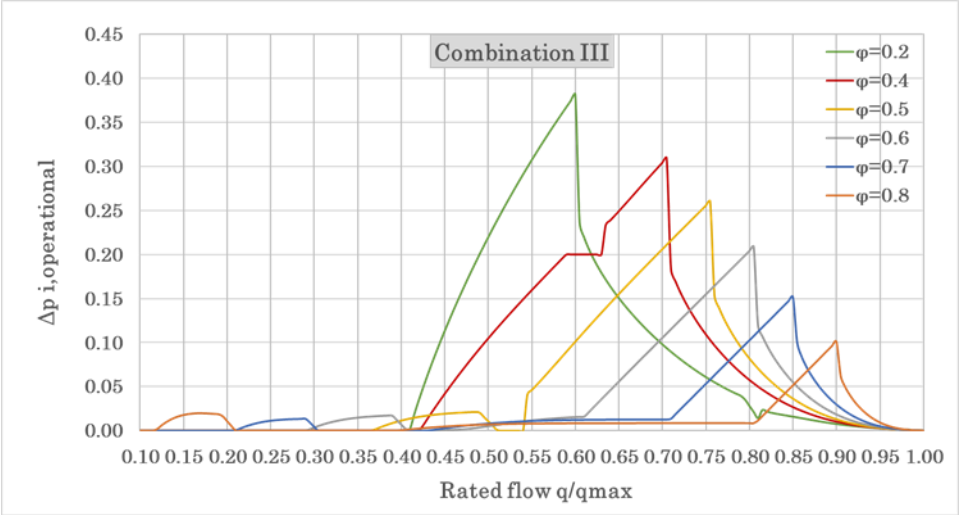

Figure 4.9 : Combination III of the deviation of dimensionless power production between optimal and hierarchical scheduling.

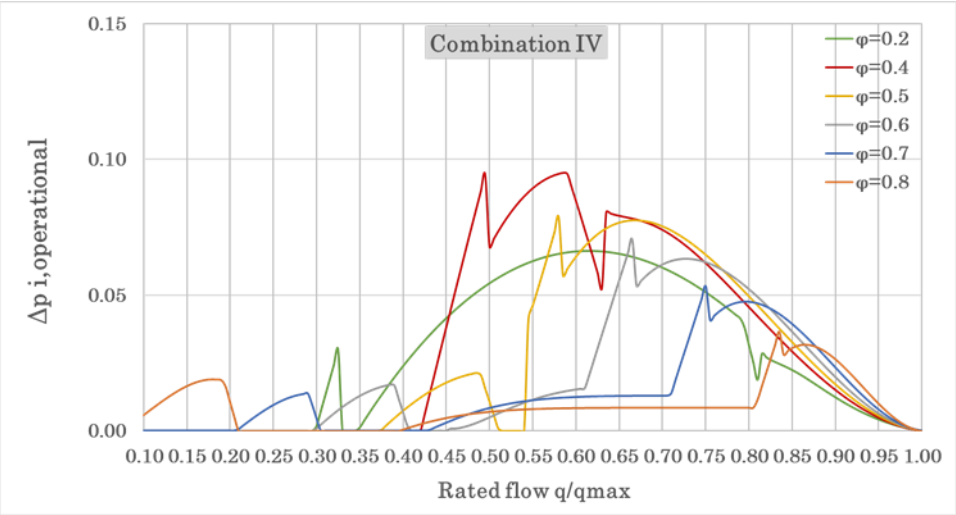

Figure 4.10 : Combination IV of the deviation of dimensionless power production between optimal and hierarchical scheduling.

Through the **Figures 4.3, 4.4, 4.5** and **4.6**, we can examine which combination is closer to the ideal operation of our system. As is shown in the aforementioned figures, in **Combination I** (*two Francis with identical* $\theta_i = 0.5$) the best sharing scheme is the one with $\varphi_i = 0.8$ and $\varphi_i = 0.2$, which are the same since the turbine mixing is symmetrical and the above sharing factors are complementary, and the worst is for $\varphi_i = 0.5$. In **Combinations II** (*two Francis with identical* $\theta_i = 0.15$), **III** (*one Pelton with* $\theta_i = 0.10$ *and one Francis with* $\theta_i = 0.50$), and **IV** (*one Pelton with* $\theta_i = 0.10$ *and one Francis with* $\theta_i = 0.15$) closer to the ideal operation happens to be achieved with sharing factor $\varphi_i = 0.7$. On those combinations, the less efficient schemes regarding the sharing factor differ depending on the range of $^{q}/_{q_{max}}$. To be more specific, in **Combination II,** the worst performance is obtained when $\varphi_i = 0.5$ and $\varphi_i = 0.8$, for high and low discharge rate, respectively, in **Combination III,** $\varphi_i = 0.2$ leads to the least appealing scenario and in the end in **Combination IV**, $\varphi_i = 0.2$ for low discharge rates and $\varphi_i = 0.4\,, 0.5$ for higher discharge rates but in smaller ranges, are the sharing factors which we should avoid in terms of better efficiency.

On the other hand, the **Figures 4.7, 4.8, 4.9** and **4.10** remark how much the optimal power production outnumbers the one produced from the hierarchical scheduling, regarding the above selected efficient scenarios. The usage of these observations is twofold: first we can conclude of how important is the use of the synergetic scheduling versus the hierarchical and secondly if the above divergence isn't in a great scale, to reconsider which scheduling to choose since the optimal might lead to more complex operation management. Depending the combination and the value of φ_i, the above figures combined with the given hydrological regime of the, under research, SHHP, can quantify the benefit of exploited discharge we gain or not by using the optimal (synergetic) rule instead of the hierarchical.

In order to assess the actual benefit (i.e., in power production terms) from the application of the synergetic vs. the hierarchical rule, we use the historical inflow data and the energy production resulting by them, sorted in descending order, thus forming the so-called energy and flow-duration curve (**Figure 4.11** and **Figure 4.12**), respectively. For each value of sorted inflow data, we estimate the power production by the two management policies, and assign it to the corresponding exceedance probability (**Figure 4.13**).

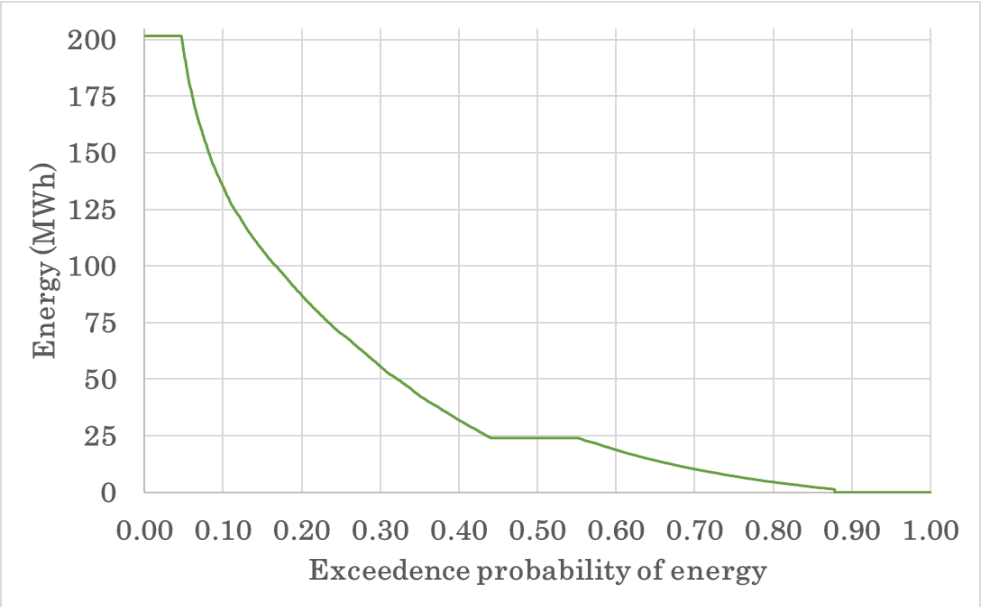

Figure 4.11 : Energy–duration curve.

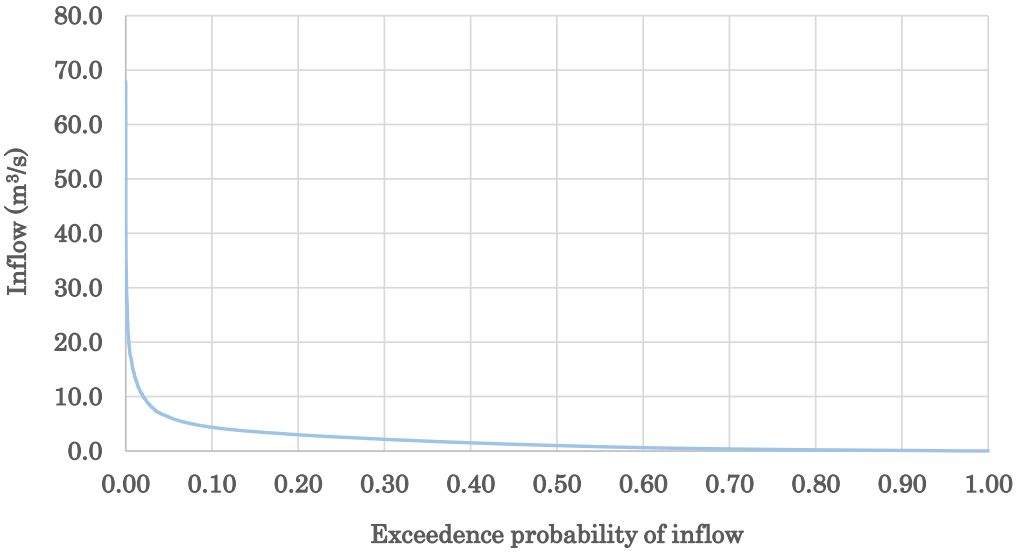

Figure 4.12 : Flow-duration curve.

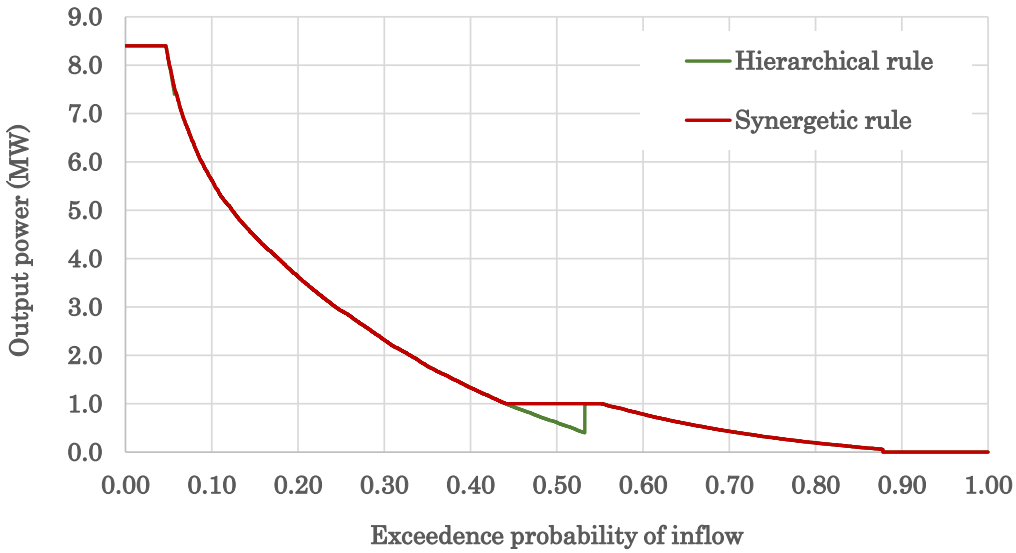

Figure 4.13 : Simulated power production as function of the empirical exceedance probability of inflow, according to the two operation policies.

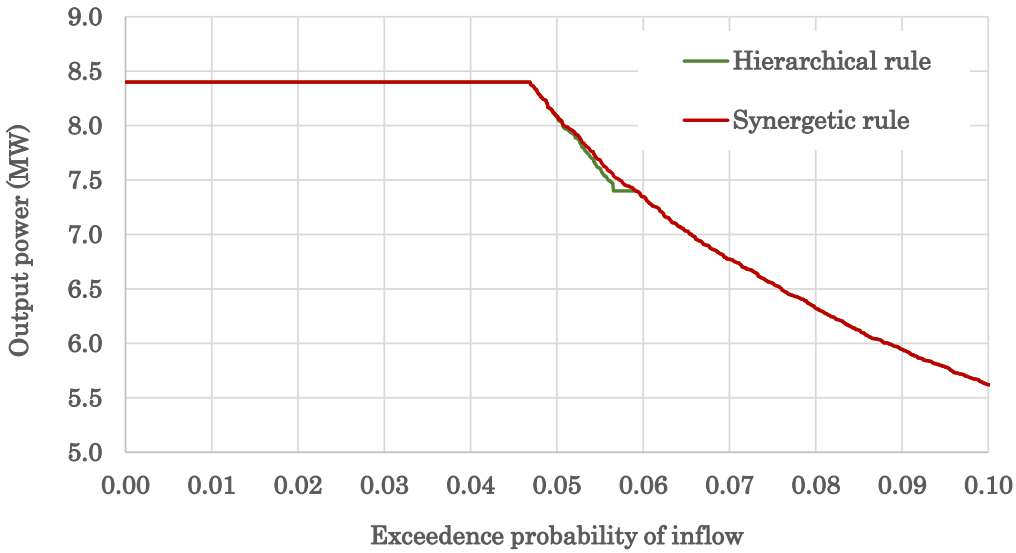

Figure 4.14 : Detail of previous figure, focusing on donation area II.

As shown in **Figure 4.13** the synergetic rule outperforms the hierarchical one particularly within donation area I, in which the system is driven by medium-scale inflows having exceedance probability from 45 to 55%. Thus, this mode is applied about 10% of time, resulting to an obvious benefit for the system. On the other hand, the gain within donation area II is not as much significant, as the rule is activated for a limited portion of time (see detailed graph in **Figure 4.14**). This highlights that the optimal performance of a mixed turbine system is subject to both the management rule and the flow regime.

5 Setting the problem of energy production forecasting in Small Hydropower Plants

5.1 The Target Model Era

Today, the energy market is subject to a new legal framework, called "Target Model". This model has been recently introduced as the new legal framework of the electricity market across Europe. Its main goal is to create a well-organized electricity market and an unified power system across European borders, through the cooperation of different markets by exchanging their natural sources in the most efficient scheduling.

The above legislation is a part of the European Union's third energy package, which aims at a new and improved function of the internal energy market by redefining the role of each participant (producers, aggregators) and the nature of their interaction.

Regarding the application of the "Target Model" in the Greek energy market, a variety of challenges arise, especially in the field of Renewable Energy Sources (RES) considering that new renewable energy projects are obliged to participate in the Greek wholesale electricity market. The above can be executed either directly or through renewable energy aggregators –meaning assigning them some of the balancing responsibilities.

This new role-allocation, leaves the RES producers financially responsible for the additional balancing cost between their forecasts and their actual energy production. From that point of view, it is clear that the contractual framework governing and representing the relations between RES producers and RES aggregators in the market, becomes of high importance.

Another significant measure which changes the structure of the energy market due to the "Target Model" and also intensify the need of credible forecasting predictors, are the additional costs for RES producers such as deviation between their forecasts and their actual energy production, clearance and non- compliance charges.

In this concept, RES aggregators' concerns focus on the commercially successful operation of their represented units, in terms of energy-schedule optimization or of power-system control services. As a result, they could ensure a better prediction of the actual production of RES units, leading to low level deviation charges accounting to RES producers.

Till our days, traditional units are mostly used on order to provide stable energy generation. Since the later are starting to be replaced by RES, it comes to question whether RES units are capable to autonomously maintain this stability by adapting with flexibility variable and possible unforeseen changes in operating conditions which also depends on the weather processes.

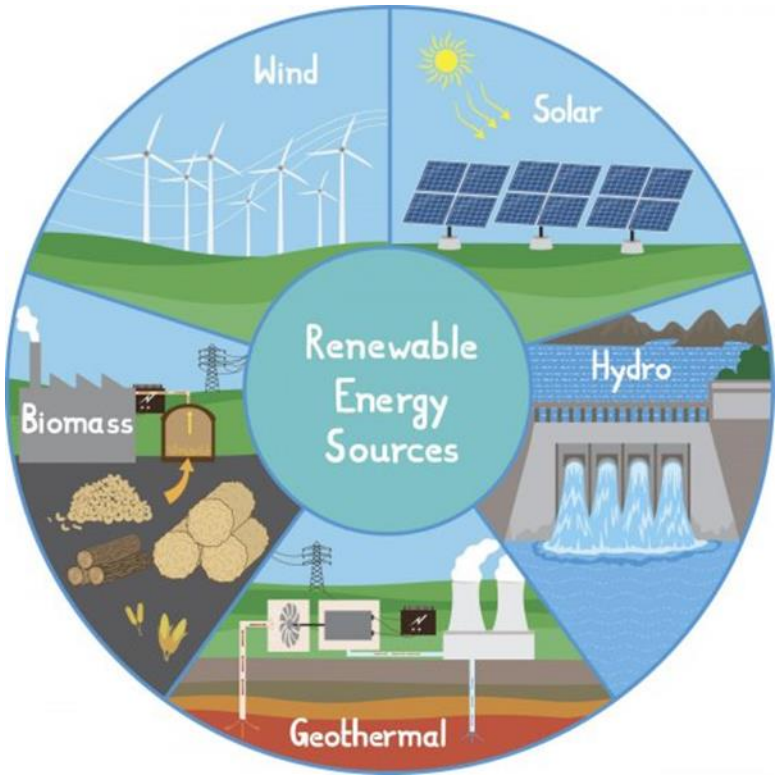

Figure 5.1 :Representation of various forms of renewable energy and their dependence on weather processes. (Source: https://www.deccanherald.com/content/661665/impacts-renewable-energy-projects.html)

5.2 Research advances and limitations

The associated research and operational applications so far mostly span over two main directions, regarding the forecasting of energy production.

The first refers to the short-term energy production forecasting by solar and wind power systems. Numerical Weather Prediction (NWP) models, are used by providing deterministic point forecasts.

The second field of interest deals with the long-term energy production by large hydropower reservoirs and is based on projections of their inflows (e.g., Cassagnole et al., 2021).

Nowadays, emphasis is given to data-driven approaches (e.g., machine learning), also combined with stochastic-probabilistic schemes for representing uncertainties that are ignored by NWP models (Felder et al., 2018; Talari et al., 2018; Croonenbroeck and Stadtmann, 2019).

Small hydroelectric works are classified as one of the most cost-effective technologies, establishing them as one of the most widespread form of renewable energy. We remind that this concerns hydropower systems up to a specific capacity value (e.g., 15 MW in Greece), commonly of negligible storage capacity, where the energy production is a direct conversion of the streamflow arriving at the intake. In contrast to other renewables, the short-term energy forecasting problem, in the field of SHPPs without storage, has not gained the necessary attention from the research community (Yildiz and Açikgöz, 2021). The typical

input information used in forecasting schemes appears to be the observed energy production and rainfall (e.g., Li et al., 2015), while some researchers also use forecasted precipitation, provided by NWP models (Monteiro et al., 2013). However, we should highlight that the accuracy of NWPs with respect to rainfall forecasting is still questionable, particularly in complex mountainous reliefs (Ólafsson and Ágústsson, 2021).

Surprisingly, streamflow forecasting procedures, followed by turbine operation models employing flow-energy conversions, seem to be missing. A plausible explanation is the scarcity of streamflow observations, since most of SHPPs are located in small remote catchments, lacking of hydrometric infrastructures.

On the other hand, given that the technical and operational characteristics of the SHPP are known (e.g., turbine scheduling and efficiency curves), the past inflows can be retrieved with quite satisfactory accuracy, on the basis of observed power production data, through reverse engineering (Sakki et al., 2021a).

Taking as an example a run-off-river SHPP, in the upper course of river Achelous, Western Greece, we investigate different day-ahead power forecasting approaches, driven by alternative data sources.

Since the limited scale of the SHPP industry makes difficult to support highly sophisticated operational forecasting systems, we seek for establishing simple and parsimonious regression-type approaches, instead of more complex schemes, e.g., from the domain of machine learning (ML) (cf. Papacharalampous et al., 2020), that yet require significant expertise to be properly used and often demanding computational infrastructures. This fact is probably associated with the growing interest in explain ability of such techniques (cf. discussion by Ribeiro et al., 2016). Key objective, and at the same time novelty of this research, is the maximization of information gathered from the available data, by taking advantage of the hydrological expertise and knowledge about the system's operation. Our research also highlights the training and evaluation procedure of each forecasting approach, as well as the representation of uncertainty and its practical interpretation.

In this vein, our overall objective is to move beyond the standard, yet risky, point forecasting methods, providing a single expected value of hydropower production, thus quantifying the overall predictive uncertainty of each method, and use it as a guidance for modelling energy market behaviors and support decision-making.

6 Study area and data

6.1 Overview and hydrological data

In the context of our analysis, we consider a hypothetical run-of-river plant under study, in the upper course of river Achelous, Western Greece. The flow arriving at the intake is diverted through an open channel to a forebay and next conveyed to the power station through a penstock, thus creating an elevation difference of 150 m.

The available hydrological information comprises spatially-averaged daily precipitation data from ten representative meteorological stations, and daily streamflow data at the intake. The latter input is extracted by adjusting the observed inflows to a downstream site, i.e., Kremasta reservoir (Efstratiadis et al., 2014), by accounting for the ratio of the corresponding drainage areas (about 1:40). The common period of the two records extends over 39 years (May 1969 to December 2008). **Figure 6.1** illustrates the adjusted flow time series, the mean annual value of which is 2.15 m^3/s.

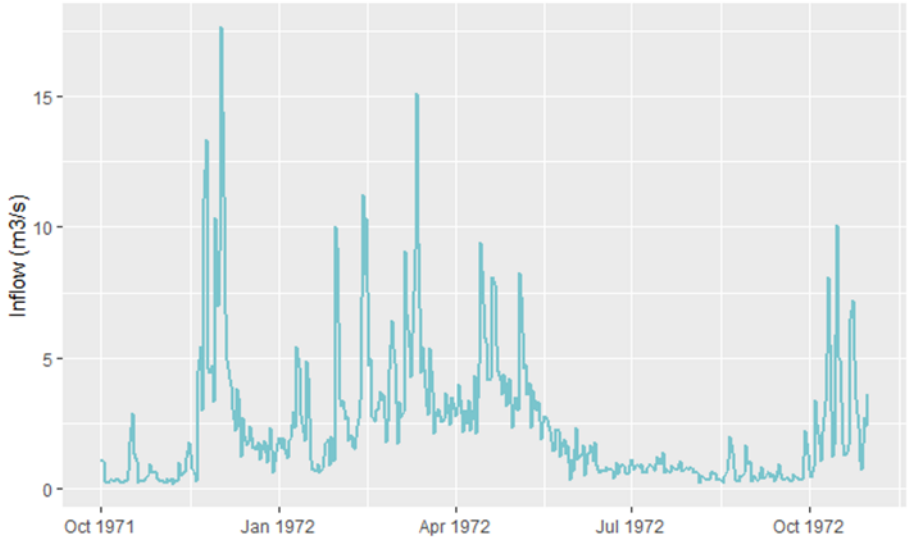

Figure 6.1: Streamflow time series at the intake for hydrological year 1971-72.

6.2 Technical characteristics

Before proceeding with the forecasting problem, it is essential to specify the technical characteristics of the project.

First, we estimate the environmental flow to be released downstream of the intake, in order to sustain the riverine ecosystems (Efstratiadis et al., 2014). According to Greek legislation, the time-constant environmental flow which should be preserved downstream of the Small Hydropower Plant, is defined as the maximum of the following quantities:

- 30% of average streamflow during the summer period (June, July, August);
- 50% of average streamflow of September;
- 30 L/s, in any case.

Following this, we defined a constant flow of 0.25 m^3/s as the 30% of mean discharge of September.

We should highlight that in next computations, we consider a constant net head, for simplicity. This comes in agreement with reality, by placing a penstock with quite large diameter (1500 mm), thus causing minimal hydraulic losses, even at the maximum discharge capacity.

Moreover, as it has already implied, in our case study, we set as an optimal operational system, a mixing of two Francis-type turbines, which characteristics are summarized in **Table 4.2**. The two capacities have been selected by the estimations, after solving an optimization problem (Sakki et al., 2021b). In this respect, a standard technoeconomic optimization problem is formalized by setting as goal the maximization of financial quantities such as the net present value (NPV). In this concept, the discounted value of future net cash flows should exceed the investment cost, so as to ensure a sustainable investment. The cash flows derived from the production of electrical energy during the entire life-cycle of the system, while the investment cost (involving the E/M equipment and the civil works) was directly or indirectly associated with the power capacity.

The objective function of the design optimization problem is expressed in annual profit terms as:

$$F\left(I, \underline{p}\right) = \underline{u}\, E_a(I, \underline{p}) - A(I) \tag{6.12}$$

This function is strongly nonlinear and contains two conflicting components, namely the mean annual energy production, $E_a(I, \underline{p})$, to maximize, and the equivalent annual cost, $A(I)$, to minimize.

To ensure robust solutions, the research also accounted for the resulting capacity factor of the RES, since they consider it may also comprise a mixing of different sources. This factor is a fundamental performance metric of power systems, defined as the ratio of the mean annual electrical energy output to the maximum possible one (Mamassis et al., 2021), i.e.:

$$F\left(\boldsymbol{I}, \underline{p}\right) = \frac{E_a\left(\boldsymbol{I}, \underline{p}\right)}{T_a \sum_{i=1}^{N} I_i} \tag{6.12}$$

In order insight to the optimization problem, Sakki et al. (2021b) repeated the design procedure for a large number of turbine capacity combinations, driven with the historical streamflow data. In their research they highlight that since the formulation of the problem is deterministic, it leads to a unique solution. As derives from their numerical and graphical results, two alternative operation policies with quite close performance characterized as optimal mixings. One of

them , named as “global optimum”, is the one we chose to be the selected turbine mixing in our case study.

The operation policy of the SHPP, in combination with both mathematical and graphic formulations, have been expounded extensively on **Chapter** 4. This has been obtained by seeking for the optimal hierarchy of the two turbines, in order to maximize the power production across different discharge ranges.

7 Day-ahead energy forecasting approaches

7.1 Application of energy forecasting schemes

7.1.1 Two routes leading to energy forecasting

In order to deal with the difficult task of energy prediction we established two alternative routes (direct, indirect) to the power forecasting problem of SHPP's, on a day-ahead basis. The direct route aims at predicting the next-day energy production via regression models. These models use as explanatory variables past observations, in terms of power production and the past rainfall, as the sole source of hydrological data. On the other hand, the indirect route initially aims at predicting the day-ahead discharge, given that such data exist. The forecasted flows are next introduced to the operation model of the system **Figure 7.1** , for extracting the forecasted energy. For each approach, we assess alternative forecasting schemes, in terms of model structure and data.

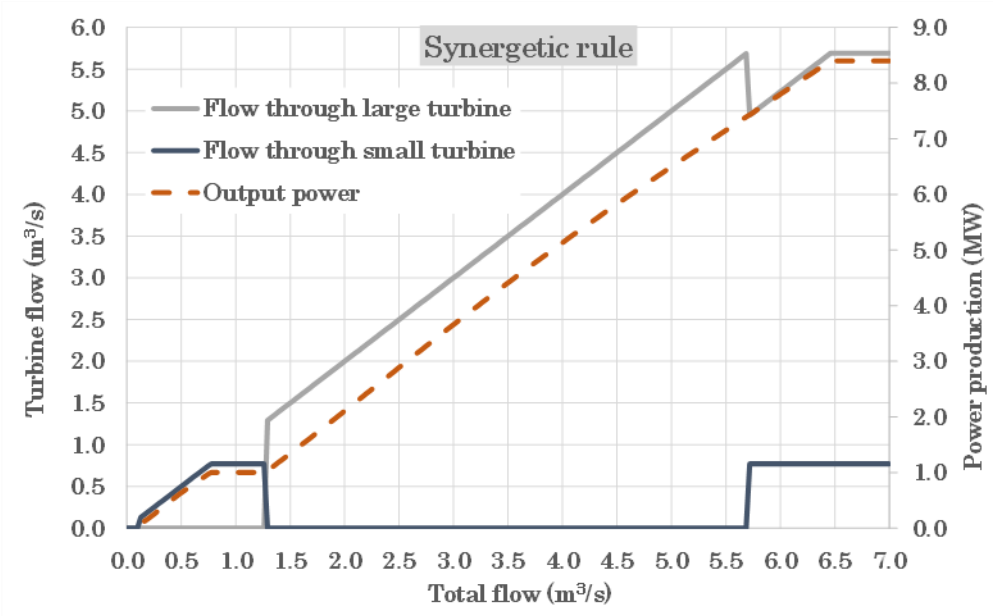

Figure 7.1 : Operational scheduling of the turbine system, ensuring an optimal power production.

7.1.2 Precipitation data

For the precipitation's information, each one of the ten stations' data were analyzed according to their degree of correlation to the observed inflow data.

In more words, since the linked relationship between the ten stations and the streamflow varies, for each one we set a relevant weight rate w_i , then for each time step t(here day) ,of our collected, n, data we calculate the following sum

product: $\sum_1^n(\boldsymbol{p_{t,i}}\,\boldsymbol{w_i})$, where $\boldsymbol{p_{t,i}}$ stands for the precipitation value of station $\boldsymbol{i}$ at day $\boldsymbol{t}$. The weighting coefficients $\boldsymbol{w_i}$ we assigned to each meteorological station, account as variables for optimization, aiming to give the best correlation value between the aforementioned sum product, and the flow value of the next day, meaning $\boldsymbol{correl}[\sum_1^n(\boldsymbol{p_{t,i}}\,\boldsymbol{w_i})\ ,\boldsymbol{q_{t+1}}]$.

The above method represents a credible approach of combining hydrological information from different recording sources. In our case, we combine the precipitation data from different meteorological stations while defining the rainfall time series $\sum_1^n(\boldsymbol{p_{t,i}}\,\boldsymbol{w_i})$, which are next used as inputs to the forecasting problem.

Table 7.1 summarizes the correlation coefficients of each precipitation data set with the flow data, for two different lag values (0 and 1). It also includes the final weight rates for each case.

Table 7.1: Correlation and weight factor for the ten different precipitation stations

	St.Vlassios	Helidona	Granitsa	Karpenisi	Katafito
$correl\ (p_{t,i}\,;q_t)$	0.340	0.407	0.397	0.370	0.364
$correl\ (p_{t,i}\,;q_{t+1})$	0.420	0.500	0.523	0.476	0.402
w_i	0.073	0.138	0.158		

	Perdikaki	Pertoulio	Sargiada	Theodoriana	Viniali
$correl\ (p_{t,i}\,;q_t)$	0.393	0.491	0.325	0.542	0.394
$correl\ (p_{t,i}\,;q_{t+1})$	0.464	0.434	0.489	0.487	0.436
w_i	0.082	0.050	0.107	0.086	0.076

7.1.3 Efficiency metric to evaluate forecasting's accuracy

In order to calibrate the free parameters of each forecasting model and evaluate their predictive capacity, we introduce a quite strict skill score in terms of the generic efficiency formula:

$$F = 1 - \frac{\sum_{t=1}^{n}\left(E_{t,\,obs} - E_{t,\,forecast}\right)^2}{\sum_{t=1}^{n}\left(E_{t,obs} - E_{t,\,bencmark}\right)^2} \tag{7.1}$$

where $E_{t,\,obs}$ is the "observed" energy at day t, which is known from the simulation model, $E_{t,\,forecast}$ is the forecasted value, which is estimated on the basis of past data ($x_{t-1,}x_{t-2,},\dots$), and differs according to each approach as presented extensively in the next paragraphs, and $E_{t,\,bencmark}$ is a reference prediction, provided by a benchmark model.

In the classical definition of efficiency, a benchmark model coincides with the mean observation (thus the daily average energy production), yet here we also

apply a stricter benchmark prediction, i.e., the so-called naïve forecasting model $E_t = E_{t+1}$ (hereafter referred to as modified efficiency). The aforementioned expression ensures an efficiency up to 78%, for the entire period of historical data (1969-2008; see **Table 7.2**).

In **Figure 7.2** we present the timeseries of the produced energy in comparison with the naïve- benchmark model, for the hydrological period 1971-1972. In addition, in **Figure 7.3** we demonstrate, in the form of a scatter plot, the correlated relationship between energy production at t day and $t + 1$,through the 39 years of collected data.

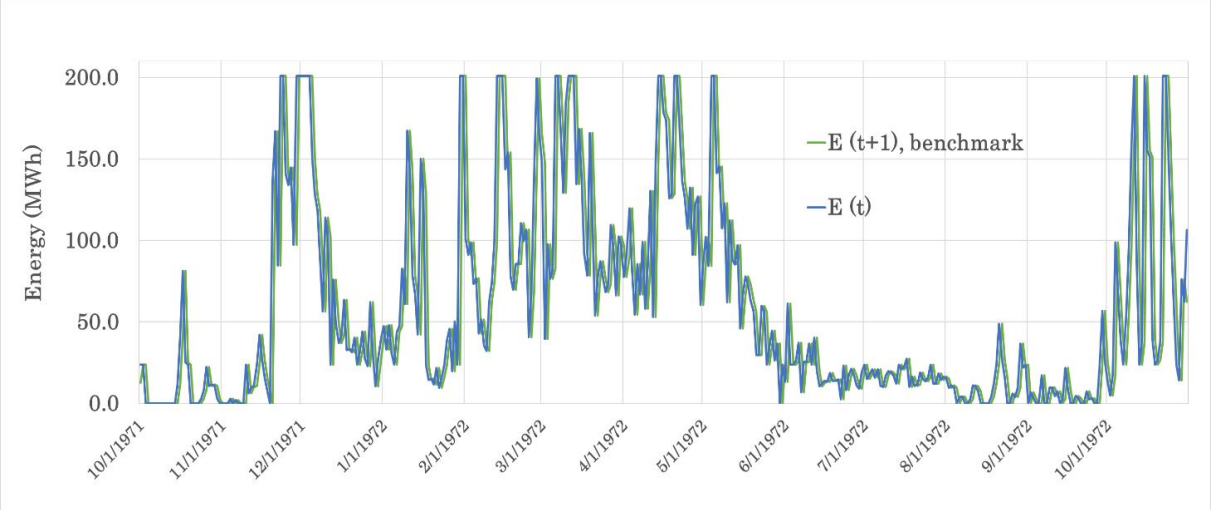

Figure 7.2 : Comparison of actual energy production with itself placed one day later (benchmark model) for hydrological year 1971-72.

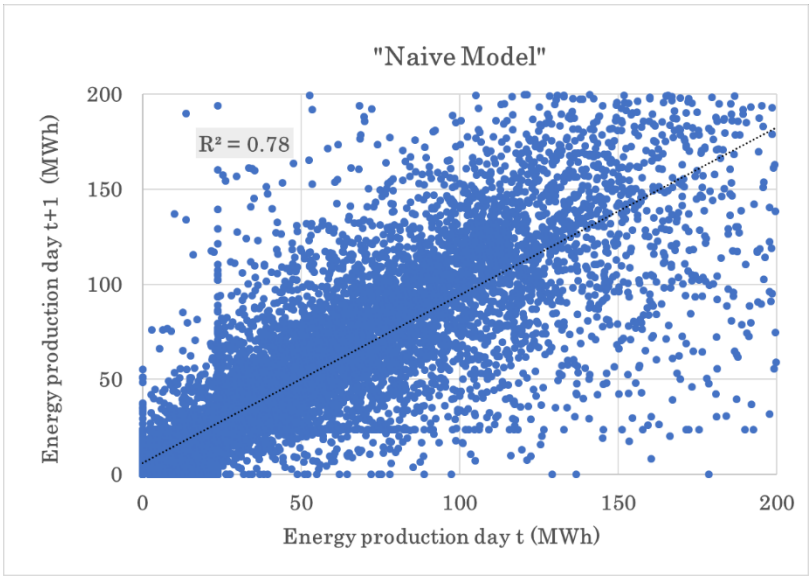

Figure 7.3 : Scatter plot of energy production at day t comparing to the energy production of the "Naïve model" at day t+1.

7.1.4 Direct (energy-based) approaches

In the direct approaches we use as independent variables (predictors) for the energy generated at time step (day) $t+1$,the past energy production, E, as well as the available hydrological data, by means of rainfall, p, from a representative meteorological station or the spatially-aggregated rainfall from a set of stations (paragraph 7.1.2). After investigations, we concluded to two possible models, for expressing the day-ahead energy, the "Generic Model" and "Crossroad Model".

Both models are expressed in the form of branched equations that take into consideration the appearance of a rainfall event at day t, which is expected to influence the generation of streamflow due to the increase of soil moisture over the basin. We highlight that the "Generic Model" **(7.2)** represents a simpler approach, since for minor precipitation events from the previous day, we assume an equal energy production as in the day before. On the other hand, the "Crossroad Model" **(7.3)**, is more complex ,yet more efficient (see **Table 7.2**), model since even for negligible precipitation events, is designed to relate the next day energy with the energy from the two previous days. Also, the "Generic Model" takes into consideration the extracted discharge of the day before.

$$E_{t+1} = \begin{cases} 4.79\,(E_t)^{0.48}\,(q_t)^{0.06}(E_{t-1})^{0.12}(p_t)^{0.15}, & p_t > 0.1\ mm \\ E_t, & p_t \le 0.1\ mm \end{cases} \tag{7.2}$$

$$E_{t+1} = \begin{cases} 3.88\,(E_t)^{0.54}(E_{t-1})^{0.12}(p_t)^{0.16}, & p_t > 0.1\ mm \\ 1.51\,(E_t)^{0.63}(E_{t-1})^{0.25}, & p_t \le 0.1\ mm \end{cases} \tag{7.3}$$

Following the typical split-sample approach, we estimated each model's parameters by calibrating against the actual energy production values in the half of observations, and validating its predictive capacity in the other half. From the aforementioned calculations the skill scores in calibration and validation, expressed in terms of classical and modified efficiency, which resulted, as well as the statistical characteristics of the model error, $w_t = E_{t,\,obs} - E_{t,\,forecast}$, are summarized in **Table 7.2 .**

In an effort to visualize the correlation of each direct (energy-based) forecasting model, with the energy which was actually produced, we present two representative figures for each one of the above approaches. Those being, a timeseries of the forecasted energy in comparison with the real energy produced (**Figure 7.4** and **Figure 7.6**) for the hydrological year 1971-72, and a scatter plot of the above values,(**Figure 7.5** and **Figure 7.7**) during the 39 years of our data set (May 1969 to December 2008).

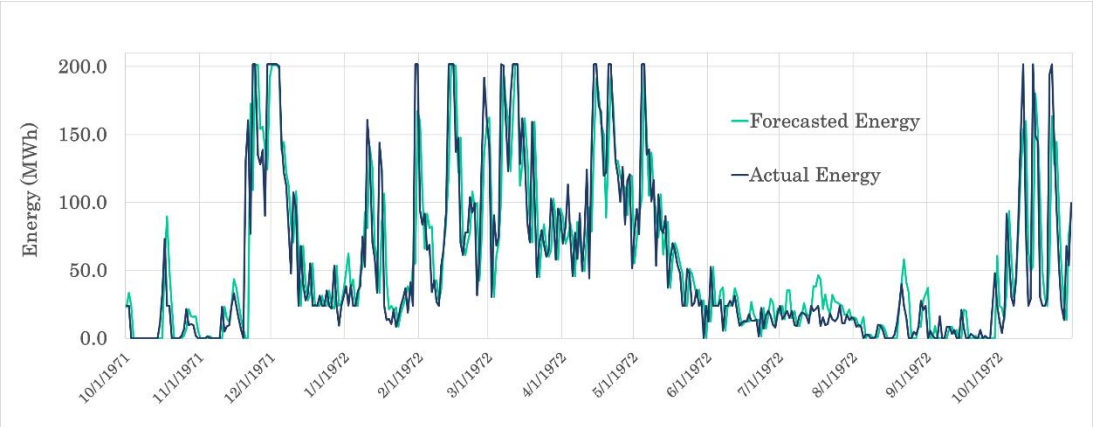

Figure 7.4: Comparison of actual energy production with the forecasted energy by the "Generic Model", during the hydrological year 1971-72.

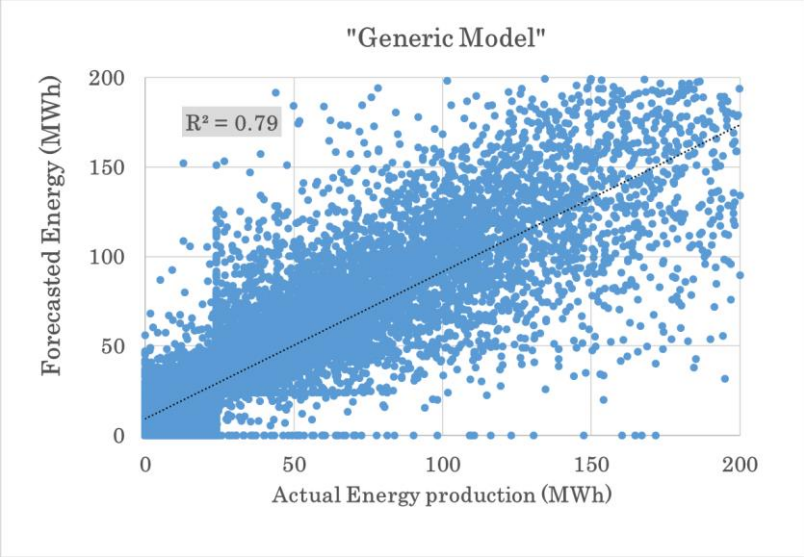

Figure 7.5 : Scatter plot of actual energy production comparing to forecasted energy by the "Generic model".

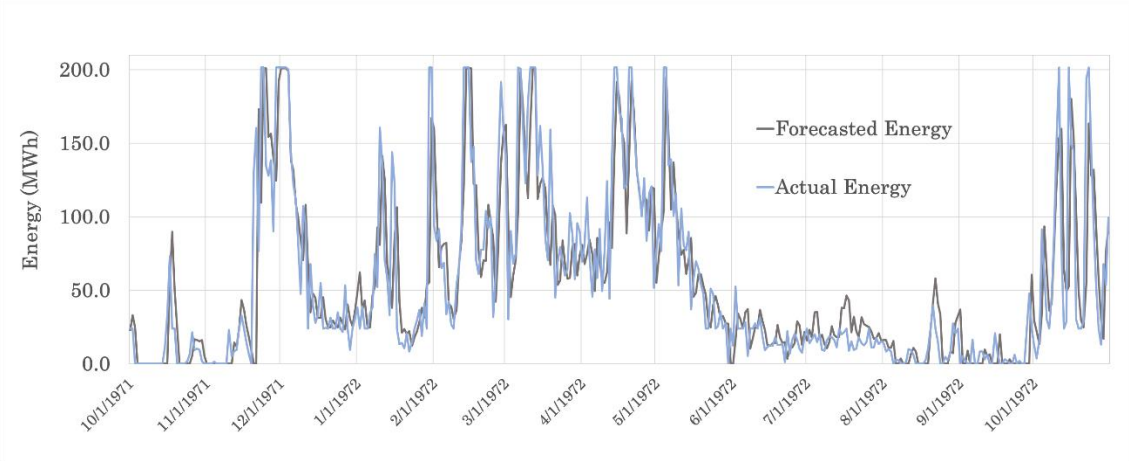

Figure 7.6 : Comparison of actual energy production with the forecasted energy by the "Crossroad Model", during the hydrological year 1971-72.

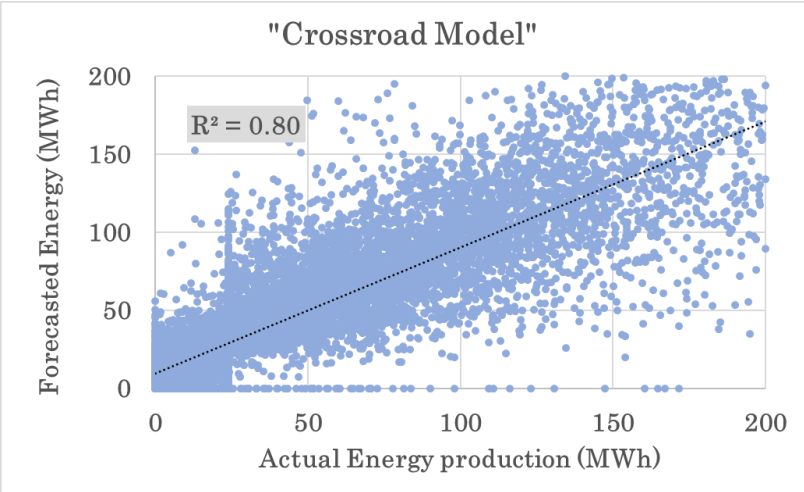

Figure 7.7 : Scatter plot of actual energy production comparing to forecasted energy by the "Crossroad Model".

As the above figures and **Table 7.2** summarize, the "Crossroad Model" in terms of classical efficiency surpasses slightly the "Generic Model", leading to the assumption that they are of same credibility, yet when we advise a stricter skill score, meaning the modified efficiency, the rate of exceedance of the Crossroad approach comparing to the Generic becomes clearer to us.

7.1.5 Indirect (flow-based) approaches

In the indirect approaches we aim to provide day-ahead forecasts of the discharge to feed the flow-energy conversion model, which is summarized in the diagram of **Figure 7.1** . In this respect we use as predictors, of streamflow at day $t+1$, the past streamflow and the rainfall. In order to account for the baseflow component of streamflow, we also extract the minimum value of last five days, q_{min5} , and the mean monthly value of the full data sample.

We remark that the baseflow component may incorporate several slow-flow elements, associated with groundwater runoff, snow melting (which is quite significant, during the spring period) as well as the falling limb of floods. After investigations, we conclude to the parametric expression:

$$q_{t+1} = \begin{cases} a_1\,(q_{min5}) + \beta_1(q_t) + \gamma_1(q_{meant}), & p_t < 0.1\ mm \\ a_2\,(q_{min5}) + \beta_2(q_t) + \gamma_2(q_{meant}) + \delta(p_t), & p_t \geq 0.1\ mm \end{cases} \tag{7.4}$$

The above expression can be defined by different values of its parameters, depending on under which conditions we calibrate the above model **(7.4)** by the use of a performance metric (Root Mean Square Error -RMSE) as goal for minimization.

In our case, the calibration was reached by two approaches, the one called "Simple Model" and the other "Smart Model". As it is indicated by their names, the

first approach is simpler since the calibration has as goal to ensure the optimal fitting of the modeled to actual discharge data by minimizing the RMSE. On the other hand, the second approach, is baptized with the characterization of *smart* , since it uses the knowledge about the technical properties of the system in the model calibration by minimizing the RMSE after taking into consideration that should count it only when the passing flow belongs into the limits of the turbines operation range, meaning that through the logic of the "Smart Model", errors are not been account for if the model correctly predicts that the flow is outside of the operation range.

As shown in **Table 7.2** , by employing a typical calibration on the basis of maximizing the efficiency of the simulated against the observed stream flows, in terms of day-ahead energy prediction we obtain a small only improvement with respect to the direct modelling approach, namely from 79.4("Generic Model"),79,9 ("Crossroad Model") to 80.7%("Simple Model") -for the full data.

On the other hand, the model error characteristics are less satisfactory, since the forecasting model underestimates the energy production by about -3.8 MWh, on average, while with the direct approach the bias is negligible. This is due to the attempt of the calibration procedure to predict stream flows outside of the operational range of turbines, and particularly the peak flows, which result to large errors. Yet, these errors are beyond our concerns, since during these periods the system operates continuously in its nominal capacity.

In order to remedy the above shortcomings, as we already have mentioned, we adjusted the fitting metric, i.e., RMSE, to the turbine operation range ($q_{min,tot}$, $q_{max,tot}$), in order to ignore the errors that are produced from the flow forecasting model, if this correctly predicts that the flows being outside this range. Moreover, if the forecasted flow is inside the range, whereas the observed is outside, we only account from the distance from the two flow limits. Under this premise, the error is calculated as follows:

$$e = \begin{cases} q_{max,tot} - q_{forecast}, & q_{obs} > q_{max,tot} \; and \; q_{forecast} < q_{max,tot} \\ q_{forecast} - q_{min,tot}, & q_{obs} < q_{min,tot} \; and \; q_{forecast} > q_{min,tot} \\ q_{obs} - q_{forecast}, & q_{obs} > q_{min,tot} \; and \; q_{obs} < q_{max,tot} \end{cases} \quad (5)$$

The above error expression incorporates within calibration, apart from the hydrological data, the expert's knowledge about the technical properties of the system that affect the flow-energy conversions. The knowledge-based calibration approach, herein called "Smart Model", ensures a clearly better skill score in terms of modified efficiency than the typical calibration approach (Indirect "Simple Model"), and good error properties as well (practically zero mean and autocorrelation-see **Table 7.2**).

In the following figures are presented the inflow timeseries which were predicted by each one of the indirect models, in comparison with the real inflow through the hydrological year 1971-72 (**Figure 7.8** and **Figure 7.12**).After using the forecasted discharge as input to the operational rule (Chapter **4.4**), we

received the energy production thus creating the energy timeseries resulting from the above models and setting in comparison with the actual energy production, as shown in **Figure 7.10 Figure 7.14** .Moreover, in order to have a more supervisory view, the scatter plots of both forecasted inflow and energy in relation with the real inflow and energy for the 39 years data, are provided through the **Figures 7.9,7.11,7.15,7.13**.

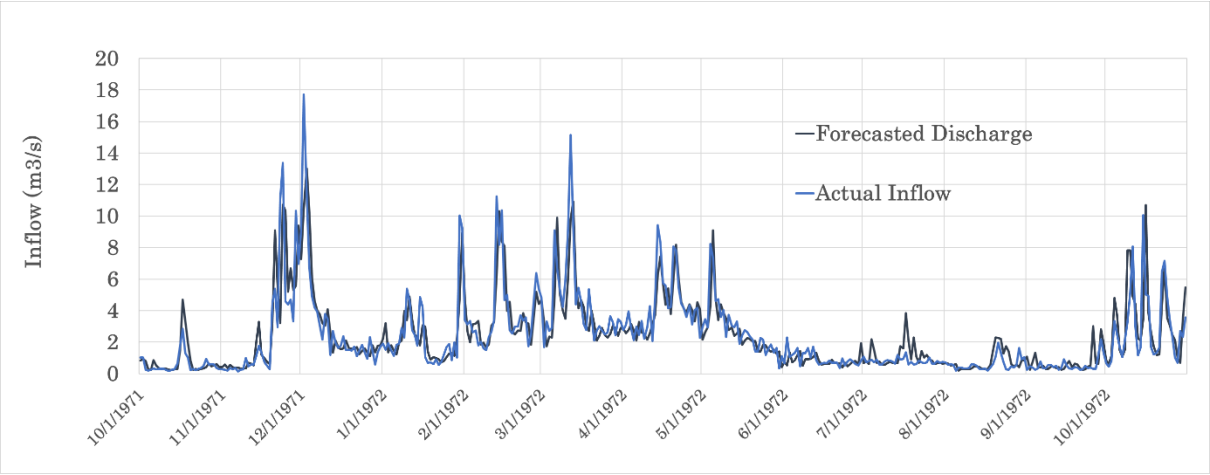

Figure 7.8 : Comparison of actual inflow with the forecasted discharge by the "Simple Model", during the hydrological year 1971-72.

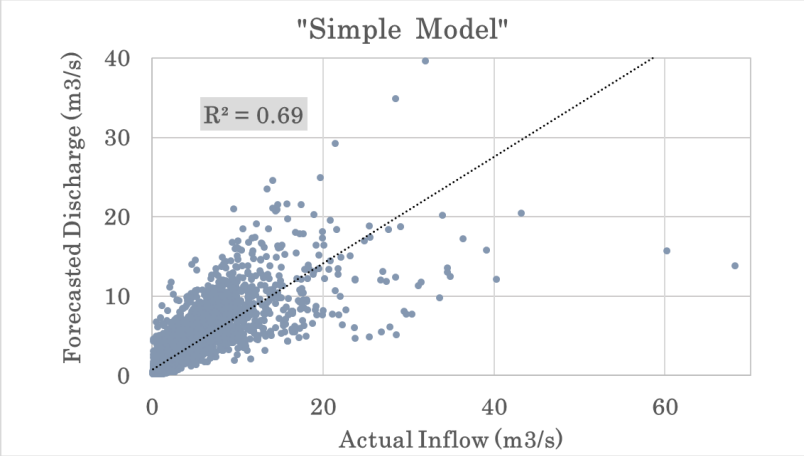

Figure 7.9 : Scatter plot of actual inflow comparing to forecasted discharge by the "Simple model".

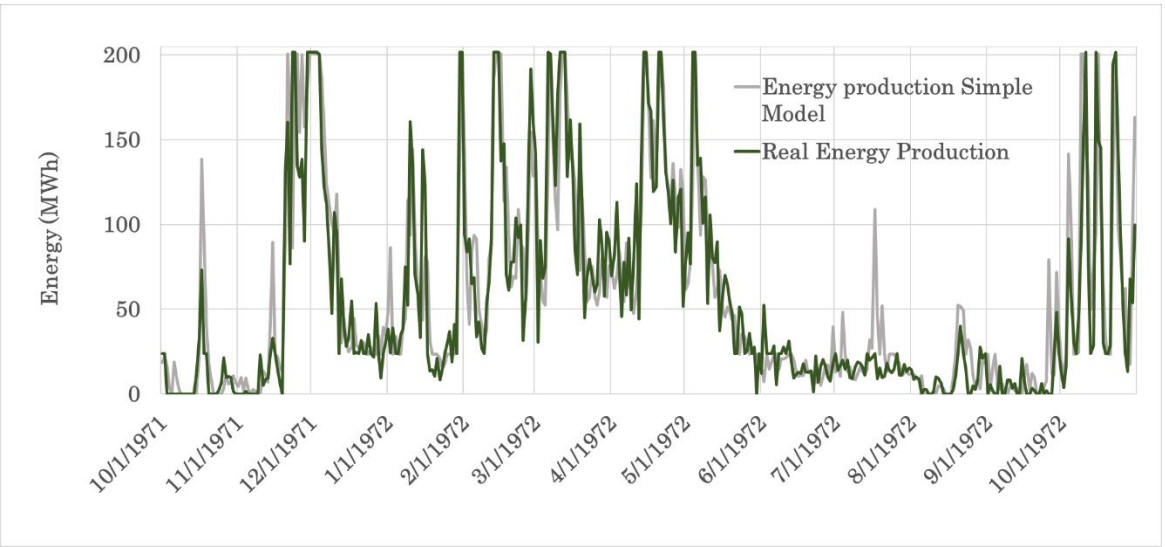

Figure 7.10 : Comparison of actual energy production with the resulting energy by the "Simple Model", during the hydrological year 1971-72

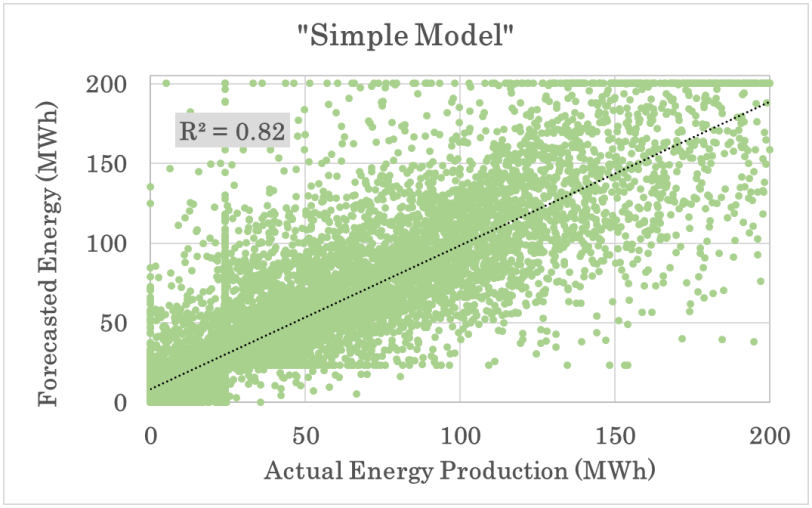

Figure 7.11 : Scatter plot of actual energy production comparing to resulting energy by the "Simple model".

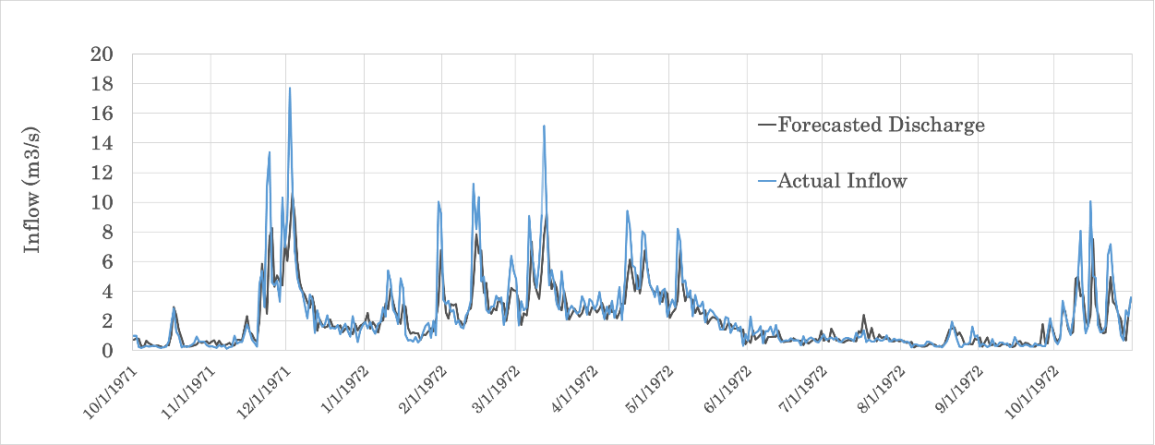

Figure 7.12 : Comparison of actual inflow with the forecasted discharge by the "Smart Model", during the hydrological year 1971-72.

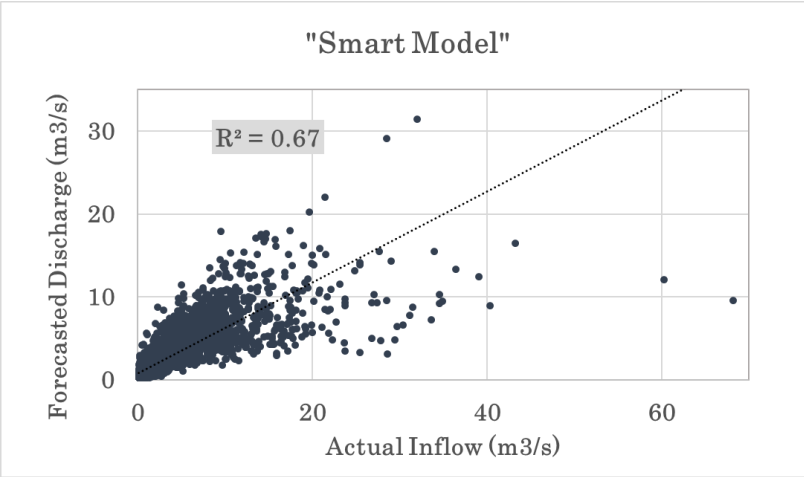

Figure 7.13 : Scatter plot of actual inflow comparing to forecasted discharge by the "Smart model".

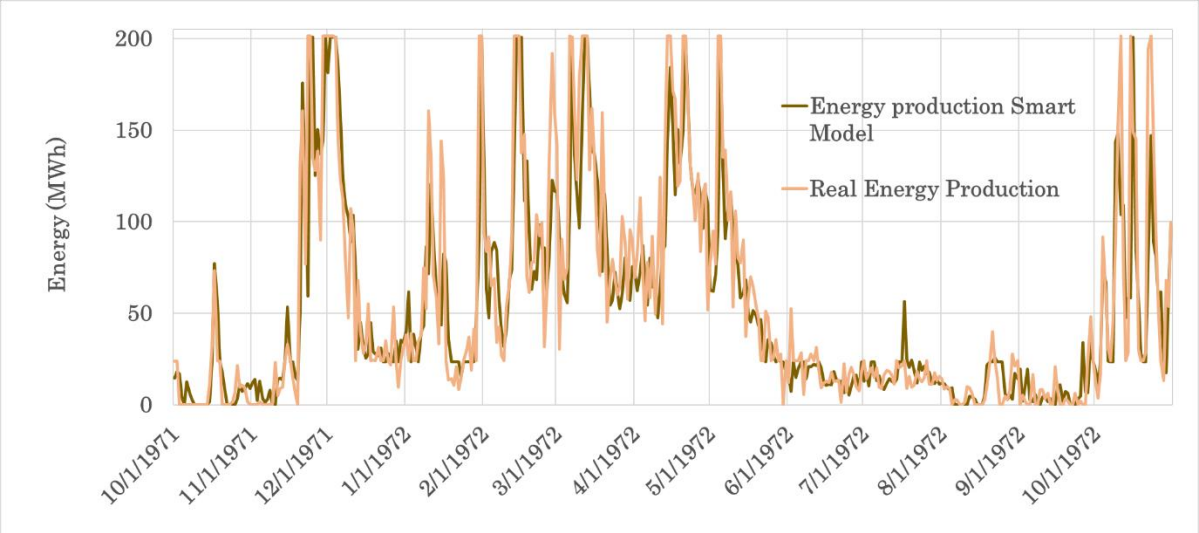

Figure 7.14 : Comparison of actual energy production with the resulting energy by the "Smart Model", during the hydrological year 1971-72.

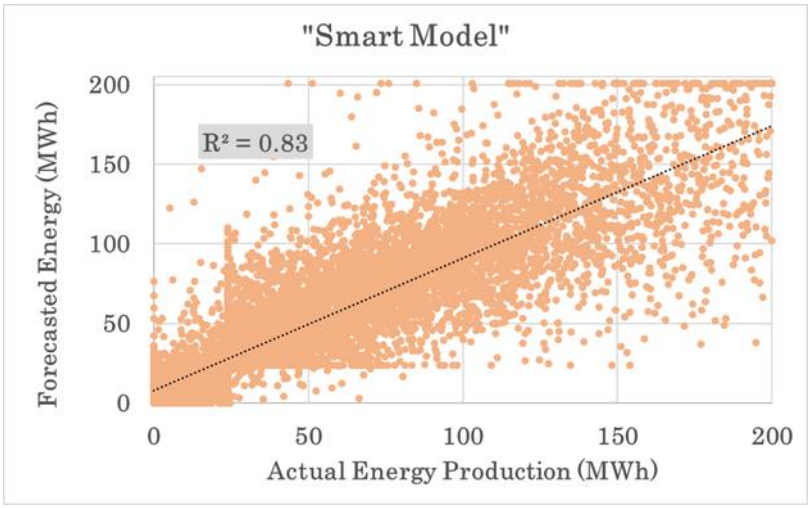

Figure 7.15 : Scatter plot of actual energy production comparing to resulting energy by the "Smart model".

7.1.6 Introduction to a Machine Learning approach

In addition to the aforementioned regression forecasting models, an interesting question arises on whether just a better day-ahead flow forecasting model that does not account for the operational characteristics of the system, would outperform the optimal model so far. In this respect, we apply a more complex approach from the Machine Learning (ML) family, namely a Deep Feedforward Neural Network (DNN). The DNN model is composed by three hidden layers with 128, 64 and 32 neurons, respectively, while the Rectified Linear Unit (ReLu) activation function is adopted for all neurons.

As inputs, we use the streamflow of past 5 days and the rainfall of past two days. The model is fitted on the basis of Mean Square Error (MSE), for a number of 100 epochs, by using a batch size of 64.

The results of the above approach are summarized through the **Figures 7.16, 7.18 , 7.19** and **7.21** , in terms of timeseries and scatter plots, of both inflow and energy compared to the real streamflow and actual resulting energy production.

In addition, in **Figures 7.17** and **7.20** we compare the actual and forecasted flow and energy values provided by the "Smart Model", as the most efficient model of the indirect approach, and the ML approach, for hydrological year 1971-72. Surprisingly, while the ML model ensures a much better fitting to the observed flows than the simple regression expression (4), (82% vs. 67%), the conversion to energy is rather disappointing. In particular, the classical efficiency metric is only 50.7%, while the modified efficiency is strongly negative. Therefore, the data-driven approach results to a worse predictive capacity even than the naïve benchmark model. Furthermore, the derived error properties are clearly non satisfactory (underestimation of the average energy up to 1 MW, quite large standard deviation, and, significant autocorrelation).

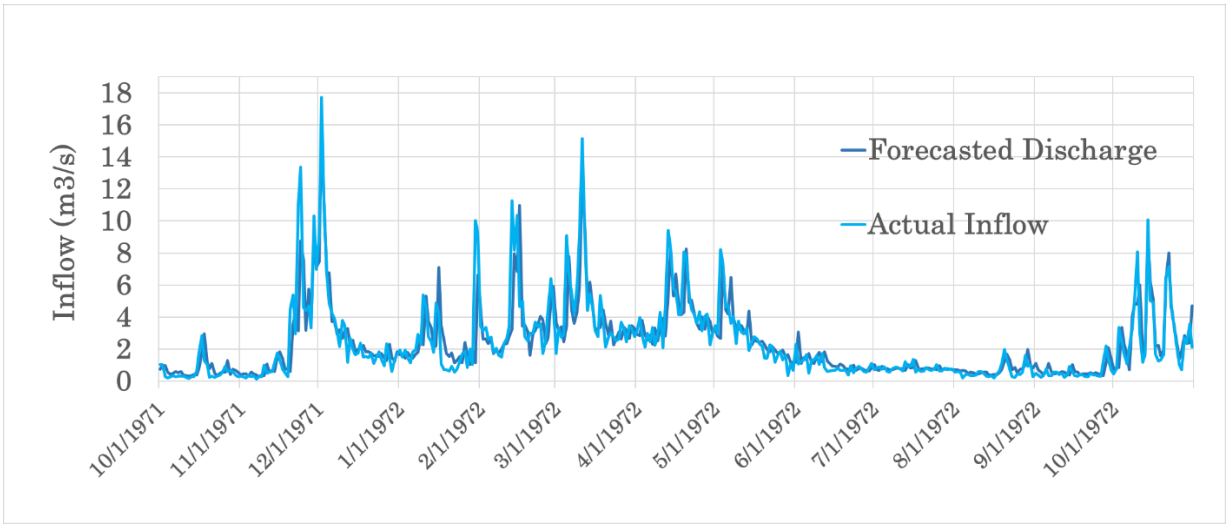

Figure 7.16 : Comparison of actual inflow with the forecasted discharge by the "DNN", during the hydrological year 1971-72.

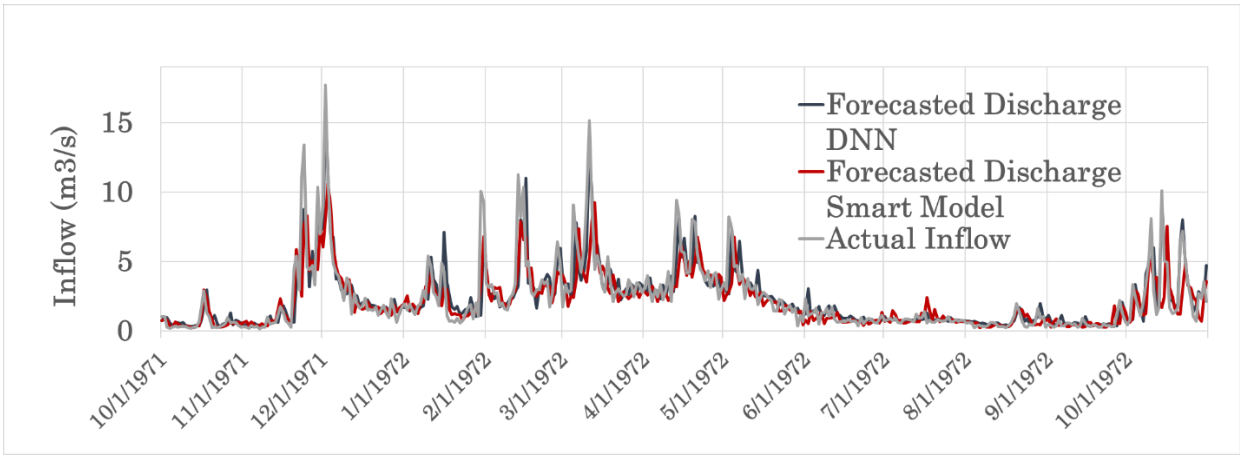

Figure 7.17 : Comparison of actual inflows with the forecasted ones from "DNN" and "Smart Model", during the hydrological year 1971-72.

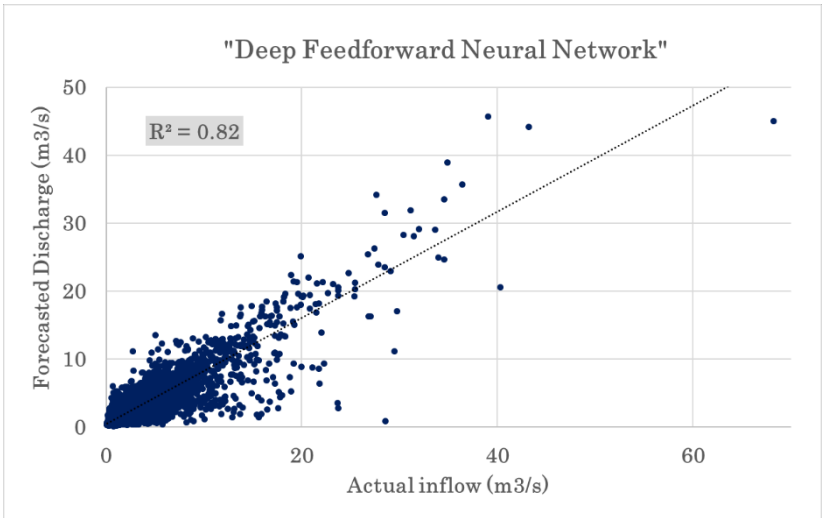

Figure 7.18 : Scatter plot of actual inflow comparing to forecasted discharge by the "DNN".

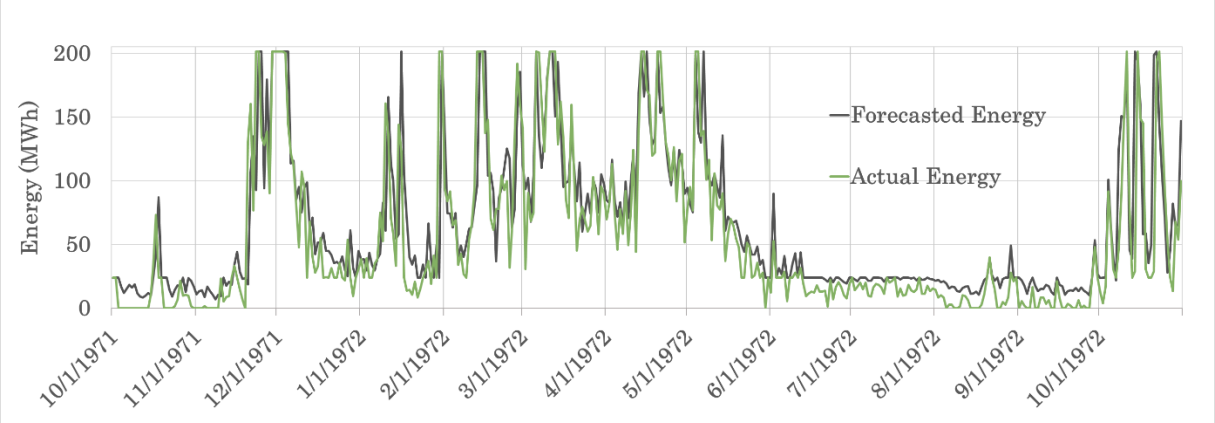

Figure 7.19 : Comparison of actual energy production with the resulting energy by the "DNN", during the hydrological year 1971-72.

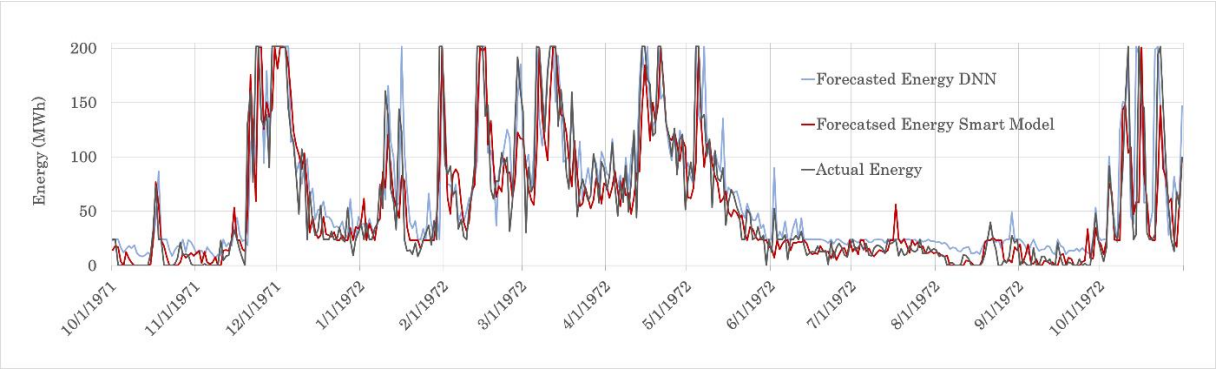

Figure 7.20 : Comparison of actual energy production with the resulting energy from "DNN" and "Smart Model", during the hydrological year 1971-72.

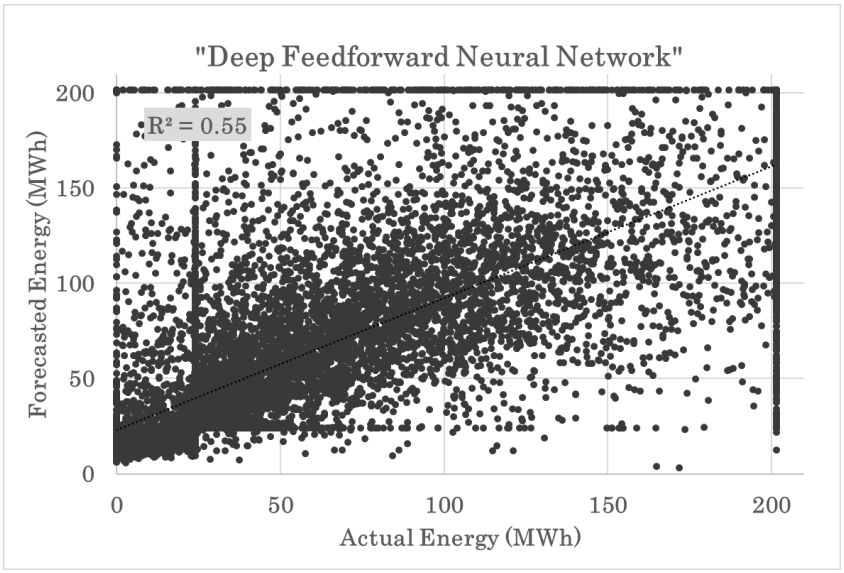

Figure 7.21 : Scatter plot of actual energy production comparing to resulting energy by the "DNN".

For each forecasting approach, we compute the marginal statistical characteristics of residuals, $w_t = E_{t,\,obs} - E_{t,\,forecast}$ (mean, standard deviation, coefficient of skewness) and the lag-1 autocorrelation, which is measure of auto-dependence (**Table 7.2**).**Table** 7.2 These are used in next chapter, where we establish a more integrated energy forecasting framework, which takes into account the model uncertainty.

Table 7.2 : Comparison of different forecasting schemes.

Model type	Efficiency of Energy			Modified efficiency of Energy			Energy error statistics			
	Calibr.	Valid.	Full data	Calibr.	Valid.	Full data	Mean (MWh)	St. dev. (MWh)	Coeff. of skewness	Lag-1 auto-correlation
Naïve	n/a	n/a	0.766	n/a	n/a	n/a	0.00	27.76	1.21	-0.119
Direct Generic	0.782	0.809	0.794	0.171	0.166	0.169	-1.11	25.28	1.34	-0.012
Direct Crossroad	0.790	0.813	0.799	0.201	0.182	0.193	-0.51	24.86	1.45	0.043
Indirect Simple	0.817	0.796	0.807	0.228	0.226	0.227	-3.83	24.11	-0.37	0.079
Indirect Smart	0.848	0.819	0.833	0.356	0.314	0.331	0.112	22.64	1.23	0.066
DNN	n/a	n/a	0.55	n/a	n/a	-0.977	-0.99	39.04	-0.42	0.540

8 Uncertainty through forecasting and their reconciliation in practice

8.1 Generator of ensembles to estimate uncertainty

A typical means to quantify the total uncertainty of a deterministic simulation model, is to add a random component (noise), w_t, to its output, y_t, where the random process w_t should be consistent with the statistical and stochastic regime of the associated residuals (Efstratiadis et al., 2015). In the generic case of autocorrelated errors, the process w_t can be obtained by a stochastic generator (e.g., Kossieris et al., 2019; Tsoukalas et al., 2020), or a statistical distribution model, provided that the errors do not exhibit significant dependencies in space and time. By generating a large enough set of random variables $y_{i,t}^{'} = y_t + w_{i,t}$, where $i = 1, \dots, n$, we obtain an ensemble of n model realizations at each time step t, which allows for the detection of empirically-derived probabilistic quantities. In our case, we use the more robust forecasting scheme ("Smart Model") and provide $n = 100$ realizations of the day-ahead energy at each time step (day), from which we get the median and the 10th and 90th largest values (quantiles) of forecasted energy production, as estimators of the 80% empirical confidence intervals.

8.1.1 Statistical distribution to describe residual ensemble

Given that the observed residuals resulting from the "Smart Model" are uncorrelated, the errors are considered as a stationary process that follows a three-parameter gamma distribution (i.e., Pearson type III), which reproduces the mean value, μ_e, the standard deviation, σ_e, and the coefficient of skewness, γ_e, of the entire sample of residuals (**Table 7.2**).The expression of the above distribution with its parameters are defined according to the following equation (**eq. 8.1,8.2**).

$$f_x(x) = \frac{\lambda^\kappa}{\Gamma(\kappa)}(x-c)^{\kappa-1}e^{-\lambda(x-c)} \tag{8.1}$$

where κ, λ and c are shape, scale and location parameters, respectively, which are estimated by the method of moments as follows :

$$\kappa = \frac{4}{{\gamma_e}^2} \qquad \lambda = \frac{\sqrt{\kappa}}{\sigma_e} \qquad c = \mu_e - \kappa/\lambda \tag{8.2}$$

Following, we produce the 100 realizations of the day-ahead energy, we first result to a stationary representation of the forecasting uncertainty in energy production through the years, since the different weather conditions depending the seasonality and specifically the monthly customization of the errors statistical characteristics have not been taken into consideration.

In addition, through **Figure 8.1** ,we present the timeseries for hydrological year 1971-72 in which we compare the actual energy production with the three characteristic prediction quantiles (10, 50 and 90%). The aftermath for developing a stationary model , is as shown in more details in **Figures 8.2** and **8.3** that through summer the forecasting is characterised by high range of uncertainty since the statistical characteristics of those dry months are equalized with the ones of the much wet months of autumn and winter season.

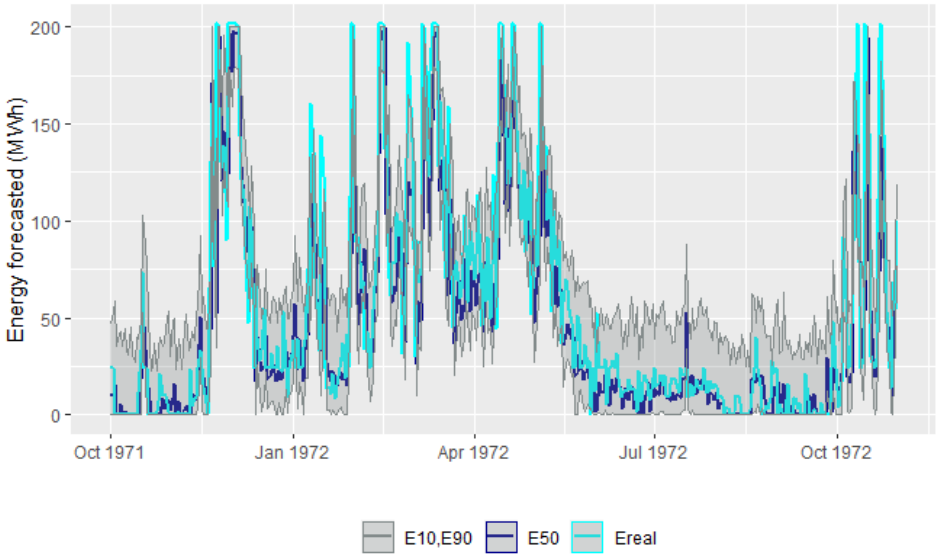

Figure 8.1 : Comparison of actual energy production for hydrological year 1971-72 with three characteristic prediction quantiles (10, 50 and 90%), by considering the error process as stationary.

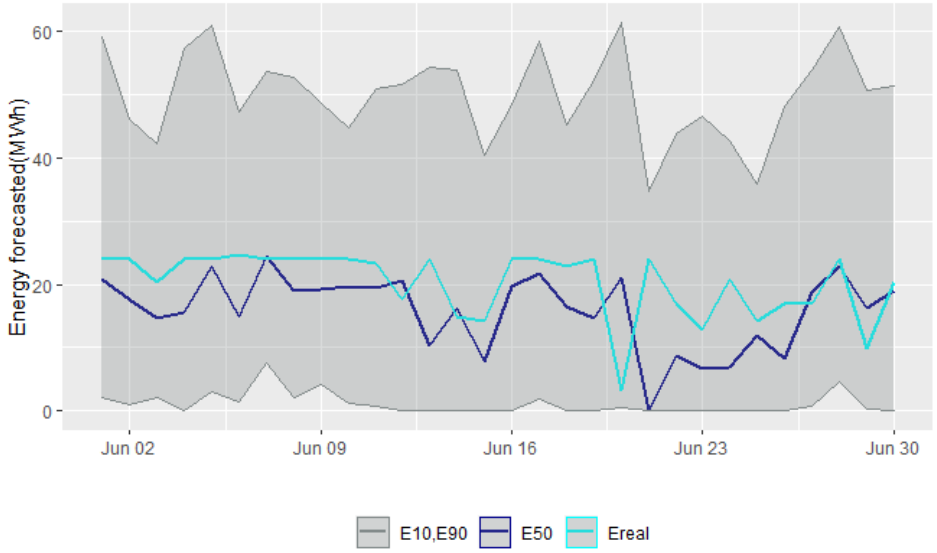

Figure 8.2 : Detailed comparison of actual energy production for year 1972 with three characteristic prediction quantiles (10, 50 and 90%), by considering the error process as stationary, for the month of June.

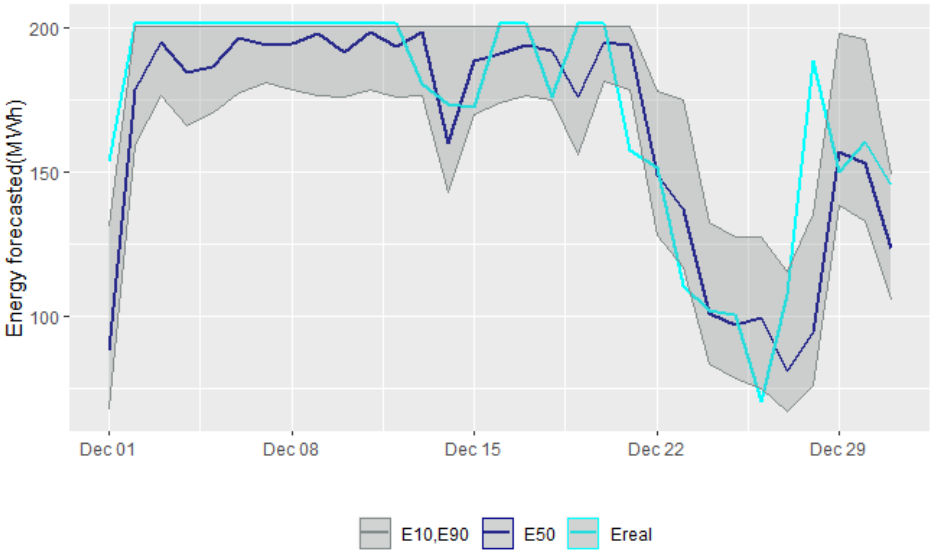

Figure 8.3 : Detailed comparison of actual energy production for year 1971 with three characteristic prediction quantiles (10, 50 and 90%), by considering the error process as stationary, for the month of December.

8.1.2 Accounting for seasonality within uncertainty quantification

In order develop a more credible and more consistent with the underlying hydrological regime forecasting procedure under uncertainty, we implement the same error modelling analysis by applying seasonally-varying (cyclostationary) generation models, which accounts for the individual statistical characteristics per month (Tsoukalas et al., 2018). As shown in **Table 3.1** , these is a considerable difference of the statistical behavior of the error across different seasons, that is also reflected in the uncertainty of energy predictions. In **Figure 8.4** we compare the uncertainty bounds obtained by the two methods, for hydrological year 1971-72. In combination with **Figures 8.5** Figure 8.5 and **8.6** Figure 8.6 we observe that during the low-flow period, these bounds are substantially reduced, by accounting for the issue of seasonality. This indicates that the more detailed analysis, where the prediction error is represented as a cyclostationary process, is much more realistic.

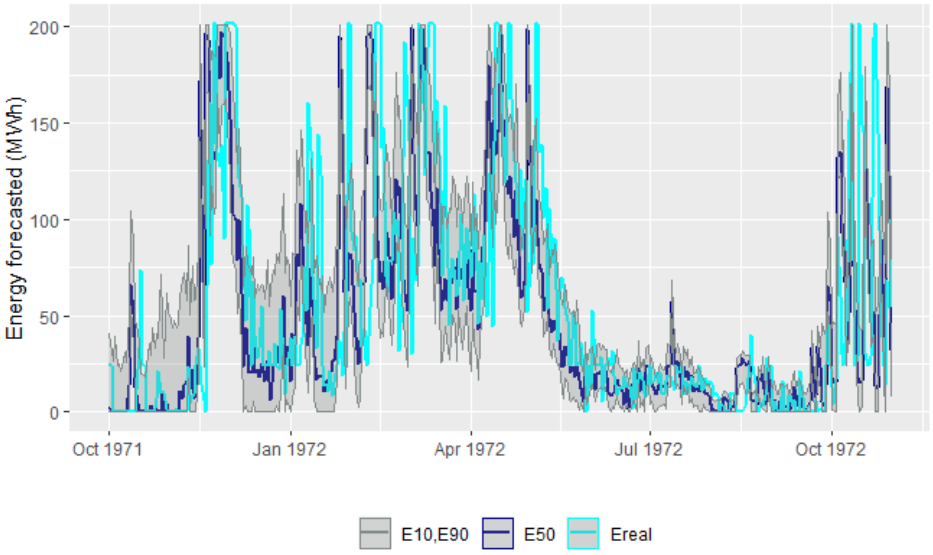

Figure 8.4 : Comparison of actual energy production for hydrological year 1971-72 with three characteristic prediction quantiles (10, 50 and 90%), by considering the error process as cyclostationary.

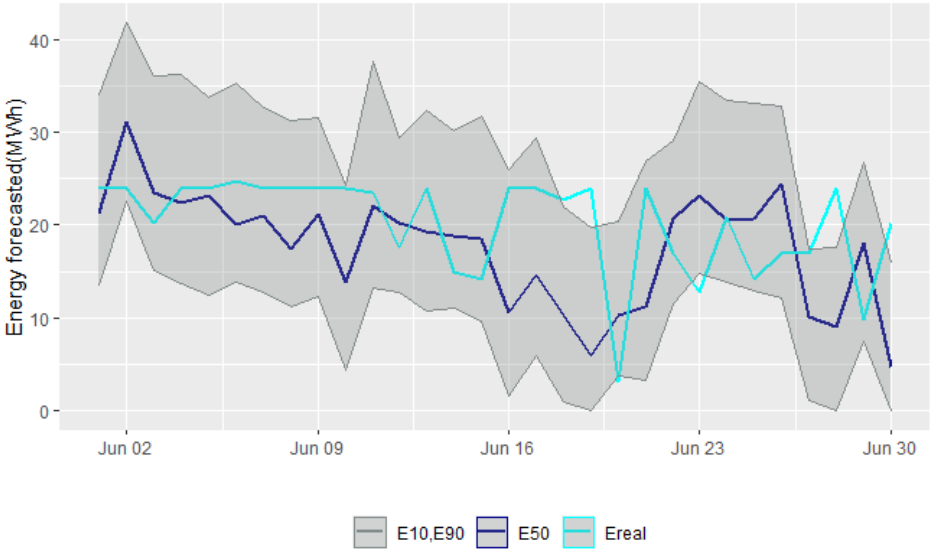

Figure 8.5 : Detailed comparison of actual energy production for year 1971 with three characteristic prediction quantiles (10, 50 and 90%), by considering the error process as cyclostationary, for the month of June.

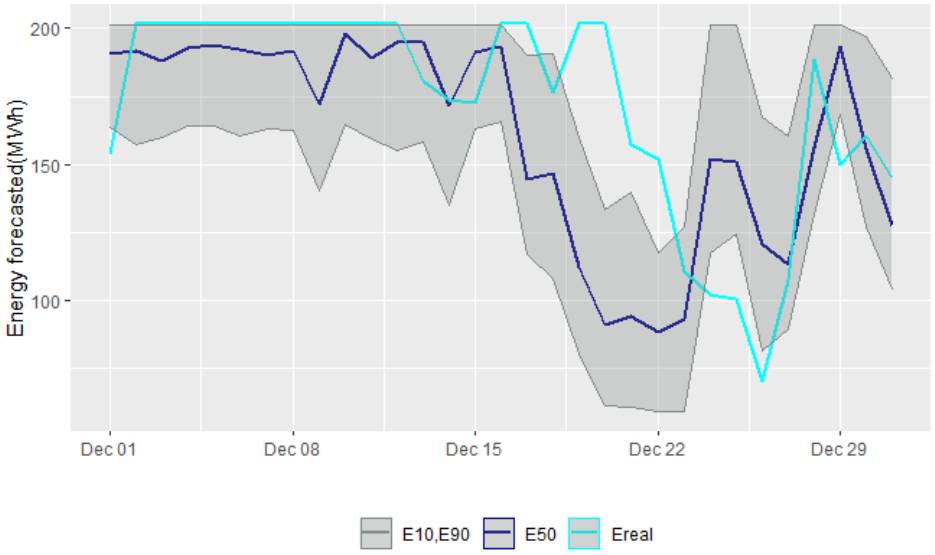

Figure 8.6 : Detailed comparison of actual energy production for year 1971 with three characteristic prediction quantiles (10, 50 and 90%), by considering the error process as cyclostationary, for the month of December.

Table 3.1 : Monthly statistical characteristics of residuals derived from the application of Smart Model.

Month	Mean (MWh)	Standard deviation (MWh)	Skewness	Lag-1 correlation
JAN	0.82	28.65	1.23	0.069
FEB	1.59	29.07	0.87	0.138
MAR	4.87	28.05	0.95	0.066
APR	1.91	26.53	0.48	0.059
MAY	1.53	19.06	1.37	0.089
JUN	-0.16	8.42	0.95	-0.062
JUL	0.11	7.74	-0.25	-0.014
AUG	-0.72	7.11	-1.85	0.056
SEP	-1.91	11.06	-1.39	0.044
OCT	-2.51	20.75	1.76	-0.050
NOV	-0.45	31.51	1.34	0.043
DEC	-2.74	30.64	0.84	0.045

8.2 Alternative market policies

In order to take advantage of the concept of uncertainty in practice, as would be made in a real-world energy market, we can determine alternative market policies in terms of quantiles. In particular, we can apply the upper, middle and low quantiles as representatives of a risky, mild and conservative forecast of the day-ahead energy, predicted from our most credible approach, the "Smart Model" and evaluate them in economic terms, by assigning a unit profit value for delivering the energy produced up to the forecasted value, and a unit penalty for the deviations (i.e., deficits with respect to the forecasted value). For instance, we account for the 90, 50 and 10% quantiles and apply a fixed profit of 60 €/MWh, a price for secondary energy equally to 30€/MWh and a penalty value of 50 €/MWh; the aforementioned values are representative of the recent system marginal price and price of deviations, respectively, of the Hellenic Electricity Market. Under this premise, the mild policy ensures a mean annual profit of 0.86 M€, the conservative 0.81 M€, and the risky 0.43 M€. This quick pseudo-financial analysis allows for comparing the different interpretations of a forecasting approach under uncertainty. In **Figure 8.7** we mention the profit resulting from the three above market policies through the year 1971-72 in relation with the profit that we would gain if the forecasting was ideal, meaning to have zero uncertainty thus predicting the actual energy production (Real profit).

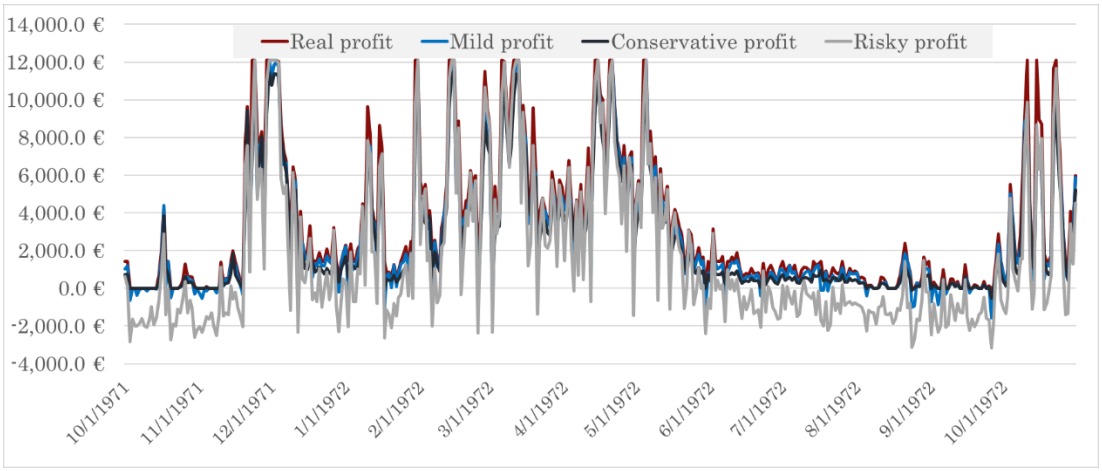

Figure 8.7 : Representation of profit produced from three alternative market policies in comparison with the actual profit, for hydrological year 1971-72.

9 Model simulation in R environment

9.1 Data information produced in excel environment

The calculations which were first conducted through Excel, and next transferred in R environment, are the following :

- Optimization of the operational rule of the turbine mixing, thus the optimal energy production for given inflow timeseries.
- Optimal calibration of each forecasting model (direct, indirect) in terms of maximizing the efficiency skill score.

9.2 Calculations in R

After obtaining from excel the forecasted discharge, derived from our most efficient approach, "Smart Model" in combination with its resulting optimal energy production (synergetic operational rule), we proceed to define the uncertainty of our forecasting through the following algorithm :

- First, we create a function (**P3params**) which calculates the three parameters of the selected gamma distribution (i.e., Pearson type III) that the statistical characteristics of energy residuals follow. The above function has as insert values the following [1 x 12] vectors :
- 1. m: mean value of each month's forecasted energy production;
  2. s: standard deviation of each month's forecasted energy production;
  3. Csk: skewness of each month's forecasted energy production.
- In addition we create the code which will return the residual value (**x**) expressed by the gamma distribution and the aforementioned parameters, through the function named as **rp3**.

```
P3params<-function(m,s,csk) {

  k=4/(csk^2) # shape
  l=sqrt(k)/s # scale
  ci=ifelse(csk>=0,m-k/l,m+k/l) # location
  l=1/l
  return (list("k"=k,"l"=l,"ci"=ci))

}

rp3=function(n, shape, scale, location, csk) {

  if (csk<0) {
   x= -rgamma(n =1, shape = shape, scale =  scale) + location

  } else {
    x= rgamma(n = 1, shape =  shape, scale = scale) + location

  }

  return(x)
}
```

Figure 9.1 : Definition of gamma distribution residual value and its parameters.

To continue, we call the above functions and set as inputs the values defined as before and named through our code with the following correspondence :

1. "Statistics_of_eah_month_final_matrix" is a [12 x 4] matrix, each line represents the equivalent month and columns 1,3 and 4 express the values m,s and Csk respectively;

```
params=list()

for (i in 1:12) {
  params[[i]]=P3params(m =Statistics_of_eah_month_final_matrix[i,1],
                       s = Statistics_of_eah_month_final_matrix[i,3],
                       Csk =Statistics_of_eah_month_final_matrix[i,4] )
  }
```

Figure 9.2 : Call of params function for calculating the parameters of the gamma distribution according to the statistical characteristics of each month's data.

2. M corresponds with the third column of the matrix named "data" and accounts for the month which each forecasted value belongs to;
3. "DEfor_gam" is a [14474 x 100] matrix and its values represent the 100 different scenarios of each day, for our 39 years of data collection. The above ensemble of energy residuals is calculating by calling the function **rp3.**

```
for (i in 1: 14474 ){

  M=data[i,3]

  for (j in 1:100){


    DEfor_gam[i,j]=rp3(n=1,shape=params[[M]]$k,location = params[[M]]$ci,
                       scale = params[[M]]$l,
                       csk = Statistics_of_eah_month_final_matrix[M,4])
    }
}
```

Figure 9.3 : Calling of rp3 function for producing the ensemble of energy residuals.

4. "energyfinal" is the final matrix, in which we gathered the final energy production data, by adding to the forecasted energy production (**data [j,5]**) the value of deviation (**DEfor_gam [j,i]**) thus expressing the uncertainty of weather prediction and modeling calibration.

```
energyfinal=matrix(NA,nrow=14474,ncol=100)

for (i in 1:100) {
  for (j in 1:14474) {

    energyfinal[j,i]=max(0,min(Emax,data[j,5]+DEfor_gam[j,i]))

  }

}
```

Figure 9.4 : Defining the forecasted energy production, after considering the factor of uncertainty.

5. Lasty, we created three vectors, "energylarge", "energylow" and "energymedian" for expressing the three characteristic quantiles (10%,90%,50% respectively) of energy production from our best forecasting approach.

```
energylarge=c()
energylow=c()
energymedian=c()
for (i in 1:14474){

  #load Rfast package

  energylarge[i]=nth(energyfinal[i,],10,descending=TRUE)
  energylow[i]=nth(energyfinal[i,],10,descending =FALSE )
  energymedian[i]=nth(energyfinal[i,],50,descending =FALSE )}
```

Figure 9.5 : Defining the three characteristic quantiles of energy production (10%,90%,50%)

10 Conclusions

10.1 Summary and innovations

Through this research, two were the main fields that we aimed to investigate and contribute to. Both are associated with the everyday management of small hydropower plants, where the key objective is the optimal energy production. The first research field approaches this problem in terms of turbine scheduling and the other in terms of efficient forecasting of the day-ahead energy.

In more details, our first area of research handled the challenge of optimizing the scheduling of turbine systems, given its technical characteristics, such us type, nominal power, and flow-efficiency curves. Through this attempt, we introduced an optimal operational policy, named "Synergetic rule", and proved that it outperforms the hierarchical rule across two specific areas of the feasible operation range of the system, named as "Donation areas I and II". Donation area I starts at $q_{1,min}$ where all discharge is conveyed to the small instead of the large turbine, meaning the former operates with its maximum efficiency. On the other hand, donation area II starts at $q_{1,max}$, where the discharge which is conveyed to the large turbine is reduced by $q_{2,max}$, in order to feed the small turbine with its maximum discharge and thus operating with its maximum efficiency. This policy is applied until the system reaches its total power capacity, thus $q = q_{1,max} + q_{2,max}$. The two operation policies have been contrasted by taking as example a real-world SHPP, also used in the investigations of the day-ahead energy forecasting problem.

In order to establish a rigorous theoretical framework for the "Synergetic rule", we expressed the problem in dimensionless form, using generic formulas for multiple potential combinations of turbines. In order to investigate the impacts of two key design characteristics, namely the turbine type and their minimum operation point (which differs significantly across different turbine types, particularly for Francis machines), with respect to the sharing factor φ, we created two types of theoretical experiments. The first refers to different combinations of the above values focusing on how its combination affects the relationship between the power produced by our established optimal operational rule (after been fitted to the values of each combination) and by an ideal operational rule with turbine efficiency equals to 100%. The second experiment uses the same combinations, with the difference that the relationship which we investigate is between the power produced by the hierarchical rule and the optimal, synergetic, rule. Our extended analyses allowed to obtain a broader knowledge regarding the connection among some basic characteristics of turbine systems and the resulting total efficiency for numerous potential combinations.

Our second domain of interest was the problem of day-ahead power forecasting in the case of small hydropower plants without storage capacity, which has

(surprisingly) received little attention so far. Taking as an example a typical project of this category, and by using simple yet effective modeling schemes, we attempted to revisit several issues that may have been well-addressed in the generic context of hydrological forecasting, but not in the specific case of SHPPs, namely:

(a) the essential information as input to hydropower forecasting;

(b) the advantages of the indirect forecasting approach, involving the use of a streamflow forecasting model, against the direct one, that does not account for the inflow input, but relies solely on the energy production data;

(c) the importance of past precipitation data as exogenous predictor, providing macroscopic information about the catchment state (e.g. antecedent soil moisture conditions);

(d) the training procedure and the skill score to be applied;

(e) the representation of the predictive uncertainty around the point forecast of day-ahead energy;

(f) and the use of uncertainty-aware forecasts from the practicians' point-of-view (investors, power engineers, stakeholders).

Our investigations indicated that the proposed flow-based approach is more flexible and physically consistent, since it provides forecasts of the hydropower system's driver, i.e., the inflow arriving at the intake. We also revealed that apart from the inflow data per se, additional information should be introduced within prediction schemes in order to better reflect our hydrological knowledge, in terms of statistical characteristics. In the particular example, these were the mean monthly inflows and the past five-day average values, as representative of the long and short-term regime of the upstream catchment, respectively. However, it is worth mentioning that even a very good prediction of inflows (as quantified in terms of efficiency), does not guarantee an equally good performance in energy prediction. Equivalently important is the training procedure and the associated performance measure, where the system's characteristics, i.e., the range of operation of turbines, are embedded as inputs to calibration.

Key outcome of this research was also the quantification of uncertainty, by means of empirical quantiles, which were estimated through a Monte Carlo approach, after fitting a suitable probability distribution to the model residuals. This task, although proved to be simple and effective in its implementation, requires more careful examination, including analysis of the error properties and their seasonal variability, as well as could be benefited from more advanced concepts and tools, such as copulas and conditional non-Gaussian distributions (cf. Tsoukalas, 2018, for a development of this kind). Nevertheless, the interpretation of uncertainty is essential as a guidance for modelling energy market behaviors and providing decision support in the Target model era.

10.1 Future research goals

Regarding the first area of research, an interesting point for further investigation is the evaluation of the real gain from the implementation of the synergetic instead of the hierarchical operation policy across different flow regimes.

As far it concerns the day-ahead energy forecasting problem, there is a plethora of options offered by state-of-the-art approaches, from weather prediction tools to advanced artificial intelligence techniques. In this respect, one of our future goals could be the enrichment of the DNN approach with the technical information thus defining the Mean Square Error (MSE) metric in a more realistic form. The expected outcome will be an even more efficient energy production forecasting than the so far best, meaning the Smart model. However, it is important to remark the risk of employing more advanced approaches, both in terms of complexity and uncertainty. From the user's perspective, the significant requirements by means of computational tools and expertise may pose significant obstacles towards using such solutions in the everyday practice. In this vein, the ultimate challenge from our perspective is ensuring a good balance between the effectiveness and accuracy of forecasting methods, on the one hand, and the limited human, technical and financial resources, as well as the limited data availability, on the other.

References

Cassagnole, M., Ramos, M.-H., Zalachori, I., Thirel, G., Garçon, R., Gailhard, J., and Ouillon, T.: Impact of the quality of hydrological forecasts on the management and revenue of hydroelectric reservoirs – a conceptual approach, Hydrol. Earth Syst. Sci., 25, 1033–1052, https://doi.org/10.5194/hess-25-1033-2021, 2021.

Croonenbroeck, C., and Stadtmann, G.: Renewable generation forecast studies – Review and good practice guidance, Renew. Sust. Energ. Rev., 108, 312–322, https://doi.org/10.1016/j.rser.2019.03.029, 2019.

Efstratiadis, A., Tegos, A., Varveris, A., and Koutsoyiannis, D.: Assessment of environmental flows under limited data availability – Case study of the Acheloos River, Greece, Hydrol. Sci. J., 59(3-4), 731–750, https://doi.org/10.1080/02626667.2013.804625, 2014.

Efstratiadis, A., Nalbantis, I., and Koutsoyiannis, D.: Hydrological modelling of temporally-varying catchments: Facets of change and the value of information, Hydrol. Sci. J., 60 (7-8), 1438–1461, https://doi.org/10.1080/02626667.2014.982123, 2015.

Felder, M., Sehnke, F., Ohnmeiß, K., Schröder, L., Junk, C., and Kaifel, A.: Probabilistic short term wind power forecasts using deep neural networks with discrete target classes, Adv. Geosci., 45, 13–17, https://doi.org/10.5194/adgeo-45-13-2018, 2018.

Kossieris, P., Tsoukalas, I., Makropoulos, C., and Savic, D.: Simulating marginal and dependence behaviour of water demand processes at any fine time scale, Water, 11(5), 885, https://doi.org/10.3390/w11050885, 2019.

Li, G., Li, B.-J., Yu, X.-G., and Cheng, C.-T.: Echo state network with Bayesian regularization for forecasting short-term power production of small hydropower plants, Energies, 8(10), 12228-12241, https://doi.org/10.3390/en81012228, 2015.

Monteiro, C., Ramirez-Rosado, I. J., and Fernandez-Jimenez, L. A.: Short-term forecasting model for electric power production of small-hydro power plants, Renew. Energ., 50, 387-394, https://doi.org/10.1016/j.renene.2012.06.061, 2013.

Papacharalampous, G., Tyralis, H., Langousis, A., Jayawardena, A. W., Sivakumar, B., Mamassis, N., Montanari, A., and Koutsoyiannis, D.: Probabilistic hydrological post-processing at scale: Why and how to apply machine-learning quantile regression algorithms, Water, 11(10), 2126, https://doi.org/10.3390/w11102126, 2019.

Ólafsson, H., and Ágústsson, H.: Mesoscale orographic flows, in: Ólafsson, H., and Bao, J.-W., Uncertainties in Numerical Weather Prediction, Chapter 11, 297-308, Elsevier, https://doi.org/10.1016/B978-0-12-815491-5.00011-2, 2021.

Papantonis, D. E.: Small Hydroelectric Works, 2nd edition, Symeon Editions, Athens, 2008 (in Greek).

Ribeiro, M. T., Singh, S., and Guestrin, C.: Why should I trust you? Explaining the predictions of any classifier, Proceedings of the 22nd ACM SIGKDD International Conference on Knowledge Discovery and Data Mining, 2016.

Sakki, G.-K., Tsoukalas, I., and Efstratiadis, A.: A reverse engineering approach across small hydropower plants: a hidden treasure of hydrological data?, Hydrol. Sci. J., https://doi.org/10.1080/02626667.2021.2000992, 2021a.

Sakki, G.-K., Tsoukalas, I., P. Kossieris, and Efstratiadis, A.: A dilemma of small hydropower plants: Design with uncertainty or uncertainty within design?, EGU General Assembly 2021, online, EGU21-2398, European Geosciences Union, https://doi.org/10.5194/egusphere-egu21-2398, 2021b.

Mamassis, N., Efstratiadis, A., Dimitriadis, P., Iliopoulou, T., Ioannidis, R., & Koutsoyiannis, D. (2021). Water and Energy. In Handbook of Water Resources Management: Discourses, Concepts and Examples (pp. 619–657). Cham: Springer International Publishing.

Talari, S., Shafie-Khah, M., Osório, G. J., Aghaei, J., and Catalão, J. P. S.: Stochastic modelling of renewable energy sources from operators' point-of-view: A survey, Renew. Sust. Energ. Rev., 81, 1953-1965, https://doi.org/10.1016/j.rser.2017.06.006, 2018.

Tsoukalas, I.: Modelling and simulation of non-Gaussian stochastic processes for optimization of water-systems under uncertainty, PhD thesis, Dept. of Civil Engineering, National Technical University of Athens, 2018 (available at: https://www.itia.ntua.gr/ 1933/).

Tsoukalas, I., Efstratiadis, A., and Makropoulos, C.: Stochastic periodic autoregressive to anything (SPARTA): Modelling and simulation of cyclostationary processes with arbitrary marginal distributions, Water Resources Research, 54(1), 161–185, WRCR23047, https://doi.org/10.1002/2017WR021394, 2018.

Tsoukalas, I., P. Kossieris, and C. Makropoulos, Simulation of non-Gaussian correlated random variables, stochastic processes and random fields: Introducing the anySim R-Package for environmental applications and beyond, Water, 12(6), 1645, https://doi.org/10.3390/w12061645, 2020.

Yildiz, C., and Açikgöz, H.: Forecasting diversion type hydropower plant generations using an artificial bee colony based extreme learning machine method, Energy Sources, Part B: Economics, Planning, and Policy, 16(2), 216-234, https://doi.org/10.1080/15567249.2021.1872119, 2021.